

ผลของการฉายรังสีแกมมา และกระบวนการอบแห้งแบบพ่นฝอยต่อสมบัติของอนุภาคยางละเอียด
ที่ยึดที่วัลคะไนส์อย่างสมบูรณ์สำหรับเป็นสารตัวเติมเพิ่มความเหนียวในพอลิเมอร์



นางสาวระพีพรรณ แต่วัฒนา

จุฬาลงกรณ์มหาวิทยาลัย

CHULALONGKORN UNIVERSITY

บทคัดย่อและแฟ้มข้อมูลฉบับเต็มของวิทยานิพนธ์ตั้งแต่ปีการศึกษา 2554 ที่ให้บริการในคลังปัญญาจุฬาฯ (CUIR)
เป็นแฟ้มข้อมูลของนิสิตเจ้าของวิทยานิพนธ์ ที่ส่งผ่านทางบัณฑิตวิทยาลัย

The abstract and full text of theses from the academic year 2011 in Chulalongkorn University Intellectual Repository (CUIR)
are the thesis authors' files submitted through the University Graduate School.

วิทยานิพนธ์นี้เป็นส่วนหนึ่งของการศึกษาตามหลักสูตรปริญญาวิศวกรรมศาสตรมหาบัณฑิต

สาขาวิชาวิศวกรรมเคมี ภาควิชาวิศวกรรมเคมี

คณะวิศวกรรมศาสตร์ จุฬาลงกรณ์มหาวิทยาลัย

ปีการศึกษา 2559

ลิขสิทธิ์ของจุฬาลงกรณ์มหาวิทยาลัย

EFFECT OF GAMMA IRRADIATION AND SPRAY DRYING ON PROPERTIES OF ULTRAFINE FULLY VULCANIZED POWDERED RUBBER (UFPR) AS TOUGHENING FILLERS IN POLYMERS

Miss Rapiphan Taewattana



A Thesis Submitted in Partial Fulfillment of the Requirements
for the Degree of Master of Engineering Program in Chemical Engineering

Department of Chemical Engineering

Faculty of Engineering

Chulalongkorn University

Academic Year 2016

Copyright of Chulalongkorn University

5770283821 : MAJOR CHEMICAL ENGINEERING

KEYWORDS: UFPR, GAMMA RADIATION, SPRAY DRYING, POLYBENZOXAZINE

RAPIPHAN TAEWATTANA: EFFECT OF GAMMA IRRADIATION AND SPRAY DRYING ON PROPERTIES OF ULTRAFINE FULLY VULCANIZED POWDERED RUBBER (UFPR) AS TOUGHENING FILLERS IN POLYMERS. ADVISOR: ASSOC. PROF. SARAWUT RIMDUSIT, Ph.D., CO-ADVISOR: PHIRIYATORN SUWANMALA, Ph.D., 119 pp.

The aim of this research was to prepare ultrafine fully vulcanized powdered rubbers (UFPRs) from natural rubber (NR), styrene-butadiene rubber (SBR) and nitrile rubber (NBR) by combination technologies of radiation vulcanization and spray drying. The latex form of these rubbers was changed to the vulcanized rubber latex by gamma vulcanization using gamma ray doses in a range of 0 to 250 kGy and the UFPRs particles were observed in a spray drying step. The effect of gamma radiation dose on properties such as swelling behaviors and thermal properties of irradiated rubber latices and UFPRs were investigated. An increase of gamma radiation dose affects to a decreasing of both swelling ratio and molecular weight between crosslink (M_c) of the vulcanized rubber. On the other hand, gel fraction, crosslink density, glass transition temperature and thermal stability of vulcanized rubber increased with increasing the dose of gamma rays. Moreover, the obtained UFPRs were used as toughening filler in polybenzoxazine (PBA-a) matrix. Comparing with the neat PBA-a, the glass transition temperature of PBA-a/UFPRs composites increased. Moreover, PBA-a/UFPNBR composites shows the highest value of flexural strength and flexural modulus over other composites systems at 150 kGy of gamma irradiation dose for UFPNBR vulcanization. The impact strength of all types of composites were also evaluated by izod impact test. The results show that all UFPRs can improve impact resistance of PBA-a based composites. From all results, it can be concluded that three types of UFPRs can be used as toughening fillers in polybenzoxazine matrix.

Department: Chemical Engineering

Student's Signature

Field of Study: Chemical Engineering

Advisor's Signature

Academic Year: 2016

Co-Advisor's Signature 

ACKNOWLEDGEMENTS

I am sincerely grateful to my advisor, Assoc. Prof. Dr. Sarawut Rimdusit, for his kindness, invaluable guidance and valuable suggestions including constant encourage throughout this study.

I am also grateful to my co-advisor, Dr. Phiriyatorn Suwanmala, and my thesis committee members, who provided constructive and scientific advices for the completion of this thesis. This includes, Assoc. Prof. Dr. Siriporn Damrongsakkul and Asst. Prof. Dr. Apinan Soottitantawat , from the Department of Chemical Engineering, Faculty of Engineering, Chulalongkorn University and Asst. Prof. Dr. Chanchira Jubsilp from the Department of Chemical Engineering, Faculty of Engineering, Srinakharinwirot University.

This research is supported by Ratchadapisek Sompoch Endowment Fund (2016), Chulalongkorn University, the Institutional Research Grant (The Thailand Research Fund), IRG 5780014, and Chulalongkorn University, Contract No. RES_57_411_21_076 and the 90th Anniversary of Chulalongkorn University Fund.

My appreciation also goes to Thailand Institute of Nuclear Technology (Public Organization), Dow Chemical (Thailand), Ltd, Bangkok Synthetics Co., Ltd, and Chemical Innovation Co., Ltd. for their technical and chemicals support in this research.

Additionally, I am very thankful for every inspiration that they have made throughout my difficult years. They are more than my best friends. Thank are also extended to all members of Polymer Engineering Laboratory of the Department of Chemical Engineering, Faculty of Engineering, Chulalongkorn University, for every constructive discussion they contributed and all their help.

Finally, my deepest regard to my beloved family and parents, who have always been the source of my understanding, support and encouragement. Also, every person who deserves thanks for encouragement and support that cannot be listed.

CONTENTS

	Page
THAI ABSTRACT	iv
ENGLISH ABSTRACT	v
ACKNOWLEDGEMENTS	vi
CONTENTS	vii
LISTS OF FIGURES	x
LISTS OF TABLES	xiv
CHAPTER I INTRODUCTION.....	1
1.1 General introduction.....	1
1.2 Objectives	4
1.3 Scopes of this study	4
1.4 Procedure of the Study	6
CHAPTER II THEORY	7
2.1 Ultrafine Fully Vulcanized Powdered Rubber (UFPR).....	7
Advantages of UFPR.....	8
2.2 Types of Rubber	9
2.2.1 Natural Rubber	9
Vulcanization of Natural Rubber	11
Applications of Natural Rubber	14
2.2.2 Nitrile Rubber.....	16
2.2.3 Styrene Butadiene Rubber	18
2.3 Radiation Processing of Materials.....	20
2.3.1 Radiation Crosslinking of Polymers	22

	Page
2.4 Spray Drying Process.....	29
Functional Principle of Spray Dryer	31
Advantages of Spray Drying.....	31
CHAPTER III LITERATURE REVIEWS	33
CHAPTER IV EXPERIMENTAL.....	50
4.1 Materials.....	50
4.2 Benzoxazine resin preparation	50
4.3 Preparation of Ultrafine Rubbers.....	51
4.4 Preparation of Ultrafine Rubbers-modified Polybenzoxazine Composites.....	51
4.5 Characterization Methods	52
4.6.1 Swelling Measurements.....	52
4.6.2 Differential Scanning Calorimetry.....	53
4.6.3 Thermogravimetric Analysis.....	53
4.6.4 Fourier transform infrared spectroscopy (FT-IR).....	54
4.6.5 Morphology of UFPRs.....	54
4.6.6 Particle Size and Size Distribution of UFPRs	54
4.6.7 Mechanical Properties of UFPRs filled Polybenzoxazine Composites (Flexural Mode).....	55
4.6.8 Impact Resistance of UFPRs filled Polybenzoxazine Composites.....	56
CHAPTER V RESULTS AND DISCUSSION	57
5.1 Characterization of Properties of Un-irradiated and Irradiated Rubber Latices..	57
5.1.1 Solubility and Swelling Behavior of Un-irradiated and Irradiated Rubber Latices.....	57
5.1.2 Glass Transition Temperature of Rubber Latices	62

	Page
5.1.3 Thermal Stability of Rubber Latices.....	63
5.1.4 Spectroscopic Property of Rubber Latices	63
5.2 Characterization of Properties of Ultrafine Rubber	66
5.2.1 Morphology of UFPRs	66
5.2.2 Particle Size of UFPRs	67
5.2.3 Swelling Properties of UFPRs.....	67
5.2.4 Thermal Properties of UFPRs: Glass Transition Temperature and Thermal Stability	70
5.3 Characterization of Ultrafine Rubber Filled Polybenzoxazine Composites	71
5.3.1 Thermal Properties of Benzoxazine Resin (BA-a) Filled with Ultrafine Rubber	72
5.3.2 Mechanical properties of Polybenzoxazine Composites Filled with Ultrafine Rubber	73
5.3.3 Impact strength of Polybenzoxazine Composites Filled with Ultrafine Rubber	75
CHAPTER VI CONCLUSIONS.....	101
REFERENCES	103
APPENDIX A	113
VITA.....	119

LISTS OF FIGURES

Figure	Page
Figure 2.1 Rubber particles.....	7
Figure 2.2 Natural rubber latex from rubber tree.....	9
Figure 2.3 Structure of cis-1,4-polyisoprene (Natural rubber).....	10
Figure 2.4 Vulcanization of natural rubber that changed the dependence long chain into cross-linked structure.....	12
Figure 2.5 Interaction between natural rubber molecules and sulfur bridges in vulcanization process.....	12
Figure 2.6 Compression molded (cured) rubber boots.....	15
Figure 2.7 Applications of natural rubber.....	16
Figure 2.8 Structure of nitrile rubber.....	16
Figure 2.9 Applications of NBR.....	17
Figure 2.10 Structure of styrene-butadiene rubber.....	18
Figure 2.11 Applications of SBR.....	19
Figure 2.12 Sumitomo Electric's heat-shrinkable tubing and heat-resistant tubing/tapes take advantage of cross-linking effects of plastics achieved by electron beam irradiation.....	21
Figure 2.13 Schematic diagram of the preparation of UFPR.....	28
Figure 2.14 Principles and equipment of spray dryer.....	30
Figure 3.1 Particle size distribution of rubber latex prepared at different radiation doses.....	34
Figure 3. 2 FE-SEM micrographs of spray dried rubber latexes prepared in radiation dose of: (a) 200 kGy, (b) 75 kGy.....	36

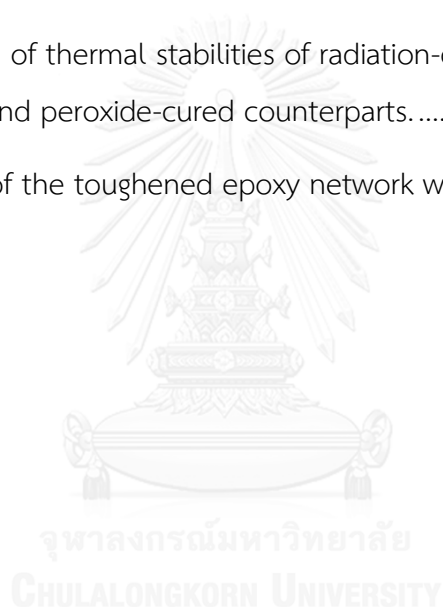
Figure	Page
Figure 3.3 The gel content and swelling ratio (Q) of different rubber powders versus radiation dose.....	37
Figure 3.4 Effect of radiation dose on the molecular weight between crosslinks (M_c) and crosslink density (CLD).	37
Figure 3.5 DSC thermograms of the rubber powders irradiated at (1) unirradiated, (2) 100 kGy, (3) 200 kGy.....	38
Figure 3. 6 FT-IR spectrums of rubber powder prepared at different radiation doses: (a) 75 kGy, (b) 100 kGy, (c) 200 kGy.....	39
Figure 3.7 SEM micrographs of the NRP at different magnifications (a) $\times 1,000$ and (b) $\times 10,000$	41
Figure 3.8 TEM images of UFSBRPR/EPDM blends.....	42
Figure 5.1 Swelling ratio of radiation irradiated rubber latex in toluene solvent at 0, 10, 30, 50, 100, 150, 200 and 250 kGy of gamma radiation doses: (●) rubber latex of NR, (■) rubber latex of SBR and (◆) rubber latex of NBR.....	77
Figure 5.2 Gel fraction of rubber latex at 0, 10, 30, 50, 100, 150, 200 and 250 kGy of gamma radiation doses: (●) rubber latex of NR, (■) rubber latex of SBR and (◆) rubber latex of NBR.	78
Figure 5.3 Molecular weight between crosslink of rubber latex that irradiated by radiation vulcanization in toluene solvent at 0, 10, 30, 50, 100, 150, 200 and 250 kGy of gamma radiation doses: (●) rubber latex of NR, (■) rubber latex of SBR and (◆) rubber latex of NBR.	79
Figure 5.4 Crosslink density of un-irradiated and irradiated rubber latex in toluene solvent at 0, 50, 100, 150, 200 and 250 kGy of gamma radiation doses: (●) rubber latex of NR, (■) rubber latex of SBR and (◆) rubber latex of NBR.	80
Figure 5.5 Sol–gel analysis of radiation crosslinking of rubber latices by Charlesby–Pinner equation (equation 5-1): (●) rubber latex of NR, (■) rubber latex of SBR and (◆) rubber latex of NBR.	81

Figure	Page
Figure 5.6 Glass transition temperature of rubber latex at 0, 50, 100, 150, 200 and 250 kGy of gamma radiation dose: (●) NR latex, (■) SBR latex and (◆) NBR latex...	82
Figure 5.7 Degradation temperature at 5 percent weight loss of rubber latex at 0, 50, 100, 150, 200 and 250 kGy of gamma radiation doses: (●) NR latex, (■) SBR latex and (◆) NBR latex.	83
Figure 5.8 FT-IR spectra of (a) un-irradiated NR latex (b) 100 kGy, and (c) 200 kGy of gamma radiation irradiated NR latex.	84
Figure 5.9 FT-IR spectra of (a) un-irradiated SBR latex and (b) 100 kGy, and (c) 200 kGy of gamma radiation irradiated SBR latex.....	85
Figure 5.10 FT-IR spectra of (a) un-irradiated NBR latex and (b) 100 kGy, and (c) 200 kGy of gamma radiation irradiated NBR latex.	86
Figure 5.11 Morphology of ultrafine fully vulcanized powdered SBR for ×2500 (a) 0 kGy, (b) 50 kGy, (c) 100 kGy, (d) 150 kGy, (e) 200 kGy and (f) 250 kGy.....	87
Figure 5.12 Morphology of ultrafine fully vulcanized powdered NBR for ×2500 (a) 0 kGy, (b) 50 kGy, (c) 100 kGy, (d) 150 kGy, (e) 200 kGy and (f) 250 kGy.....	88
Figure 5.13 Morphology of ultrafine fully vulcanized powdered NBR for ×2500 (a) 0 kGy, (b) 50 kGy, (c) 100 kGy, (d) 150 kGy, (e) 200 kGy and (f) 250 kGy.....	89
Figure 5.14 Average particle size of ultrafine SBR and NBR at various gamma radiation dose.....	90
Figure 5.15 Swelling ratio of ultrafine rubber in toluene solvent at 0, 50, 100, 150, 200 and 250 kGy of gamma radiation doses: (●) ultrafine-NR (UFPNR), (■) ultrafine-SBR (UFPSBR) and (◆) ultrafine-NBR (UFPNBR)	91
Figure 5.16 Gel fraction in toluene solvent of ultrafine rubber at 0, 50, 100, 150, 200 and 250 kGy of gamma radiation doses: (●) ultrafine-NR (UFPNR), (■) ultrafine-SBR (UFPSBR) and (◆) ultrafine-NBR (UFPNBR).....	92

Figure	Page
Figure 5.17 Molecular weight between crosslink of ultrafine fully vulcanized powdered rubber at different gamma radiation dose: (●) UFPNR, (■) UFPSBR and (◆) UFPNBR.	93
Figure 5.18 Crosslink density of ultrafine rubber at various gamma radiation doses after spray drying process: (●) ultrafine-NR (UFPNR), (■) ultrafine-SBR (UFPSBR) and (◆) ultrafine-NBR (UFPNBR).	94
Figure 5.19 Glass transition temperature of UFPRs at different gamma irradiated dose: (●) ultrafine-NR (UFPNR), (■) ultrafine-SBR (UFPSBR) and (◆) ultrafine-NBR (UFPNBR).	95
Figure 5.20 Degradation temperature at 5% weight loss of ultrafine rubber at 0, 50, 100, 150, 200 and 250 kGy of gamma rays: (●) ultrafine-NR (UFPNR), (■) ultrafine-SBR (UFPSBR) and (◆) ultrafine-NBR (UFPNBR).	96
Figure 5.21 Glass transition temperature of polybenzoxazine composites at different doses of gamma rays: (▲) neat polybenzoxazine (PBA-a), (●) filled with ultrafine-NR (UFPNR), (■) filled with ultrafine-SBR (UFPSBR) and (◆) filled with ultrafine-NBR (UFPNBR).	97
Figure 5.22 Flexural strength of (▲) neat polybenzoxazine and polybenzoxazine composites filled with (●) ultrafine-NR (UFPNR), (■) ultrafine-SBR (UFPSBR) and (◆) ultrafine-NBR (UFPNBR) at various gamma radiation doses.	98
Figure 5.23 Flexural modulus of (▲) neat polybenzoxazine and polybenzoxazine filled with (●) UFPNR, (■) UFPSBR and (◆) UFPNBR at 0, 50, 100, 150, 200 and 250 kGy of gamma rays.	99
Figure 5.24 Impact strength of composites based on PBA-a at difference gamma dose irradiated UFPRs: (●) PBA-a/UFPNR, (■) PBA-a/UFPSBR and (◆) PBA-a/UFPNBR.	100

LISTS OF TABLES

Table	Page
Table 2.1 Typical analysis of natural rubber	10
Table 2.2 Comparison between raw natural rubber and vulcanized natural rubber..	13
Table 2.3 Notable products made using radiation crosslinking	24
Table 2.4 Advantages and disadvantages of radiation crosslinking.....	26
Table 3.1 Different types of gels and their properties.....	44
Table 3.2 Comparison of thermal stabilities of radiation-cured vulcanizates of SBR and NBR with sulfur and peroxide-cured counterparts.....	46
Table 3.3 Properties of the toughened epoxy network with ENP and CTBN	47



CHAPTER I

INTRODUCTION

1.1 General introduction

Rubber is an important raw material that can be used in many manufacturing applications, such as footwear, transportation, and different engineering product [1]. In general, rubber can be combined with other materials such as plastics and other kind of rubber to enhance overall properties including toughness of the final products. Mixing of different types of these raw materials would be quite difficult since raw material as blocks, rods, sheets, or pellets need to be crushed into smaller particles. Therefore materials in the form of small particles or even fine powder of raw rubber are widely used to manufacture various types of products with accepted physical, mechanical and chemical properties [2].

There have been several works carried out showing ultrafine fully vulcanized powdered rubber (UFPR), i.e. between micro- to nano- dimensions that can be produced from natural rubber, styrene-butadiene rubber, carboxylated styrene-butadiene rubber, nitrile rubber, carboxylated nitrile rubber, chloroprene rubber, polybutadiene rubber, butadiene-styrene-vinylpyridine rubber, ethylene propylene rubber, synthetic-isoprene rubber and urethane rubber. UFPR can be used to improve toughness of plastics such as propylene [3, 4], polyethylene [5], epoxy [6], and nylon [7, 8], and modify asphalt for greater elasticity and less prone to cracking as well as aging. Also this can improve friction behavior within the materials [9].

Liu, Y et al. studied eight series of nano-powdered rubbers modified with phenolic resin for improving friction properties of materials. It was found that nano-rubber powder had good compatibility and chemical interaction at interface with the modified resin for friction material applications. Nano-scale particle size of the rubber was able to disperse well in matrix resulting in better interface and more chemical interaction between the rubber particles and the matrix. In their study, it was determined that phenolic resin modified with rubber particle had much higher impact strength and heat resistance than that of the pure phenolic resin [9].

Primarily, rubber latex should be treated by curing or vulcanizing procedure. In a typical treatment of rubber latex, curing agents such as sulfur and peroxide, are used in vulcanization process. For this process, rubber is changed from plastic material, linear or slightly cross-linked structure, to hard material, highly cross-linked structure, due to its chemical structure were linked to each other. However, this process is complex and requires high heating cost. Ionization radiation is one of vulcanization process which do not require heating and usually do not use any curing agents. Therefore, it's easier and results in a clean technology [10]. Compared to the products which are produced by chemical or thermal crosslinking techniques, radiation vulcanized soft rubber powder possesses some advantages because of its very fine particle sizes and good controllability about the crosslinking density of the rubber. Its major application is as a property modifier for thermoplastics and other elastomers and to produce thermoplastic vulcanizates (TPVs) [2-9].

Recently, Yoshida, K et al. invented a method for producing silicone rubber powder which can be divided into 3 steps. The first is preparing a dispersion of a heat-vulcanized liquid silicone rubber composition in water at 0 to 25 °C. Next, dispersing the obtained rubber in a prior step into a liquid at least 50 °C to vulcanize the liquid silicone rubber composition into powders. And then, separating the vulcanized powdery silicone rubber [11]. Another invention, Harashima, A *et al.* exposed a vulcanized powdery silicone rubber. The process consists (1) vulcanizing a vulcanizable silicone composition comprising a specific organopolysiloxane to form a vulcanized silicone rubber, and (2) drying the vulcanized silicone rubber by spray drying [12].

It was rather complicated process to manufacture ultrafine rubber particles until Sinopec Corp developed a method to reduce particle size of rubber in a range of from 20 nm to 2000 nm by irradiation vulcanization and spray drying method. First, rubber latex was vulcanized by gamma irradiation, which transforms rubber latex to crosslink rubber latex. After that, the spray drying process was used to dry the latex to solid powder [13].

There are many advantages for using spray drying to produce UFPR such as an ease to control the size of the rubber particles, or obtaining particles in spherical shape. In addition each particle will be of the same chemical composition with the feed and experience very short residence time during the spray drying thus shorten processing time of UFPR (3-40 seconds), which permits spray drying less chance of thermal degradation of the obtained powder [14].

Consequently, the objective of this study is to prepare ultrafine fully vulcanized powdered rubber from rubber latex including natural rubber, styrene-butadiene rubber and nitrile rubber based on previous crosslinking by irradiation curing process in a prior step to spray drying. And then the crosslinking ultrafine rubbers will be analyzed for their particle size, morphology, swelling behavior, and their essential thermal and physical properties. Effect of those three types of UFPRs on toughening behavior of rigid polybenzoxazine will also be compared.

1.2 Objectives

1. To prepare ultrafine fully vulcanized powdered rubber from natural rubber, nitrile butadiene rubber and styrene butadiene rubber by gamma radiation and spray drying.
2. To characterize physical and thermal properties of the obtained ultrafine fully vulcanized powdered rubber.
3. To compare effect of the obtained UFPRs on toughening behaviors of a rigid type polybenzoxazine.

1.3 Scopes of this study

1. Preparation of vulcanized rubber latices include natural rubber, nitrile rubber, and styrene butadiene rubber by gamma radiation at dose range 0-250 kGy.

2. Preparation of vulcanized rubber latices that dilute to 25 % solid content.
3. Preparation of ultrafine rubber particles by spray drying process with range of temperature between 100-180 °C.
4. Characterize physical and thermal properties of the ultrafine fully vulcanized powdered rubber.
 - Physical Properties
 - Particle size measurement : Mastersizer
 - Morphology characterization : Scanning electron microscope (SEM)
 - Swelling behaviors : gel content, swelling ratio, molecular weight between crosslink and crosslink density in toluene solution
 - Chemical bonding of ultrafine rubber : Fourier transform infrared spectroscopy (FT-IR)
 - Thermal Properties
 - Glass transition temperature : Differential scanning calorimetry
 - Thermal degradation : Thermogravimetric analysis
5. Synthesis of bisphenol-A aniline based benzoxazine resin (BA-a).
6. Preparation of benzoxazine resin filled with ultrafine rubber at 15 phr

7. Comparison of toughness enhancement of polybenzoxazine using the above three types of the UFPRs at a fixed composition of 15 phr of the UFPR based on impact test.

1.4 Procedure of the Study

1. Review related literature.
2. Prepare of chemicals and equipment for using in this research.
3. Prepare vulcanized rubber latex from natural rubber latex, nitrile rubber latex and styrene butadiene rubber latex by irradiation of gamma rays with 0, 50, 100, 150, 200 and 250 kGy.
4. Prepare vulcanized rubber latex that dilute to 25% solid content by deionized water (DI water).
5. Prepare ultrafine fully vulcanized powdered rubber by spray drying process with range of temperature between 100 – 180 °C.
6. Evaluate about particle size, morphology, swelling properties - gel content, swelling ratio, molecular weight between crosslink and crosslink density-thermal properties of ultrafine fully vulcanized powdery rubber.
7. Test the toughness of the UFRP based on those three elastomers in polybenzoxazine a fixed UFRP content of 15 phr.
8. Analyse the experimental results.
9. Prepare of the final report.

CHAPTER II

THEORY

2.1 Ultrafine Fully Vulcanized Powdered Rubber (UFPR)



Figure 2.1 Rubber particles [15].

A new type of rubber for modifying polymer matrix that has attracted much attention in recent years is ultrafine fully vulcanized powdered rubber (UFPR). Its special manufacturing process leads to the much higher crosslinking density on the surface of UFPR than in the inner parts, which makes it a unique kind of shell-core elastomeric filler [16]. UFPR was prepared by the combined technologies of irradiation and spray drying. Firstly, the rubber latex is mixed with required additives and cross linking agents, and then irradiated by gamma rays Co-60 or electron beam from electron accelerators, and followed by spray drying. A series of UFPR has been commercialized, such as silicone rubber (S-UFPR), carboxylic acrylonitrile butadiene

rubber (CNBRUFPR), acrylonitrile butadiene rubber (NBR-UFPR), styrene butadiene vinyl-pyridine rubber (BSP-UFPR), and carboxylic styrene butadiene (CBS-UFPR) [17].

Advantages of UFPR

UFPR show many advantages properties such as [18];

- The mixing processing would be low-energy consumed and time-efficiency because the interactions between crosslinked rubber particles are much lower than cohesion of bulk rubber.
- The rubber dispersion would be pretty fine domain with the same size as that of UFPR. More importantly, UFPR would keep dispersion phase all the time no matter how high the blend ratio of UFPR to matrix rubber is.
- The co-crosslinking between two phases (polymer matrix and UFPR) would be simplified because one phase has been crosslinked state. All the ingredients could only be mixed into continuous phase because of the crosslinking of dispersed rubber, and as a result, the dispersed rubber phase would keep highly elasticity state, which is very promising for some rubber products.

2.2 Types of Rubber

2.2.1 Natural Rubber



Figure 2.2 Natural rubber latex from rubber tree.

Natural rubber; NR [19] was the first rubber and was unique until the development of polysulfide rubber in about 1927. Natural rubber supplies about one-third of the world demand for elastomer and is the standard by which other are judges. It was Charles Goodyear and Thomas Hancock's experiments with natural rubber, sulfur, and heat that led to the discovery of vulcanization, representing the birth, as it were, of compounding.

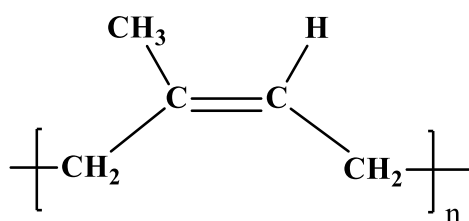


Figure 2.3 Structure of cis-1,4-polyisoprene (Natural rubber).

Natural rubber is *cis*-1,4-polyisoprene, structure is showed in figure 2.3. A linear and long-chain polymer with repeating isoprenic units (C_5H_8), it has a density of 0.93 at 20 °C. Intensive plant breeding has produced a wide range of clonal types whose Mooney viscosity (when freshly coagulated) can vary from slightly below 50 to over 90. The component of natural rubber is shown in table 2.1.

Table 2.1 Typical analysis of natural rubber

Component	(%)
Moisture	0.6
Acetone extract	2.9
Protein (calculated from nitrogen)	2.8
Ash	0.4
Rubber hydrocarbon	93.9
Total	100

Natural rubber has several outstanding properties including high flexibility, high tear resistance, high tensile strength, good friction characteristics and inexpensive. They are used to many different products due to the properties excellent in the tensile strength, although no fillers reinforced and highly flexible, very suitable to produce gloves, condoms, and rubber band. Including high flexibility (elasticity), while a high heat (heat build-up) and sticking together (tack) that is suitable for the production of truck tires, aircraft tires or mixed with synthetic rubber for tire production.

Vulcanization of Natural Rubber

Vulcanization is the process by which natural rubber, tapped from trees, is transformed into a malleable product that is more durable. Charles Goodyear discovered the process of vulcanization in 1893 to modify the properties of natural rubber. It is the addition of right amount of sulfur or peroxide to natural rubber to impart high elasticity, tensile strength and resistance to abrasion [20].

Raw dry rubber is heated with vulcanizing agents (figure 2.4 and 2.5) such as sulfur (5%-8% based on the requirement), zinc oxide (a filler, 5%) and accelerator (0.5% -1%) at 400 - 440 K for about half an hour. As the sulfur quantity increases, the rubber becomes tougher. 50% sulfur gives ebonite (vulcanite). An accelerator containing nitrogen, sulfur or both is used to increase the reaction rate and for vulcanization to occur at room temperatures.

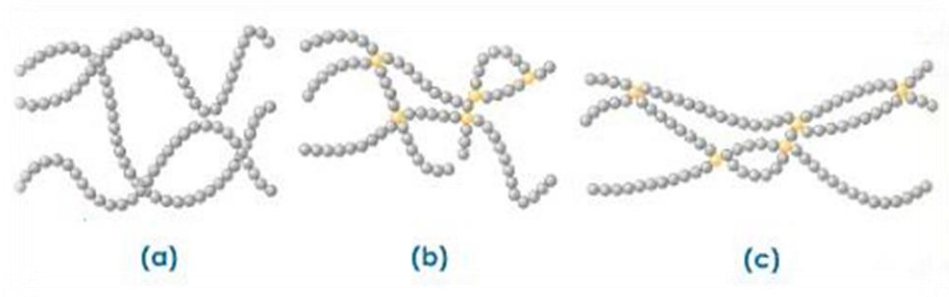


Figure 2.4 Vulcanization of natural rubber that changed the dependence long chain into cross-linked structure [20].

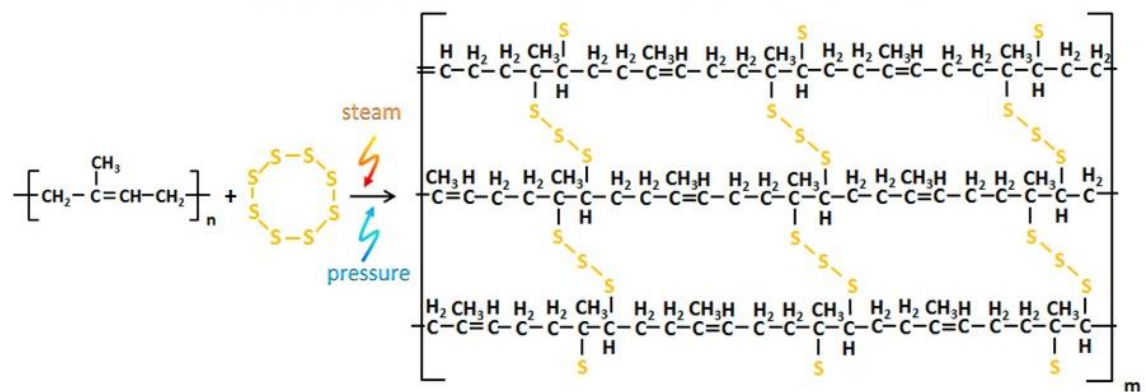


Figure 2.5 Interaction between natural rubber molecules and sulfur bridges in vulcanization process [21].

Table 2.2 Comparison between raw natural rubber and vulcanized natural rubber [20].

Raw Natural Rubber	Vulcanized Natural Rubber
Soft and sticky	Comparatively hard and non-sticky
Low tensile strength and not very strong	High tensile strength and very strong
Low elasticity	High elasticity
Can be used over a narrow range of temperature from 10 to 60 degrees centigrade	Can be used over a wide range of temperature from -40 to 100 degrees centigrade
Low abrasion resistance	High abrasion resistance
Absorbs a large amount of water	Absorbs a small amount of water
Soluble in solvents like ether, carbon disulphide, carbon tetrachloride, petrol and turpentine	Insoluble in all the usual solvents

The double bonds in natural rubber permit formation of sulfur bridges between different chains (figure 2.5). These cross-links are responsible for removing the tackiness of untreated rubber.

Rubber can be hardened by adding carbon black as a filler (solid substance added for strength and to reduce the cost) to it during the vulcanization process. This increases the strength and abrasion resistance of natural rubber. Carbon black when mixed with rubber in rubber tires, makes them more durable and cuts the cost. The vulcanized and hardened rubber is used to make tires and tubes of automobiles and conveyor belts for industrial use.

Vulcanized natural rubber is used for making: Rubber bands, football bladders, gloves and rubber tubes and Tyres and tubes of automobiles and conveyor belts for industrial use after hardening.

Applications of Natural Rubber

- Contemporary manufacturing

Around 25 million tonnes of rubber is produced each year, of which 42 percent is natural rubber. The remainder is synthetic rubber derived from petrochemical sources. Around 70 percent of the world's natural rubber is used in tires. The top end of latex production results in latex products such as surgeons' gloves, condoms, balloons and other relatively high-value products. The mid-range which comes from the technically specified natural rubber materials ends up largely in tires but also in conveyor belts, marine products, windshield wipers and miscellaneous rubber goods. Natural rubber offers good elasticity, while synthetic materials tend to offer better resistance to environmental factors such as oils, temperature, chemicals or ultraviolet light and suchlike. "Cured rubber" is rubber which has been compounded and subjected to the vulcanisation process which creates cross-links within the rubber matrix.



Figure 2.6 Compression molded (cured) rubber boots [22].

- Pre-World War II textile applications

Rubber produced as a fiber, sometimes called 'elastic', has significant value for use in the textile industry because of its excellent elongation and recovery properties. For these purposes, manufactured rubber fiber is made as either an extruded round fiber or rectangular fibers that are cut into strips from extruded film. Because of its low dye acceptance, feel and appearance, the rubber fiber is either covered by yarn of another fiber or directly woven with other yarns into the fabric. In the early 1900s, for example, rubber yarns were used in foundation garments. While rubber is still used in textile manufacturing, its low tenacity limits its use in lightweight garments because latex lacks resistance to oxidizing agents and is damaged by aging, sunlight, oil, and perspiration. Seeking a way to address these shortcomings, the textile industry has turned to neoprene (polymer of chloroprene), a type of synthetic rubber,

as well as another more commonly used elastomer fiber, spandex (also known as elastane), because of their superiority to rubber in both strength and durability.



Figure 2.7 Applications of natural rubber.

2.2.2 Nitrile Rubber

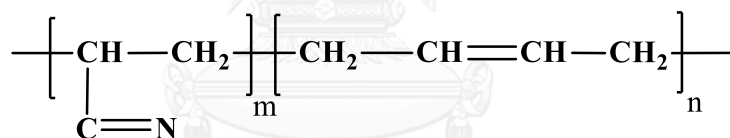


Figure 2.8 Structure of nitrile rubber.

Nitrile rubber (NBR) [19] is a synthetic rubber that a copolymer of butadiene and acrylonitrile, made in an emulsion process like styrene-butadiene rubber. It's chosen where oil and fuel resistance superior to that of neoprene is wanted or for its chemical resistance. Figure 2.8 is showed the repeating units of NBR.

Nitrile has good resistance to wide variety of nonpolar oils, fats, and solvents. This property offers advantages in making products for automotive and oil industries such as oil seals, pipe protectors, and blowout preventers. The acrylonitrile content

varies, usually from 20 to 50% by weight, with levels under 25% classified as low, 25-35% as medium, and 35-50% as high. Major properties are dependent on acrylonitrile (ACN) content, and this subject will be picked up again. Mooney viscosity ranges from 25 to 100, although the usual range is 40-80. Unlike natural rubber, NBR has no crystallinity and therefore there is no self-reinforcing effect. The density of NBR varies with acrylonitrile content, low acrylonitrile level polymer is 0.98, and high is 1.00.

This rubber is highly polarized and having featured properties is good resistant to petroleum and non-polar solvents. Increasing acrylonitrile content will greatly enhance the ability to oil resistance. It is good wear, abrasion, and tear resistant. The operating temperature range is between -40 to 100 °C.



Figure 2.9 Applications of NBR.

Most applications are applied to the exposed oil, heat resistant, abrasion resistance such as oil gasket rubber, o-ring rubber, seal rubber, conveyor belts, oil tube, reinforced rubber tube, coated rubber, roller rubber, and boots. It has been produced with a glove for protection against radioactive.

2.2.3 Styrene Butadiene Rubber

Styrene-butadiene rubber (SBR) [19] is a synthetic rubber that a copolymer of styrene and butadiene normally containing about 23.5 % bound styrene. It made both by emulsion and in solution polymerization. Figure 2.10 showed the repeating unit of the styrene-butadiene rubber.

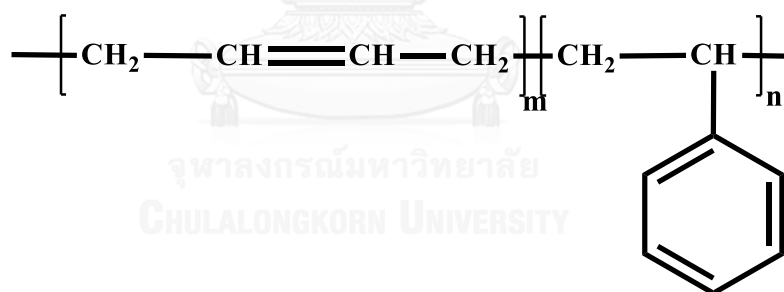


Figure 2.10 Structure of styrene-butadiene rubber

Because of the double bond present in butadiene, that portion of molecule can be present in three forms: *cis*-1,4, *trans*-1,4, and vinyl-1,2. Ordinarily the proportions are about 18% *cis*, 68% *trans*, and 17% vinyl. Solution SBR has about the same amount of styrene as emulsion product, but there is higher *cis*-butadiene content, lower *trans*-butadiene, and lower vinyl. Mooney viscosity of un-pigmented

SBR made by the emulsion process ranges from 23 to 128, with the most popular grades being in the range of 44 to 55. The density of SBR is 0.94 and the glass transition temperature (T_g) -which the rubber goes from rubbery to brittle glassy state- is higher than natural rubber, a common grade of SBR having a T_g of about $-53\text{ }^\circ\text{C}$, whereas natural rubber is about $-70\text{ }^\circ\text{C}$.



Figure 2.11 Applications of SBR

One of the most important variables is monomer ration in the copolymer. This shows up dramatically in the change in the glass trasion temperture. Polystyrene has T_g is about $-90\text{ }^\circ\text{C}$ and polybutadiene's T_g is about $-90\text{ }^\circ\text{C}$. As the weight fraction of polystyrene in copolymer increases, there is a regular increase in T_g . For example, at 0.25 weight fraction the T_g is about $-65\text{ }^\circ\text{C}$, at 0.5 about $-55\text{ }^\circ\text{C}$, and at 0.75 about $0\text{ }^\circ\text{C}$. The influence of increasing styrene ratio on the properties of the vulcanized rubber

compounds is less clear. Storey and Williams investigated this phenomenon and found that as the styrene content increased, modulus increased, but resilience decreased. Tensile strength increased as the styrene content increased to 0.5 weight fraction, and then decreased. As styrene content is increased, the polymer loses its rubberiness and becomes more like a plastic in processing.

SBR is a synthetic rubber with most widely used in the industry. Because of inexpensive rubber and more features properties. SBR has low resistant about petroleum and hydrocarbon solvent because it's a non-polar rubber. But it can resistant to dilute acid and base, alcohol, water, glycol, salt and silicone oil as well. These rubber have a high dielectric strength. The operating temperature applications ranging from -50 to 100 °C. SBR is used to produce a belt, soles, insulated wires, rubber hoses, medical rubber products, and food packaging.

2.3 Radiation Processing of Materials

Practical applications for radiation processing of materials have been evolving since the introduction of this technology nearly fifty years ago [23]. Crosslinking plastic materials, sterilizing medical products and preserving foods were the earliest developments. Processes for curing monomeric coatings and inks were developed somewhat later. The use of these and other processes has grown and they are widely practiced today.

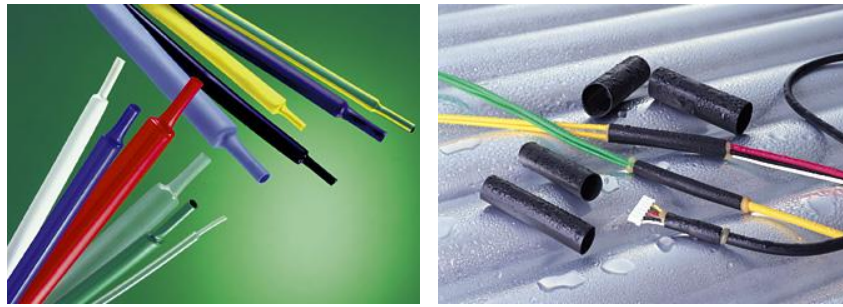


Figure 2.12 Sumitomo Electric's heat-shrinkable tubing and heat-resistant tubing/tapes take advantage of cross-linking effects of plastics achieved by electron beam irradiation [20].

Electron beam crosslinking is used to produce heat-shrinkable plastic films for packaging foods and other consumer products, heat - shrinkable plastic tubing and encapsulations for industrial products, plastic foam and hydrogels for medical applications. The insulation on electrical wires and the jackets on multi-conductor cables are crosslinked to increase heat tolerance and to improve the resistance to abrasion and solvents. Crosslinked plastic pipe is used for hot water distribution systems. Sheet rubber components for automobile tires are partially crosslinked before the tire is made to stabilize the thickness of these materials during the final thermal cure. Radiation-cured, solvent-free coatings and inks are used for magazines, newspapers and a variety of packaging materials. Other applications include reducing the molecular weight by scissioning of polymers, e.g. polytetrafluoroethylene, polypropylene and cellulose, grafting of monomers onto polymers to modify their surface properties, and curing fiber-reinforced composite material. Industrial irradiation processes using high power electron accelerators are attractive because the throughput rates are very high and the treatment costs per unit of product are often

competitive with more conventional chemical processes. The utilization of energy in electron beam processing is more efficient than typical thermal processing. The use of volatile or toxic chemicals can be avoided. Strict temperature or moisture controls may not be needed. Irradiated materials are useable immediately after processing. These capabilities are unique in that beneficial changes can be induced rapidly in solid materials and preformed products.

2.3.1 Radiation Crosslinking of Polymers

Crosslinking (or cross-linking, cross linking) is a process where the long chains of polymers are linked together increasing the molecular mass of the polymer as a result. Properties of polymer products that can be improved by crosslinking include [24]:

- Mechanical properties, such as tensile strength
- Scratch resistance
- Performance at higher temperatures, often with an increase in the melting temperature
- Resistance to chemicals because of lowered solubility in organic solvent
- Gas permeation reduction

- Shape memory retention. Elastomers may be crosslinked to a slight degree to give them “memory” – they will return to their original shape after being expanded.

Depending upon the polymer, different techniques may be used to cause crosslinking. In all cases, the chemical structure of the polymer is altered through the crosslinking process. This can be done by adding different chemicals in conjunction with heating and, sometimes, pressure. One of the earliest examples of crosslinking is the vulcanization of natural rubber by adding sulfur under heat, which creates the links between the latex molecules. Vulcanization gives the rubber its strength properties over temperature ranges in which non-vulcanized rubber could not perform.

Alternatively, the polymer may be crosslinked by using high-energy ionizing radiation, such as electron beam (e-beam), gamma ray or x-ray. Gamma irradiation is usually most economical at lower doses (~80 kGy and below) and for large, high density parts. Electron beam is commonly used for small parts, particularly low density parts, and linear product processed reel to reel such as wire, cable, and tubing.

Table 2.3 Notable products made using radiation crosslinking [24]

Products	Improving Properties
Wire and cable insulation	<ul style="list-style-type: none"> - Improved mechanical strength and insulation properties, particularly for high temperature applications. Used in automobiles, aircraft, trains, ships and other markets. - Additives are important (antioxidants, flame retardants, prorads, etc.)
Heat shrinkable products	<ul style="list-style-type: none"> - Film: Lower gas permeability and better performance at low temperatures compared to non-irradiated films. - Tubing
Polymeric positive temperature coefficient products	<ul style="list-style-type: none"> - Resettable fuses - Heat tracing products, eg self-regulating heaters
Gaskets and seals	<ul style="list-style-type: none"> - Improved temperature resistance - Improved resistance to chemicals
Hydrogels	<ul style="list-style-type: none"> - No contamination from chemical crosslinkers - Simultaneous sterilization is possible
Products from radiation crosslinked engineering plastic (eg polybutylene terephthalate, polyamide)	<ul style="list-style-type: none"> - Crosslinking promoters added - Primarily to increase temperature resistivity - Automotive underhood and other applications

Table 2.3 Notable products made using radiation crosslinking (cont')

Products	Improving Properties
Polyolefin foams	Crosslinking during the foaming process to increase melt viscosity resulting in lower density closed cell foam.
PEX-c pipe	Improved mechanical and burst strength for higher temperature plumbing and water transport pipe.
Vulcanization	<ul style="list-style-type: none"> - Radiation pretreatment of tire components to allow blending of synthetic rubber and to reduce energy costs compared to thermal methods - Extruded polysiloxane gaskets and tubes - Polysiloxane electrical insulation tape - Polysiloxane rubber based / fabric

The resins of materials that listed in Table 2.3 may be irradiated at doses lower than those used for crosslinking to create long chain branching, a precursor to crosslinking. This influences the melt flow properties of the materials by decreasing their melt flow index and enhancing melt strength during processing. Examples are irradiated polyethylenes used in products such as films and foams which can benefit from enhanced melt strength during manufacture, and ethylene vinyl acetate [24]. The advantages and disadvantages of radiation crosslinking are shown in Table 2.4.

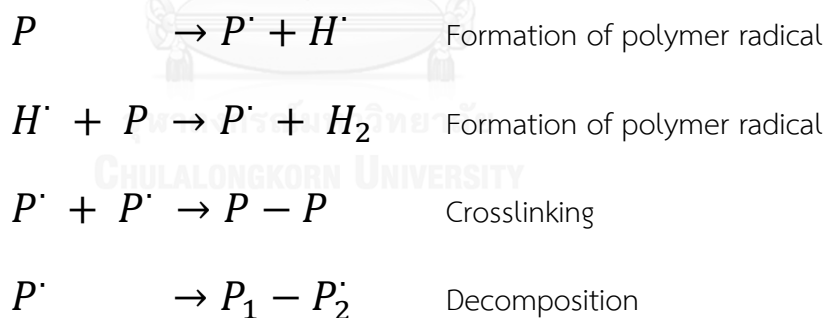
Table 2.4 Advantages and disadvantages of radiation crosslinking [24].

Advantages	Disadvantages
Many polymers can be crosslinked. When needed, compounds often relatively simpler	Benefits and process of radiation crosslinking not widely understood
A number of service centers can offer radiation crosslinking services worldwide	Use of a service center means product must be shipped and placed in the control of others during the irradiation process
Versatile technology: Degree of crosslinking can be controlled with the dose and small batches may be processed	High capital cost and equipment expertise is needed for in-house crosslinking
Reliable	
Efficient use of energy	
“Cleaner” process with the potential for no unwanted residuals in the product	

Irradiation creates free radicals which will often chemically react in various ways, sometimes at slow reaction rates. The free radicals can recombine forming the crosslinks. The degree of crosslinking depends upon the polymer and radiation dose. One of the benefits of using irradiation for crosslinking is that the degree of crosslinking can be easily controlled by the amount of dose. Other subtle influences include the additives in the base polymer and the type of radiation used (related to the dose rate). Another influence which may not be as subtle is oxidation during irradiation. This effect will be more predominant when using gamma irradiation as compared to the much

faster electron beam irradiation process. Furthermore, oxidation can continue after irradiation causing changes in properties with time. This oxidation process may reduce by antioxidants added to the polymer resin.

A competing process, called scissioning, occurs when polymers are irradiated. In this case, the polymer chains are broken and molecular mass decreases. Scissioning and crosslinking occur at the same time where one may predominate over the other, depending upon the polymer and the dose. The rate of occurrence for these two processes is the G value, defined as the number of events that occurs with the absorption of 100 eV of energy. These can be converted to units of $\mu\text{mol}/\text{J}$ by multiplying G by 0.1036.



Scheme 2.1. Simplified reaction mechanism of radiation processing of rubber latex system [10].

One of the new applications of radiation crosslinking is to prepare radiation vulcanized fine rubber powders that produce by crosslinking the rubber latex using radiation and then spray drying of them. During this process, polymer radicals formed

in rubber latex and the subsequent crosslinking or decomposition reactions occur.

Scheme 2.1 shows the simplified reaction mechanism of radiation processing of rubber latex system.

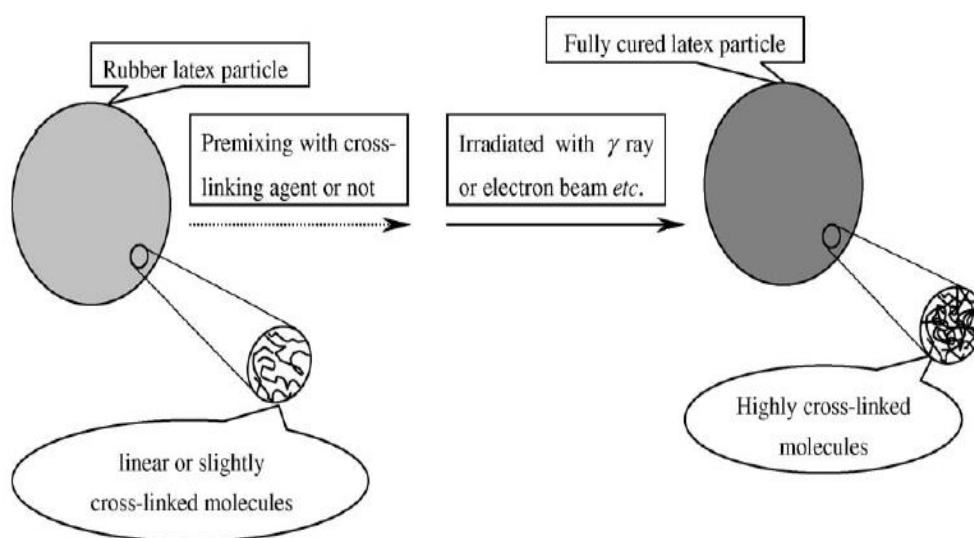


Figure 2.13 Schematic diagram of the preparation of UFPR [9].

Radiation curing, as shown in Figure 2.13, is done without heating and in the absence or presence of vulcanization agents. This process is cleaner, simpler and more homogeneous than the conventional curing methods (sulfur or peroxide). By using this vulcanization process, a rubber network in which the polymer chains are linked to each other by very stable covalent carbon-carbon bonds, can be achieved. Variables such as radiation dosage, dose rate and chemical additives can affect vulcanizate properties and microstructure. Some researchers have studied radiation crosslinking effects in rubber, rubber blends and thermoplastic elastomers.[10]

2.4 Spray Drying Process

The methods used to produce nanoparticles can be divided into three main groups [25]:

- (i) Physicochemical methods e.g. the creation of nanoparticles using preformed polymers and inducing their precipitation by emulsification–solvent evaporation, diffusion or reverse salting-out.
- (ii) In situ chemical synthesis methods of macromolecules, giving rise for instance to polymerization or interfacial polycondensation reactions.
- (iii) Mechanical methods e.g. use of high-energy devices like high pressure homogenizers, sonifiers, or high-energy wet mills.

A traditional spray dryer, the third of the above-mentioned methods, is generally used to transform liquid substances into powders rapidly and efficiently. The speed of the process and the consequently short drying time enables the drying of even temperature-sensitive products without degradation. This spray drying process is particularly used to improve product conservation in dried solid form. With the development of active compound and emulsion encapsulation used in pharmaceuticals, cosmetics and functional food preparation, this method has also been used for encapsulation purposes. The powder thus generated is a matrix system in the form of micro-particles (i.e. microspheres), exhibiting a spherical or hollowed morphology

depending on the nature of the wall material used and the operational drying conditions such as the inlet temperature, solid concentration, gas flow rate or feed rate. The powder samples are generally heterogeneous and amorphous. Overall yields of spray drying on a laboratory scale are limited, reaching around 50% to 70. Spray drying was used in pharmaceutical ingredients, drug delivery, vaccines, inhalable drugs, taste masking, functional foods, flavors, vitamins, proteins, probiotic bacteria, juice concentrate, milk powder, and materials such as nanotechnology, catalysts, fuel cells, batteries, accumulators, ceramics, UV absorbers, pigments and coatings. Figure 2.14 shows principles and equipment of spray dryer.

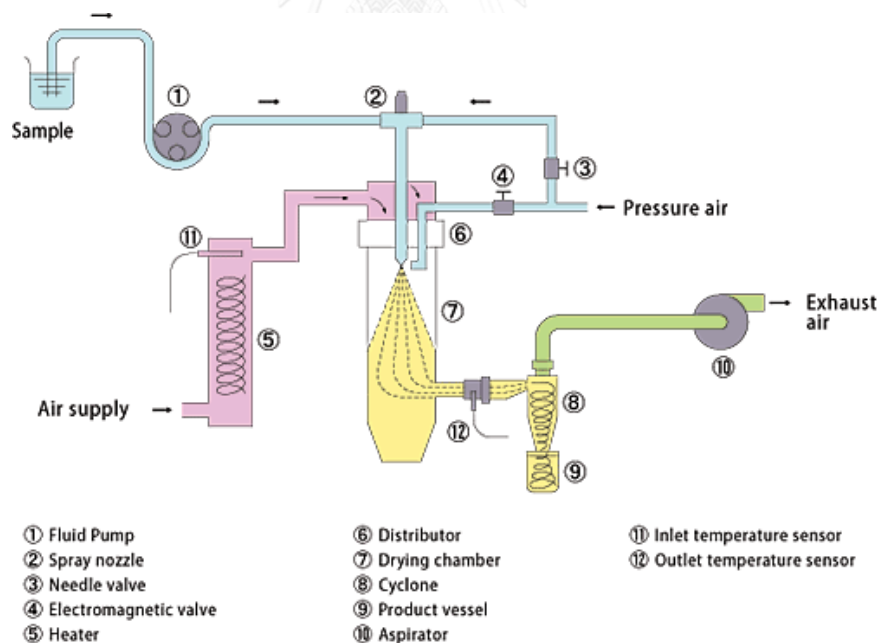


Figure 2.14 Principles and equipment of spray dryer [22].

Functional Principle of Spray Dryer

The principle of spray drying process have 6 steps [26];

- 1) Heating : Heat the inlet air to the desired temperature (max. 220 °C)
- 2) Droplet formation : Two-fluid nozzle
- 3) Drying chamber : Conductive heat exchange between drying gas and sample droplets
- 4) Particle collection : Cyclone technology
- 5) Outlet filter : Collection of finest particles to protect the user and the environment
- 6) Drying gas : Delivered by aspirator

Advantages of Spray Drying

Spray drying process have many advantages. First, the particle size can be controllable : The dry particle size can be easily controlled by atomization of the liquid feed and the design of the hot gas inlet. The correct spray dryer design and atomization technique can increase yields for products that require classification. Spray dryers can typically produce between 30 to 500 micron average particle size, in a bell shaped distribution.

Second, the flow properties of dry solids : The shape of most spray dried particles is spherical, which provides for fluid-like flow properties. This makes many downstream operations, such as packaging, pressing, filtering, and handling easier and less costly.

Third, The homogeneous solids mixture produced : Spray drying produces the most homogeneous product for multi-component solutions and slurries. Each particle will be of the same chemical composition as the mixed feed.

Next, The evaporative cooling of the product : The heat and mass transfer during drying occurs in the air and vapor films surrounding the droplet. This protective envelope of vapor keeps the particle at the saturation temperature. As long as the particle does not become "bone-dry", evaporation is still taking place and the temperature of the solids will not approach the dryer outlet temperature. This is why many heat sensitive products can be spray dried easily at relatively high inlet temperatures.

Finally, The short residence time required : The surface area produced by atomization of the liquid feed enables a short gas residence time, ranging from 3-40 seconds depending upon the application, which permits spray drying without thermal degradation. This allows for fast turn-around times and product changes because there is no product hold up in the spray drying equipment.

CHAPTER III

LITERATURE REVIEWS

Qiao *et al.* (2002) [13] have prepared a radiation vulcanized powdery rubber having a particle size of from 20 to 2000 nm. The vulcanized powdery rubber is easily to be dispersed into various plastics, and thus can be mixed with various plastic to prepare toughened plastics and radiation vulcanized thermoplastic elastomers. A process for preparing a vulcanized rubber powder having a gel content of at least 60% and a particle size ranging from 20-2000 nm, said process consisting essentially of the following steps in the following sequence:

First, providing a rubber latex comprising rubber in the form of particles having an average particle size in a range of from 20-2000 nm. Then, optionally adding a cross-linking agent to said rubber latex to form rubber latex composition and irradiating the rubber latex composition to cross-linking of the rubber with formation of particulate rubber having a gel content of at least 60% by weight. Finally, drying the irradiation rubber latex composition and obtaining the vulcanized rubber powder.

The irradiation carried out by high energy source such as gamma rays, X-rays, UV rays, and high energy electron beam. Irradiation dose is in the range of 1 to 300 kGy. The inlet and outlet temperature of spray dryer were in range of 100 to 200 °C and 20 to 80 °C. The spray dryer has an inlet temperature from 100 to 200 °C and outlet temperature from 20 - 80 °C.

The rubber latexes that is selected in this research consisting of natural rubber latex, styrene-butadiene rubber latex, carboxylated styrene-butadiene rubber latex, nitrile rubber latex, carboxylated nitrile rubber latex, chloroprene rubber latex, polybutadiene rubber latex, , acrylic rubber latex, butadiene-styrene-vinylpyridine rubber latex, isoprene rubber latex, butyl rubber latex, ethylene-propylene rubber latex, urethane rubber latex, and fluorine rubber latex.

Abadchi *et al.* (2014) [10] have prepared and characterized polybutadiene rubber (BR) powder by irradiating of rubber latices using Co-60 radiation and spray-drying at the appropriate condition. Morphology, size and size distribution of rubber particles were determined by using scanning electron microscopy (SEM) and laser particle size analyzer (LPSA) technique, respectively.

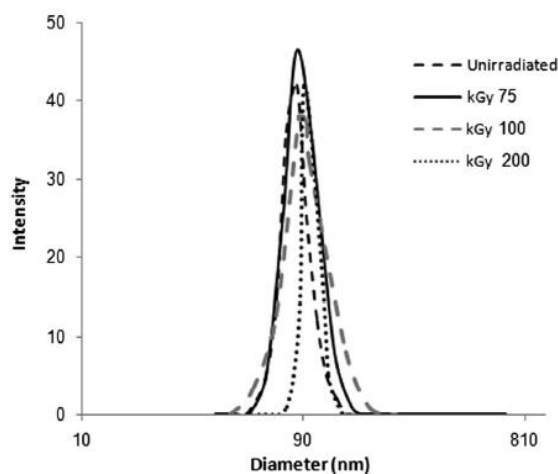


Figure 3.1 Particle size distribution of rubber latex prepared at different radiation doses [10].

The particle size and size distribution of rubber powder at different radiation doses, which was determined by a laser particle size analyzer, are shown in Figure 3.1.

As shown in this figure, mean particle size of un-irradiated rubber latex is about 87 nm. Additionally, the radiation crosslinking of rubber latexes has no significantly effect on mean particle size. However, a narrower particle size distribution is observed for the particles that irradiated in dose range of 200 kGy.

Morphology of the irradiated spray-dried rubber latexes prepared at 200 and 75 kGy are shown in Figure 3.2. In these figures, irradiated rubber powder particles are observed in spherical shape with very smooth surfaces, and the diameter size of the particles are in the range of 90 to 500 nm. However, many of the particles have a diameter of about 100 nm. These FE-SEM micrographs also show that latex particles aggregation during spray drying process cannot be prevented completely by the radiation process especially for the sample irradiated at lower dose. As an instance, for the sample irradiated at 75 kGy (Fig. 3.2b) because of the incomplete atomization, the yield of the spray drying process is low, and particles tend to stick to the walls of the chamber and therefore cannot be collected.

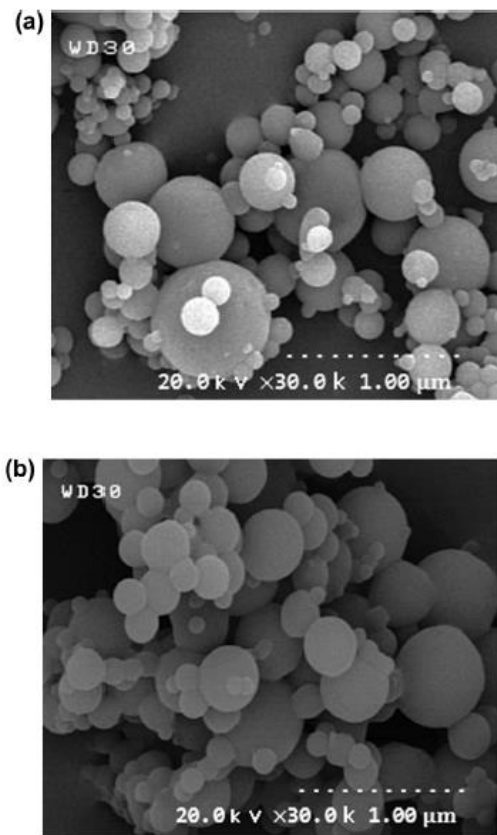


Figure 3. 2 FE-SEM micrographs of spray dried rubber latexes prepared in radiation dose of: (a) 200 kGy, (b) 75 kGy [10].

The influences of absorbed dose on the volume swelling ratio, molecular weight between crosslinks, gel fraction, and glass transition temperature of obtained powder were studied. The gel content and swelling ratio (Q) of BR rubber powders prepared at different radiation doses are shown in Figure 3.3 and the molecular weight between crosslinks (M_c), and crosslink density (CLD) of the powders are shown in Figure 3.4.

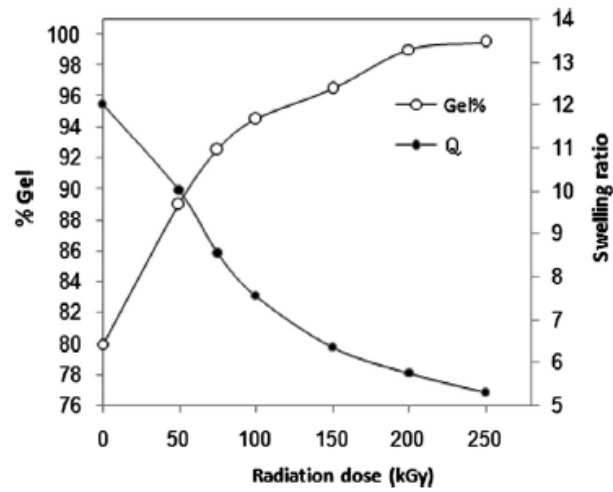


Figure 3.3 The gel content and swelling ratio (Q) of different rubber powders versus radiation dose [10].

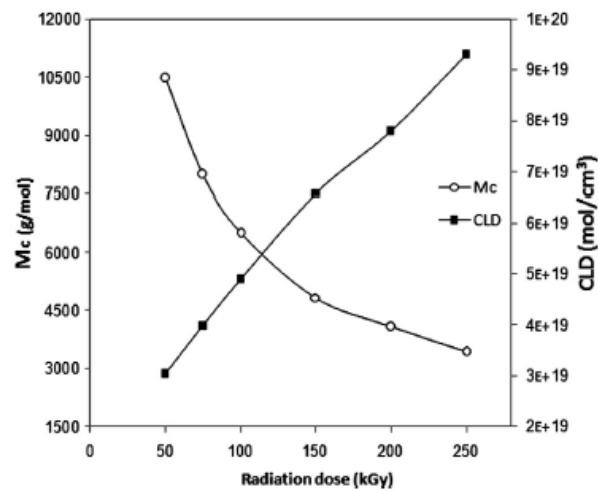


Figure 3.4 Effect of radiation dose on the molecular weight between crosslinks (M_c) and crosslink density (CLD) [10].

They can be seen that the gel fraction and crosslink density (CLD) of rubber powders, increased with increasing absorbed dose, whereas the swelling ratio (Q) and molecular weight between crosslinks (M_c), decreased. Crosslinking density increasing in the whole dose range studied can be attributed to further increase in intermolecular

radical–radical combinations and other rearrangements and indicates predominantly crosslinking behavior of BR rubber powders on irradiation process. It is well known that the main effect of the interactions of gamma rays with rubbers is the formation of free radicals, whose further evolution can cause chain crosslinking, chain branching and/or chain scission.

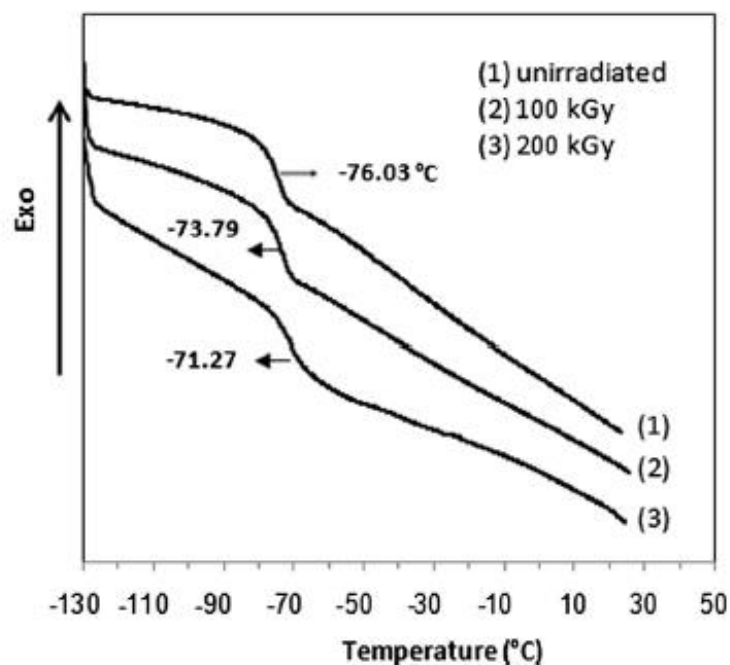


Figure 3.5 DSC thermograms of the rubber powders irradiated at (1) unirradiated, (2) 100 kGy, (3) 200 kGy [10].

The effect of the radiation on the glass transition temperature (T_g) of unirradiated and irradiated polybutadiene rubber was subjected to DSC analysis. In Figure 3.5, the thermograms shows the T_g of un-irradiated BR is -76.03°C and irradiating, dependent on the irradiation dose, causes an increase in T_g ; higher dosage results in a

higher T_g . This rise in T_g is due to the reduction in rubber chain movement resulting from increasing in both intra-molecular as well as inter-molecular crosslinks within the BR rubber chains, leading to a three dimensional network structure.

Fourier transform infrared spectroscopy of rubber powders confirmed that an increasing of the irradiation dose affect to the characteristic peak that corresponds to the C=C double bands decreased. The FTIR spectra for the rubber powder prepared at different radiation doses are shown in Figure. 3.6.

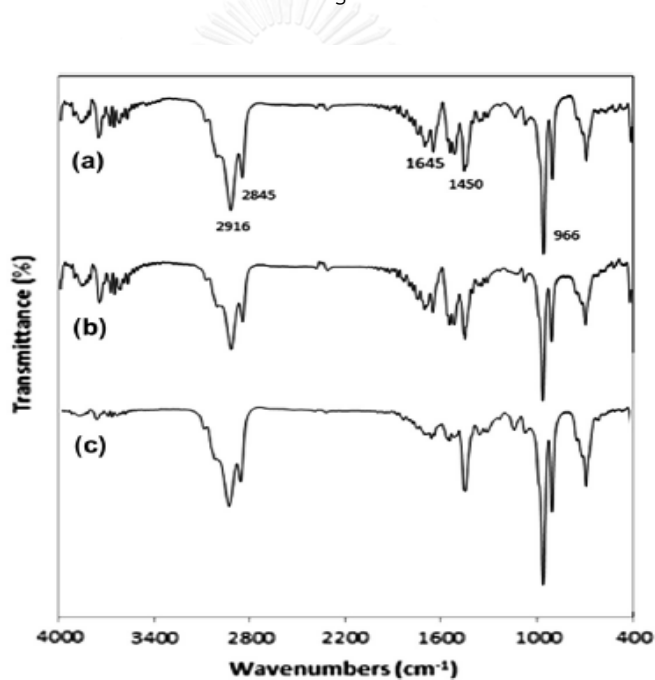
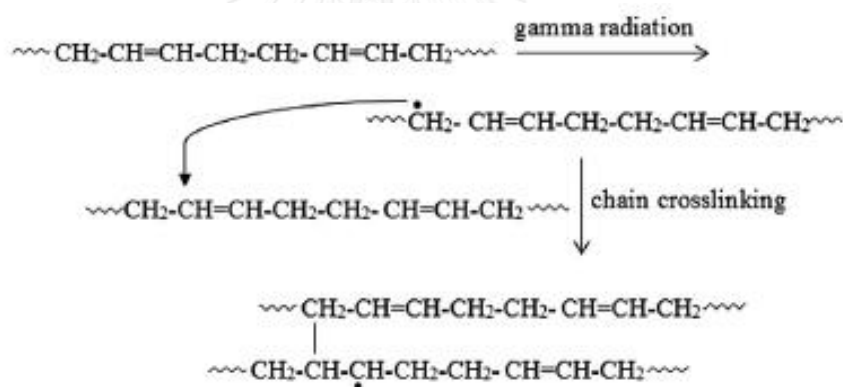


Figure 3. 6 FT-IR spectrums of rubber powder prepared at different radiation doses: (a) 75 kGy, (b) 100 kGy, (c) 200 kGy [10].

In this figure the peak at 1645 cm^{-1} indicates presence of C=C unsaturated sites in chemical structure of rubber powder. Also peaks located in the region from 2916 to 2845 cm^{-1} is correspond to -C-H stretching, peaks around 966 cm^{-1}

corresponds to C–C stretching, and peak at 1450 cm^{-1} , denotes $-\text{CH}_2$ in-plane deformation. This figure confirmed that with increasing of absorbed dose, the intensity of the double-bond peak at 1645 cm^{-1} , tend to disappear as the radiation dosage is increased, and CH_2 deformation band at 1450 cm^{-1} and C–C stretching at around 966 cm^{-1} show a sharp increase in the spectra of irradiated rubber latexes. This indicates the occurrence of radical formation on the butadiene chains and more crosslinking of the samples at higher doses. Initiation of crosslinking reaction takes place with the radical formation at the butadiene chain as mentioned in Scheme 3.1.



Scheme 3.1 Proposed mechanism of crosslinking in polybutadiene chain [10].

P. Sae-Oui *et al* (2010) [5] have prepared thermoplastic natural rubber (TPNR) that was carried out by blending high density polyethylene (HDPE) with natural rubber powder (NRP) obtained from spray drying of pre-vulcanized natural rubber latex. The natural rubber powder (NRP) obtained from the spray drying technique is a fine, light yellowish powder. Figure. 3.7 represents SEM micrographs of the NRP at different

magnifications. At relatively low magnification ($\times 1,000$), it can be observed that the particles of NRP are spherical in shape and have relatively large particle size distribution, i.e., the particle size ranges from 1 to 100 μm . At higher magnification ($\times 10,000$), it could be observed that these particles have a relatively rough surface and are partially interconnected.

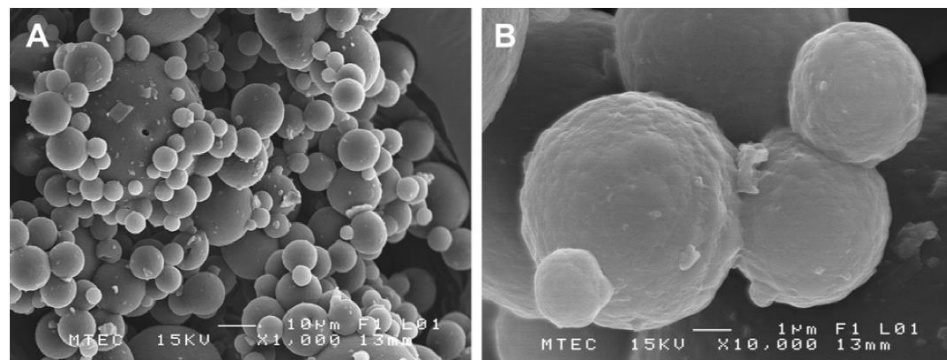


Figure 3.7 SEM micrographs of the NRP at different magnifications (a) $\times 1,000$ and (b) $\times 10,000$ [5].

M. Tian *et al.* (2006) [18] have studied about UFPR/thermoplastics blends. It have been made with good and balanced properties due to the fine dispersion and full vulcanization of rubber phase. If these cross-linked rubber particles with extremely small sizes were blended with other rubbers, the obtained rubber blend would exhibit some advantages that are very promising for some rubber products, compared with traditional rubber blends.

TEM micrographs of UFSBRPR/EPDM blends are shown in Figure 3.8. In these TEM micrographs, the deep gray dispersed phase is UFSBRPR, the light gray continuous

phase is EPDM, and the very dark parts are the inorganic fillers as separator to prevent UFPR from aggregating when drying UFPR, whose sizes and types are different depending on the type of UFPR.

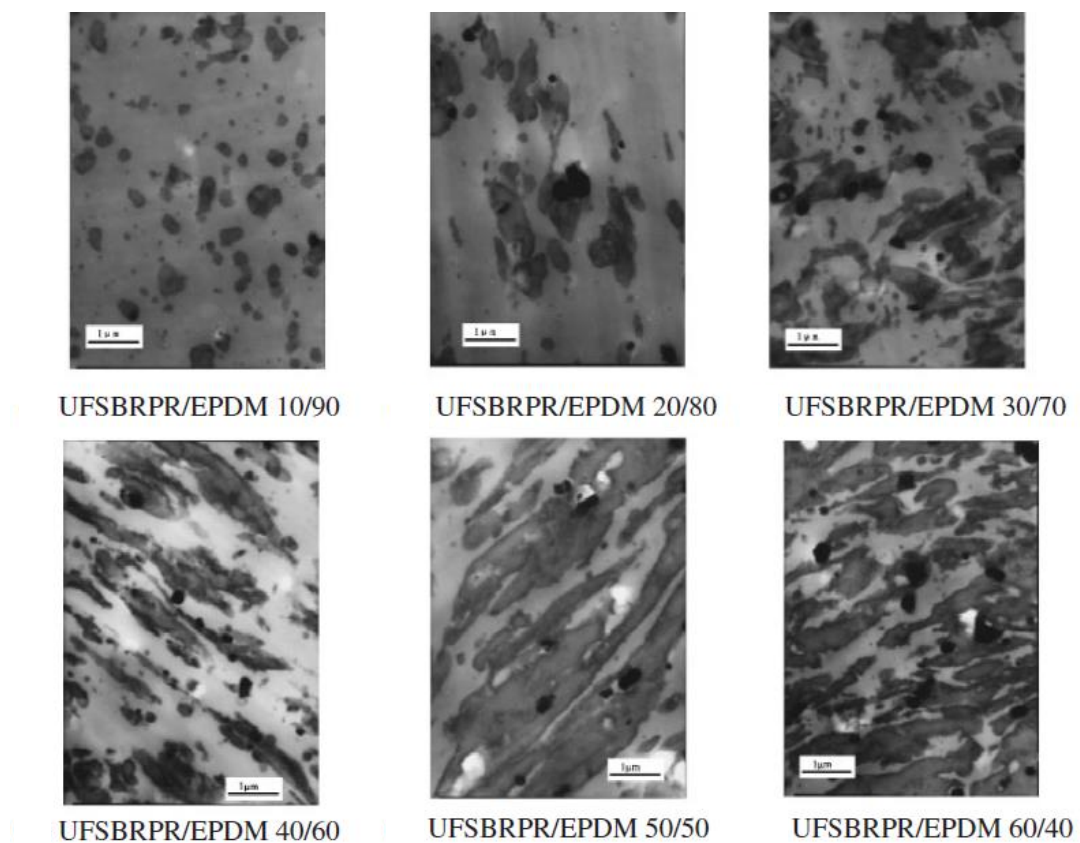


Figure 3.8 TEM images of UFSBRPR/EPDM blends [18].

UFSBRPR/EPDM blends, clearly present that all the blends exhibit the typical “sea-island” morphology under investigated range of blend ratio of UFSBRPR to EPDM. No phase reverse is observed even when the blend ratio of UFSBRPR to EPDM reaches 60/40. It is also found that when the blend ratio of UFSBRPR/EPDM is 10/90, UFSBRPR is finely and uniformly dispersed in EPDM as spherical particles with the size close to

its original particle size, about 200 nm. However, as the blend ratio of UFSBRPR to EPDM increases, the UFSBRPR particles start to agglomerate. Correspondingly, the size of dispersion becomes larger and larger, and the shape of dispersion evolves into strip from sphere.

UFPR has been vulcanized before being incorporated into rubber, so that the dispersion behavior of them should be somewhat similar to that of inorganic fillers. In this type system, the filler-filler interaction and filler-rubber interaction predominate the dispersion and aggregation of UFPR besides the processing parameters, filler characteristics, and loading of filler. There might be three mainly reasons for this phenomenon [18].

Compared with the inorganic fine particles, the filler-filler interaction of UFPR is stronger because of the entanglement of those rubber macromolecules with free segments located in surface regions of UFPR.

The lower modulus and good deformability of UFPR particles also impair dispersing because the higher shear force around UFPR particles agglomerations could not be generated according to traditional stress transfer theory. These two reasons are disadvantageous of dispersion of UFPR in rubber matrix. The filler-rubber interaction (i.e., the compatibility between UFPR and matrix rubber) is still essential for the morphology of this kind blends.

S. Mitra et al (2010) [27] have prepared crosslinked natural rubber (NR) gels by curing NR latex with EB irradiation over a range of doses from 2.5 to 20 kGy using butyl acrylate as sensitizer. The NR gels were systematically characterized by solvent swelling, dynamic light scattering, mechanical and dynamic mechanical properties. These gels were introduced in virgin NR and styrene butadiene rubber (SBR) matrices. From Table 3.1, addition of the gels improved the mechanical and dynamic mechanical properties of NR and SBR considerably.

Table 3.1 Different types of gels and their properties [27].

Gel type	Gel Content (%)	Crosslink density $\times 10^5$ (gmoL/cc)	Gel size (Z_{avg} dia.) (nm)	Tensile strength (MPa)	Elongation at break (%)	Young's modulus (MPa)	T_g ($^{\circ}$ C)
NB _{2.5}	72.9	0.18	360	5.60 \pm 0.17	1340 \pm 20	0.88 \pm 0.03	-55.2
NB ₅	82.5	0.35	290	6.10 \pm 0.18	1300 \pm 20	0.97 \pm 0.03	-54.5
NB ₁₀	89.6	0.86	310	7.90 \pm 0.20	1270 \pm 20	1.07 \pm 0.04	-53.4
NB ₁₅	93.0	1.42	320	9.40 \pm 0.25	1250 \pm 20	1.21 \pm 0.04	-52.6
NB ₂₀	94.1	1.55	300	9.70 \pm 0.28	1220 \pm 20	1.40 \pm 0.04	-50.8

Note: The butyl acrylate - sensitized NR latex gel was given NB_x designation, where x denotes the radiation dose in kGy.

Both the gel content and crosslink density increase with the increase in radiation dose, up to about 15 kGy. The increase in gel content and crosslink density with the increase in radiation dose is due to the formation of a three- dimensional network structure. The dynamic light scattering (DLS) studies give an idea about the particle size of the EB-irradiated latex gels. The particle sizes (Z_{avg} diameter) of the

gelled latex are in the range 290 to 360 nm. The Z_{avg} diameter of the virgin NR latex is 220 nm. It is apparent that on irradiation, the gel size increases. However, the significant increase in gel size is not only because of the crosslinking reaction taking place inside the latex particles, but also due to the partial coalescence of the gel particles under high-energy radiation due to damage of the protective protein layer surrounding the NR latex.

And in this table also summarizes the tensile properties of various EB cross-linked latex gels used in this study. It is quite clear that the tensile strength (TS) of the various gelled rubbers increases steadily with an increase in crosslink density. The virgin NR used in this study has TS of 1.86 MPa with an elongation at break (ϵ_b) value of 1400%. The TS increases many fold after EB crosslinking and is about 9.70 MPa in NB₂₀, whereas ϵ_b value decreases to 1220%. The increase in TS and reduction in eb values in cross-linked gels are related to the introduction of greater number of C-C interchain crosslinks initiated by the butyl acrylate in presence of EB radiation.

The effect of EB crosslinking is also very pronounced on the dynamic mechanical properties of different NR gels as compared to their virgin counterpart NR. With increase in EB dose, the $\tan\delta$ peak maxima (considered as T_g here) shifts toward higher temperature (Table 3.1). It is worth mentioning here that the virgin NR has a T_g of about -56.1 °C. Hence, considerable increase in T_g with the introduction of EB crosslinking in the rubber matrix can be observed. For example, in NB₂₀, T_g shifts by

more than +5.1 °C compared to NR. The increase in T_g with the progressive increase in electron beam dose (from 2.5 to 20 kGy) is attributed to the restriction imposed on the chain movement due to the crosslinking, as there is lesser number of free chains available at glassy to rubbery transition.

Ahmed *et al.* (2000) [28] have compared about thermal stabilities of NBR and SBR vulcanizates cured by different curing agents namely sulfur, peroxide and gamma radiation was performed by thermogravimetric analysis (TGA), assessed on the basis of comparison of DTG peak maxima and temperature for loss of 50% mass.

Table 3.2 Comparison of thermal stabilities of radiation-cured vulcanizates of SBR and NBR with sulfur and peroxide-cured counterparts [28].

Rubber type	DTG peak due to elastomer, T_{max} (°C)	Temperature for onset of degradation (°C)
Sulfur-cured vulcanizates (150°C,30 min)		
SBR	474	444
NBR	480	274
Peroxide-cured vulcanizates (160°C,60 min)		
SBR	481	313
NBR	475	300
Radiation-cured vulcanizates (ambient,11 kGy/h)		
SBR	532	480
NBR	522	445

As seen in Table 3.2, improvement in thermal stability, as demonstrated by slight increase in DTG peak maxima, was observed in case of SBR. In case of NBR, a decline in thermal stability was observed. The results showed that when compared with their sulfur-cured and peroxide-cured, radiation-cured formulations demonstrated much higher thermal stability both in case of SBR and NBR.

H. Fan *et al* (2005) [6] have studied about elastomeric nano-particles (ENP) toughened epoxy resin. Comparison of pure epoxy resin and epoxy toughened with CTBN, the composites of epoxy resin/ ENP have both higher toughness and heat resistance as shown in Table 3.3. The ENP was prepared by mixing the carboxylic nitrile-butadiene rubber latex with 5 phr crosslinking agent trimethylol propane triacrylate (TMPTA). That latex was irradiated for 25 KGy by γ ray and then spray dried. The ENP used in the study have an average size of less than 100 nm.

Table 3.3 Properties of the toughened epoxy network with ENP and CTBN [6]

Sample	Izod impact strength (KJ·m ⁻²)	Flexural strength (MPa)	Flexural modulus (GPa)	HDT (°C)
Pure epoxy network	11.4	102	3.18	113.2
Toughened by CTBN	15.9	86.6	2.66	107.6
Toughened by ENP	22.3	81.4	2.76	114.4

Note: Epoxy resin(E-44): 100 phr; MeTHPA: 75 phr; rubber: 12 phr; triethanolamine: 1.5 phr.

When rubber content was 12 phr, the Izod impact strength of epoxy network toughened by carboxylic nitrile-butadiene ENP can be increased by 96 percent, compared with CTBN being increased by only 39 percent (Table 3.3) at room temperature. However the heat distortion temperature (HDT) of CTBN/epoxy composite was decreased by 5.6 °C, but the VP501/epoxy composite's HDT was increased by 1.2°C.

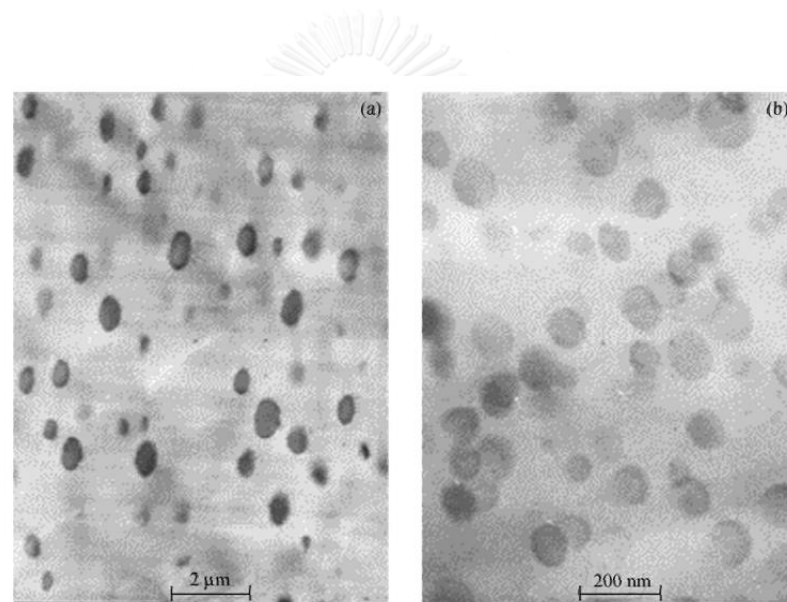


Figure 3.9 TEM image of the epoxy network toughened with rubber. (a) CTBN; (b) carboxylic nitrile-butadiene ENP [6].

CTBN was dissolved in epoxy resin before curing and the particles of CTBN were formed in epoxy matrix during curing. Therefore curing condition and process had great effect on the particle size of CTBN. Usually its particle size was over 500 nm and distribution was wide (Figure. 3.9(a)). But ENP particle formation was irrelevant to curing

condition and process. Its particle size in epoxy matrix was no more than 100 nm and distribution was narrow, Figure. 3.9(b). Difference in dispersion morphology of the two toughening agents and resultant difference in interface property were the reasons that differentiated ENP/epoxy composite with better properties.



CHAPTER IV

EXPERIMENTAL

4.1 Materials

The materials were used in this research are benzoxazine resin, natural rubber (NR), carboxylated styrene butadiene rubber (SBR), carboxylated acrylonitrile butadiene rubber (NBR) and toluene. Benzoxazine resin is based on bisphenol-A (polycarbonate grade) that supplied by PTT Phenol Co., Ltd. (TPCC), aniline (AR grade) that was obtained from Panreac Quimica SA Company and para-formaldehyde (AR grade) that was purchased from Merck Company. Natural rubber (NR) latex was purchased from Suksapanpanit. Carboxylated nitrile rubber (NBR) latex was supported by Bangkok Synthetics Co., Ltd, Thailand. Carboxylated styrene butadiene rubber (SBR) latex was supplied by Dow Chemical (Thailand), Ltd., and toluene (AR grade) was purchased from RCI Labscan Co., Ltd, Thailand. Trimethylol propane trimethacrylate (TMPTMA) that used as an accelerator for NR latex that was supported by Chemi Innovation Co., Ltd.

4.2 Benzoxazine resin preparation

The benzoxazine resin used is based on bisphenol-A, aniline and formaldehyde in the mole ratio of 1:4:2. The resin was synthesized by using a patented solventless method in the U.S. Patent 5,543,516 [29]. The obtained benzoxazine monomer is clear-yellowish powder at room temperature and can be molten to yield a low viscosity

resin about 70 °C to 80°C. The product was then ground to fine powder and kept in a refrigerator for future-use.

4.3 Preparation of Ultrafine Rubbers

The Co-60 gamma radiation (Gamma Chamber GC5000 from BRIT, India) was used to irradiate three types of rubber latices at ambient temperature with accumulated radiation doses at 10, 30, 50, 100, 150, 200, and 250 kGy and a dose rate of 4.02 kGy/h. After that, both un-irradiated and irradiated rubber latices were dried by a spray drying (Buchi Mini Spray Dryer model B-190 from BUCHI, Switzerland) with the inlet temperature in a range of 100°C to 180°C to achieve the ultrafine rubbers in bottom product.

4.4 Preparation of Ultrafine Rubbers-modified Polybenzoxazine Composites

The PBA-a/UFPR composites containing 15 phr of UFPR were prepared to yield molding compounds. The UFPRs were manually mixed with benzoxazine resin at a temperature of 110°C. The compounds were then compression-molded by hot pressing at 200°C for 3 h under a hydraulic pressure of 15 MPa. The fully-cured samples were air-cooled to room temperature in an open mold before characterizations.

The ultrafine rubber-modified polybenzoxazine composites were designated as PBA-a/UFPNR for ultrafine natural rubber, PBA-a/UFPSBR for ultrafine styrene butadiene rubber, and PBA-a/UFNBR for ultrafine nitrile rubber, respectively.

4.5 Characterization Methods

4.6.1 Swelling Measurements

The transparent film of un-irradiated and irradiated rubber latex that cast on glass plates at ambient temperature were prepared for evaluate swelling properties and gel content. The weight of dried latex film (W_1) was carefully measured immersing in toluene ($\rho_s = 0.87 \text{ g/cm}^3$, $V_1 = 106.4 \text{ mL/mol}$) for 24 h. After that, the swollen rubber latex film was immediately weighed (W_2). The swollen film was then dried in a vacuum oven for 24 h at 70°C to remove the solvent and then it was weighed again (W_3). The swelling ratio (Q), molecular weight between crosslinks (M_c), crosslink density (CLD) and gel fraction (g) were calculated by using the following equations (Flory- Rehner equation) [30, 31];

$$Q = \frac{(W_2 - W_1) / \rho_s}{W_1 / \rho_r} \quad (4.1)$$

$$M_c = \frac{-\rho_r V_1 (\varphi_r^{\frac{1}{3}} - \varphi_r)}{\ln(1 - \varphi_r) + \varphi_r + \chi_{12} \varphi_r^2} \quad (4.2)$$

$$\text{Where; } \varphi_r = \frac{1}{1 + Q}$$

$$CLD = \frac{\rho_r N}{M_c} \quad (4.3)$$

$$g = \frac{W_3}{W_1} \quad (4.4)$$

where W_1 , W_2 and W_3 are the weights of initial, swollen and dried samples, respectively, ρ_s and ρ_r are the densities of solvent (0.87 g/cm^3 of toluene) and rubber,

ϕ_r is the volume fraction of polymer in the swollen sample, V_1 is the molar volume of the toluene solvent (106.4 mL/mol), χ_{12} is the polymer–solvent interaction parameter and N is Avogadro's number.

4.6.2 Differential Scanning Calorimetry

Glass transition temperature (T_g) of the samples was measured by a differential scanning calorimeter (model DSC1 Module) from Mettler-Toledo. The sample mass of dried latex film was used in a range of 5 to 10 mg. The samples were cooled from 25°C to -100°C by liquid nitrogen at a cooling rate of 10 °C/min under nitrogen atmosphere. The temperature was constantly kept at -100°C about 2 min. The sample was then reheated from -100°C to 25°C at the same heating rate to provide DSC thermograms.

4.6.3 Thermogravimetric Analysis

Degradation temperature at 5% weight loss of the rubber samples was evaluated by using a thermogravimetric analyzer (model TGA1 Module) from Mettler-Toledo (Thailand). The initial mass of all samples were about 10 mg. The samples were scanned from 25°C to 850°C with a heating rate of 20°C/min under nitrogen atmosphere at a N_2 purge gas flow rate of 50 mL/min.

4.6.4 Fourier transform infrared spectroscopy (FT-IR)

Fourier transform infrared spectroscopy was carried out with a Spectrum GX FTIR spectrometer from Perkin Elmer to investigate the presence of double bonds and other functional groups on the rubber latices before and after gamma irradiation. The spectrum was reported in a region of 400 to 4000 cm^{-1} and was averaged from 128 scans at a spectral resolution of 4 cm^{-1} .

4.6.5 Morphology of UFPRs

Scanning electron microscopy (SEM) was performed by using a Jeol JSM-6400, scanning electron microscope with the accelerating voltage of 10 kV. The UFPRs were coated with thin gold using a JEOL ion sputtering device (model JFC-1200) for 4 min and then subjected to SEM observation.

4.6.6 Particle Size and Size Distribution of UFPRs

Laser diffraction particle size analyzer (Mastersizer, Malvern Instruments, UK) was used to characterize particle size and size distribution of UFPRs in distilled water diluted emulsion. The Mastersizer 3000 uses the technique of laser diffraction to measure the size of particles. It does this by measuring the intensity of light scattered as a laser beam passes through a dispersed particulate sample. This data is then analyzed to calculate the size of the particles that created the scattering pattern [32].

4.6.7 Mechanical Properties of UFPRs filled Polybenzoxazine Composites (Flexural Mode)

The mechanical properties of the composites such as flexural strength and flexural modulus were performed on universal testing machine (Instron Co., Ltd model 5567) based on ISO178:2010. The measurement was carried out in a three-point bending mode, with a supporting span of 32 mm and a crosshead speed of 10 mm/min. The average values of five samples at least with a dimension of rectangular specimen was 10 mm × 50 mm × 2 mm were determined.

The flexural strength and flexural modulus based on ISO178:2010 were calculated by following equations;

$$E_f = \frac{L^3 m}{4bd^3}$$

$$\sigma_f = \frac{3PL}{2bd^2}$$

Where; E_f = Flexural modulus, GPa

σ_f = Flexural strength, MPa

L = Supporting span, mm

m = Slope of the initial straight-line portion of the load

deflection

b = Width of the specimen, mm

d = Depth of the specimen, mm

P = Load at a given point on the load deflection curve, N

4.6.8 Impact Resistance of UFPRs filled Polybenzoxazine Composites

Impact strength of UFPRs filled in polybenzoxazine (PBA-a/UFPRs) composites was investigated by a pendulum impact tester (Zwick Testing Machines Ltd.) with izod mode following by ASTM D256. The energy lost that required to break the sample as the pendulum continues on its path was measured from the distance of its follow through. Impact resistance is the ability of a material to withstand a high force or shock applied to it over a short period of time. Izod impact testing is an ASTM standard method for determining the impact resistance of materials. A pivoting arm was raised to a specific height with constant potential energy and then released. The arm swings down and hits the sample. The energy absorbed by the sample can be calculated from the height of the arm swings to after hitting the sample. The Izod impact test differs from the Charpy impact test in that the sample was held in a cantilevered beam configuration as opposed to a three-point bending configuration [33].

CHAPTER V

RESULTS AND DISCUSSION

5.1 Characterization of Properties of Un-irradiated and Irradiated Rubber Latices

5.1.1 Solubility and Swelling Behavior of Un-irradiated and Irradiated Rubber Latices

Swelling behavior of polymer is an important parameter for deciding the polymer-solvent compatibility during polymer applications. The swelling measurement of rubber latices shows the ability of rubber to resist the solubility by solvent. Swelling ratio is the consequence of the interaction between solvent and polymer matrix to define the change of dimensions of crosslinked polymer. The highly crosslinked polymer provides a less degree of swelling. Figure 5.1 shows effect of gamma radiation dose on swelling ratio of un-irradiated and irradiated rubber latices after immersed in solvent i.e. toluene for 24 h. The swelling ratio of all samples was calculated based on Equation 4.1. The swelling ratio of natural rubber (NR) latex were determined to be 7.35 ± 0.23 of un-irradiated, 4.97 ± 0.15 , 4.73 ± 0.14 , 4.49 ± 0.16 , 4.29 ± 0.19 and 4.09 ± 0.11 of irradiated NR latex with gamma radiation doses of 50, 100, 150, 200 and 250 kGy, respectively. The values of SBR latex decreased from 4.83 ± 0.14 of un-irradiated to 2.41 ± 0.14 , 2.16 ± 0.11 , 2.02 ± 0.18 , 1.72 ± 0.14 and 1.62 ± 0.13 at the same gamma irradiation doses to NR latex. The values of NBR latex was 6.51 ± 0.30 of un-irradiated NBR latex and decreased to 3.34 ± 0.24 , 2.94 ± 0.21 , 2.72 ± 0.38 , 2.51 ± 0.33 and 2.35 ± 0.16 with gamma radiation doses of 50, 100, 150, 200 and 250 kGy, respectively.. It can be seen that the values of swelling ratio of SBR and NBR latices were similarly to NR latex.

An increasing of gamma radiation doses resulted in a decrease in the values of swelling ratio of irradiated rubber latices as a result of a formation of crosslinked structure. This phenomenon was due to the strong interaction in rubber chain after gamma radiation, leading in the higher solvent resistance of irradiated rubber latices compared with un-irradiated rubber latices. A solvent resistance of rubber latices refers to the ability of rubber chain to retain its important physical properties especially crosslink density of the rubber. Among these three types of rubber latices, SBR showed the highest solvent resistant that was owing to higher crosslinking ability of SBR than that of NR and NBR as shown in Figure 5.4.

Additionally, the values of gel fraction that express as the fraction of insoluble weight to initial weight of rubber at different gamma radiation doses were characterized as shown in Figure 5.2. The result showed that the gel fraction of rubber increased from 0.53 ± 0.04 for un-irradiated NR latex to 0.76 ± 0.04 , 0.80 ± 0.02 , 0.86 ± 0.02 , 0.93 ± 0.02 and 0.93 ± 0.02 with increasing gamma doses of 50, 100, 150, 200 and 250 kGy, respectively. The gel fraction of SBR latex showed similar trend to NR which was found to increase from 0.61 ± 0.02 for un-irradiated SBR to 0.83 ± 0.01 , 0.88 ± 0.02 , 0.96 ± 0.02 , 0.98 ± 0.02 and 0.99 ± 0.01 for increasing gamma doses to 50, 100, 150, 200 and 250 kGy, respectively. Meanwhile, the value of un-irradiated NBR latex was measured to be 0.59 ± 0.05 and the values of irradiated NBR latex were 0.81 ± 0.02 , 0.85 ± 0.02 , 0.92 ± 0.01 , 0.96 ± 0.03 , and 0.97 ± 0.01 with gamma doses of 50, 100, 150, 200 and 250 kGy, respectively. It can be seen that gel fraction of all rubber latices increased

with increasing gamma radiation dose which was due to the formation of a three-dimensional network structure. The results of gel fraction of rubber after radiation were similarly reported by Abachi *et al.* [10] who studied the effect of gamma radiation doses in the range of 50 to 250 kGy on gel fraction of polybutadiene rubber.

Molecular weight between crosslink (M_c) of un-irradiated rubber latices which can be calculated from Equation 4.2 was shown in Figure 5.3 The M_c of un-irradiated NR latex was $23,322 \pm 1,472$ g/mol and the M_c s of irradiated NR were $10,723 \pm 272$, $9,756 \pm 591$, $8,873 \pm 652$, $7,894 \pm 776$ and $7,231 \pm 398$ g/mol at irradiation dose of 50, 100, 150, 200 and 250 kGy, respectively. The M_c values of SBR latex were measured to be $3,974 \pm 411$, $1,257 \pm 226$, $1,071 \pm 164$, 968 ± 237 , 756 ± 159 and 681 ± 32 g/mol for gamma doses of 0, 50, 100, 150, 200 and 250 kGy, respectively. The M_c values of NBR were $10,785 \pm 924$, $2,808 \pm 406$, $2,273 \pm 323$, $1,890 \pm 561$, $1,661 \pm 449$, and $1,540 \pm 199$ g/mol for gamma doses of 0, 50, 100, 150, 200 and 250 kGy, respectively. The M_c of three types of rubber tended to decrease with an increasing of gamma doses and showed the same behavior as swelling ratio value. It was due to less soluble part in irradiated rubber than un-irradiated rubber latices resulting in the high crosslink density and solvent resistance of irradiated rubber latices.

Figure 5.4 shows the crosslink density of rubber latex which can be calculated by Equation 4.3. Crosslink density of un-irradiated NR latex was $2.37(\pm 0.15) \times 10^{19}$ mol/cm³. The values of irradiated NR latices were $5.15(\pm 0.14) \times 10^{19}$, $5.66(\pm 0.34) \times 10^{19}$, $6.23(\pm 0.46) \times 10^{19}$, $7.00(\pm 0.64) \times 10^{19}$ and $7.64(\pm 0.40) \times 10^{19}$ mol/cm³ at doses of

gamma ray of 50, 100, 150, 200 and 250 kGy, respectively. The values of crosslink density of SBR latices were calculated to be $1.49(\pm 0.56) \times 10^{20}$, $4.72(\pm 3.65) \times 10^{20}$, $5.54(\pm 4.07) \times 10^{20}$, $6.13(\pm 7.47) \times 10^{20}$, $7.84(\pm 8.64) \times 10^{20}$ and $8.71(\pm 2.15) \times 10^{20} \text{ mol/cm}^3$ at doses of gamma ray of 50, 100, 150, 200 and 250 kGy, respectively.. The crosslink density values of NBR latices were $5.57(\pm 0.48) \times 10^{19}$, $2.14(\pm 3.19) \times 10^{20}$, $2.64(\pm 3.80) \times 10^{20}$, $3.18(\pm 8.49) \times 10^{20}$, $3.62(\pm 8.92) \times 10^{20}$ and $3.90(\pm 5.13) \times 10^{20} \text{ mol/cm}^3$ at doses of gamma ray of 0,50, 100, 150, 200 and 250 kGy, respectively. As seen in Figure 5.4, crosslink density of all rubber latices increased with increasing radiation dose. It was due to the successfully crosslinking of the three types of rubber latices that form more three-dimensional network structure as a result of an increasing the radiation doses. It is prominent that the main effect of the interactions of gamma rays with rubbers is the formation of free radicals, whose further evolution can cause chain crosslinking, chain branching and/or chain scission [10].

Yields of chain crosslinking and scission are determined according to Charlesby–Pinner Equation as shown in Equation 5.1 [34]. .

$$s + s^{0.5} = \frac{p}{q} + \left(\frac{1}{qu_1} \right) \left(\frac{1}{D} \right) \quad (5.1)$$

Where, s is soluble fraction ($s = 1 - \text{gel fraction}$)

p is the scission density per unit dose

q is the crosslinking density

D is the radiation dose in kGy

u_1 is the number average degree of polymerization

The ratio of chain scission to crosslinking (p/q) can be obtained from the intercept value of the extrapolated straight line of the relationship between $s + s^{0.5}$ and $1/D$ as shown in Figure 5.5. The random radiation crosslinking generates a linear data set when $s + s^{0.5}$ was plotted against $1/D$.

In Figure 5.5 the radiation crosslinking (or radiation vulcanization) of rubber latices follows the Charlesby-Pinner equation in the gamma radiation dose up to 150 kGy. The intercept (p/q) values of NR, SBR and NBR latex were 0.392, 0.119 and 0.241, respectively. The lower value of p/q indicates a greater crosslinking rather than chain scission [10]. From the result, SBR showed the less p/q value suggesting that SBR had greater crosslinking than the NBR and NR, respectively. This shows that not only crosslinking reaction is predominant and radiation-crosslinking reaction of rubber chains proceeds easily through intermolecular reactions, but also that crosslinking occurs randomly [35]. The crosslinked chains restricted the motion of macroradicals and the main chain backbone of polymer may break into small fragments or small clusters of crosslinked polymer chains. Each of the fragments contain a number of polymer molecules that crosslinks at lower radiation doses [10, 36]. Thus, there was a competition reaction between crosslink formation and chain scission at lower doses of irradiation and the reverse trend was observed at higher doses of irradiation [36].

5.1.2 Glass Transition Temperature of Rubber Latices

Glass transition temperatures (T_g s) of un-irradiated and irradiated rubber latices at various gamma radiation doses were investigated by non-isothermal differential scanning calorimetry as shown in Figure 5.6. The T_g s of un-irradiated rubber latices were -65.4°C for NR latex, -27.2°C for SBR latex and -25.5°C for NBR latex. The T_g s of the irradiated NR latex were investigated to be -64.9 , -64.1 , -63.6 , -62.9 and -62.6°C at 50, 100, 150, 200 and 250 kGy of gamma irradiation doses, respectively. The T_g values of irradiated SBR latices were determined to be -26.6 , -25.4 , -24.8 , -24.3 and -22.8°C at gamma irradiation doses of 50, 100, 150, 200 and 250 kGy, respectively. Whereas, The T_g s of NBR latices were measured to be -24.3 , -23.5 , -22.1 , -21.5 and -21.0°C at gamma irradiation doses of 50, 100, 150, 200 and 250 kGy, respectively. The results illustrated that an increase in irradiation dose resulting in an increasing of T_g for all three types of rubber latices. An enhancement of T_g of the rubber latices was due to the gamma crosslinking in the rubber chains leading to the reduction in rubber chain movement and a formation of a three dimensional network structure [10, 27]. Furthermore, it can be observed that T_g s of SBR and NBR were higher than that of NR because these rubbers were the copolymers that a movement of the structure was more difficult than NR structure. Among three types of rubber, NBR latex was found to be the most enhancement of T_g (18%) due to gamma radiation suggesting this rubber was the most sensitivity to vulcanization by gamma radiation. This result was consistent

with crosslink density of this rubber which showed the most enhanced in value due to gamma irradiation as seen in Figure 5.4.

5.1.3 Thermal Stability of Rubber Latices

Thermal stability of rubber lattices was considered by degradation temperature at 5 % weight loss (T_{d5}) of rubber lattices as exhibited in Figure 5.7. The T_{d5} s of NR latex improved from 334°C for the un-irradiated NR latex to 336, 337, 337, 338 and 338 °C of irradiated NR lattices at gamma irradiation doses of 50, 100, 150, 200 and 250 kGy, respectively. The T_{d5} s of the SBR lattices were observed to be 363, 369, 376, 377, 378 and 378°C at gamma doses of 0, 50, 100, 150, 200 and 250 kGy, respectively. For NBR lattices, the T_{d5} value was 380°C for un-irradiated NBR latex and were 381, 384, 386, 387 and 388°C for gamma radiation doses of 50, 100, 150, 200 and 250 kGy, respectively. The reason of an increment in thermal stability of irradiated rubber latex was the higher crosslinking structure led to the need of higher activation energy than un-irradiated rubber latex to thermally decompose the irradiated rubber [37].

5.1.4 Spectroscopic Property of Rubber Latices

FT-IR spectroscopy is used to verify the chemical change produced by gamma irradiation in un-irradiated and irradiated rubber lattices. Figure 5.8 (a) shows spectrum of un-irradiated NR latex which exhibited the characteristic peak at 836 cm^{-1}

attributed to the CH out-of-plane bending of cis-1,4 addition [38] that presence in disappearance of intensity with increasing gamma dose to 100 and 200 kGy. The bands of 2962 and 2854 cm^{-1} were attributed to CH_3 and CH_2 asymmetric and symmetric stretching [39-41], respectively. Additionally, a peak at 1662 cm^{-1} indicated the presence of C=C unsaturated sites in chemical structure of rubber [38-41]. After gamma vulcanization, FTIR spectra of irradiated NR latex were also observed. The spectra of irradiated NR latex exhibits similar characteristic peaks with un-irradiated NR latex. But absorbance intensities of this vulcanized rubber were shown in difference. In this case, the intensity of 1662 cm^{-1} band decreased because of the broken chains of C=C in rubber and its change to formation of C-C bonding that presence in 970 cm^{-1} for crosslinking network in rubber structure.

In addition, Figure 5.9 shows FTIR spectra of un-irradiated and irradiated SBR latex at gamma radiation doses of 100 kGy and 200 kGy, respectively. In this figure, the characteristic peaks at 2920 and 2846 cm^{-1} attributed to the CH stretching of aromatic rings and the peak at 1600 cm^{-1} presented the stretching vibration of the CH_2 and CH_3 [42]. In the other peaks at 910 and 759 cm^{-1} were attributed to trans 1,4 structure (γ -CH) of the single substituted benzene ring and the CH out-of-plane deformation, respectively [42]. Moreover, the absorbance band at 1493 cm^{-1} was featured to in-plane scissor vibration of CH_2 linking aromatic ring and band in the range of 820 – 660 cm^{-1} were indicated to aromatic-H out-of-plane bending vibration [43] that tended to disappear with increasing gamma irradiation dose. This phenomenon

might be due to the benzene ring of styrene unit was formed crosslinking reaction with other units both of styrene and butadiene as similarly reported by Barrera *et al.* [44] that have studied polystyrene-SBR blends. From their results, the most important change of the benzene ring in polystyrene was meta-substituted with polybutadiene chains of SBR at high gamma irradiation dose due to the crosslinking effect.

The spectra of un-irradiated and irradiated NBR latex were observed as seen in Figure 5.10. The characteristic peak at 2238 cm^{-1} was attributed to nitrile ($\text{C}\equiv\text{N}$) stretching [45] that absence in intensity with increasing gamma absorbed dose. The disappearance of peaks at 2924 and 2849 cm^{-1} in the rubber latex corresponds to the C-H stretching vibration of CH_2 groups in the rubber back bone [46]. The disappearance of peak at 969 cm^{-1} corresponded to the stretching of butadiene double bond of NBR latex that confirmed by a decrease in unsaturated rubber structure during gamma vulcanization. Figure 5.10 (b) and 5.10 (c) show a decrease of peak at 1449 cm^{-1} corresponding to CH in-plane deformation of methylene group and peaks at 1698 and 1731 cm^{-1} indicated to carbonyl stretching vibration of H-bonded COOH group and carbonyl stretching of monocarboxylic acid stretching in carbonyl compound [47]. These peaks were indicated to a reduction of carbonyl terminate group in NBR latex from gamma vulcanization. On the other hand, an increment of peak intensity at 738 cm^{-1} that featured to C-C bonding in irradiated NBR latex that confirmed by a formation of three-dimensional network structure in rubber chains.

5.2 Characterization of Properties of Ultrafine Rubber

5.2.1 Morphology of UFPRs

After the first step of gamma vulcanization, the rubber latices were dried by a spray dryer without any additional treatment. The spray dried conditions included inlet temperature in the range of 100 to 160°C, hot air flow in the range of 6.7 to 17.4 L/h and rubber feed in the range of 0.57 to 1.40 mL/h. The UFPRs with different gamma radiation doses were obtained from spray dried irradiated rubber latices. The SEM micrographs of UFPSBR, UFPNBR and UFPNR were shown in Figure 5.11, 5.12 and 5.13, respectively. For un-irradiated rubbers, agglomerated and tackiness particles were observed in the obtained UFPNBR and UFPNR as seen in Figures 5.12(a) and 5.13(a). . Figures 5.11(a) to 5.11(f) illustrate un-irradiated and irradiated UFPSBR particles. The irradiated UFPSBR showed smaller particle size than un-irradiated UFPSBR. Moreover, spherical shape with very smooth surface of irradiated UFPSBR was noticed at the high doses of gamma radiation. For UFPNBR and UFPNR, the samples gained from irradiated rubber at low gamma dose illustrated gather particles and spherical aspect. However, these SEM micrographs also showed latex particles aggregation of these samples with a lower radiation dose. This behavior was also reported by Abadchi *et al.* [10] that have studied gamma irradiation of polybutadiene latex. They found the formation of aggregated polybutadiene particles after 75 kGy of gamma irradiation dose.

5.2.2 Particle Size of UFPRs

Particle sizes of UFPRs were detected by the laser diffraction particle size analyzer. However, particle size of UFPNR and un-irradiated UFPNBR cannot determine by this method due to the agglomerated particle cannot separate and distribute in water. Figure 5.14 shows the particle size of UFPSBR and UFPNBR at various gamma radiation doses. The average particles size of UFPSBR were determined to be 586, 186, 59, 40, and 21 μm with gamma radiation doses of 0, 100, 150, 200 and 250 kGy, respectively. The particle size of UFPNBR were 1430, 756, 163 and 27 μm for 100, 150, 200 and 250 kGy of gamma radiation doses, respectively. As a result, an increase of gamma dose led to a decrease in particle size for both UFPSBR and UFPNBR.

5.2.3 Swelling Properties of UFPRs

The swelling behaviors of UFPRs including swelling ratio, gel fraction, molecular weight between crosslink and crosslink density were also characterized as presented in Figure 5.15, 5.16, 5.17 and 5.18, respectively.

Swelling ratio of all UFPRs was studied by the same method with latices sample. For UFPNR particles, the swelling ratio of un-irradiated UFPNR was 1.93 ± 0.05 whereas the swelling ratio values of irradiated UFPNR were measured to be 1.92 ± 0.03 , 1.88 ± 0.02 , 1.82 ± 0.05 , 1.80 ± 0.04 and 1.76 ± 0.03 at gamma irradiation doses of 50, 100, 150, 200 and 250 kGy, respectively. In addition, the swelling ratio of UFPSBR was calculated to be 1.65 ± 0.04 , 1.62 ± 0.03 , 1.59 ± 0.04 , 1.54 ± 0.04 , 1.45 ± 0.03 and 1.37 ± 0.04

at gamma irradiation doses of 0, 50, 100, 150, 200 and 250 kGy, respectively. For UFPNBR system, the values were 1.85 ± 0.03 , 1.76 ± 0.02 , 1.68 ± 0.04 , 1.61 ± 0.04 , 1.57 ± 0.03 and 1.46 ± 0.03 at gamma irradiation doses of 0, 50, 100, 150, 200 and 250 kGy, respectively. The swelling ratio of all UFPRs was found to decrease with increasing gamma irradiation dose. The results were in good agreement with rubber latices system. Furthermore, it can be observed that swelling ratio of all rubbers was improved after spray drying process. It probably because the thermal energy stimulated rubber latex to generate more crosslink structure by the remained free radicals from gamma irradiation that led in improved the swelling properties of UFPRs. In the other word, the soluble part in all UFPRs was decreased. According to this reason, other swelling properties such as gel fraction, molecular weight between crosslink and the most important factor i.e. crosslink density were also improved via spray drying process.

An enhancement of gamma irradiation dose affected to the increasing of the gel fraction and crosslink density of all UFPRs as shown in Figure 5.16. The gel fraction of UFPNR was increased from 0.892 ± 0.007 of un-irradiated UFPNR to 0.988 ± 0.001 , 0.989 ± 0.009 , 0.996 ± 0.008 , 0.997 ± 0.006 and 0.998 ± 0.006 with an increase of gamma irradiation doses of 0, 50, 100, 150, 200 and 250 kGy, respectively. In addition, gel fraction of UFPSBR and UFPNBR exhibited similar trend with UFPNR. The gel fraction of values UFPSBR were 0.863 ± 0.005 , 0.985 ± 0.004 , 0.986 ± 0.010 , 0.989 ± 0.007 , 0.993 ± 0.005 and 0.998 ± 0.005 at gamma irradiation doses of 0, 50, 100, 150, 200 and 250 kGy, respectively. Gel fraction of UFPNBR were measured to be 0.887 ± 0.006 , 0.978 ± 0.003 ,

0.989±0.005, 0.991±0.006, 0.994±0.011 and 0.997±0.007 at gamma irradiation doses of 0, 50, 100, 150, 200 and 250 kGy, respectively.

Molecular weight between crosslink of all UFPRs were determined as seen in Figure 5.17. M_c of un-irradiated UFPNR was 1921±96.9 g/mol whereas M_c of irradiated UFPNR were measured to be 1909±62.5, 1834±40.9, 1726±72.7, 1684±63.1 and 1609±51.0 g/mol at gamma irradiation doses of 50, 100, 150, 200 and 250 kGy, respectively. The M_c of UFPSBR were found to be 1213±44.5 g/mol for un-irradiated UFPSBR and 1174±33.5, 1132±42.9, 1070±45.3, 968±39.9 and 884±43.7 g/mol for irradiated UFPSBR at gamma irradiation doses of 50, 100, 150, 200 and 250 kGy, respectively.. The molecular weight between crosslink of UFPNBR were 1298±41.5, 1186±28.4, 1094±43.0, 1026±38.5, 981±26.5 and 870±34.6 g/mol at gamma irradiation doses of 0, 50, 100, 150, 200 and 250 kGy, respectively.

Additionally, the crosslink density of all three types of rubber was presented in Figure 5.19. The crosslink density of UFPNR were found to be $2.88(\pm 0.149) \times 10^{20}$ mol/cm³, $2.89(\pm 0.102) \times 10^{20}$, $3.01(\pm 0.068) \times 10^{20}$, $3.20(\pm 0.130) \times 10^{20}$, $3.28(\pm 0.119) \times 10^{20}$ and $3.43(\pm 0.111) \times 10^{20}$ mol/cm³ at gamma irradiation doses of 0, 50, 100, 150, 200 and 250 kGy, respectively. For UFPSBR rubber, the values of un-irradiated UFPSBR was $4.89(\pm 0.179) \times 10^{20}$ mol/cm³ and the values of irradiated UFPSBR were $5.05(\pm 0.019) \times 10^{20}$, $5.24(\pm 0.201) \times 10^{20}$, $5.54(\pm 0.232) \times 10^{20}$, $6.12(\pm 0.250) \times 10^{20}$ and $6.71(\pm 0.326) \times 10^{20}$ mol/cm³ at gamma irradiation doses of 0, 50, 100, 150, 200 and 250 kGy, respectively. Whereas the crosslink density of UFPNBR was increased from 4.63 ± 0.148 mol/cm³ of

un-irradiated UFPNBR to $5.06(\pm 0.122) \times 10^{20}$, $5.74(\pm 0.242) \times 10^{20}$, $5.86(\pm 0.216) \times 10^{20}$, $6.08(\pm 0.167) \times 10^{20}$ and $6.18(\pm 0.276) \times 10^{20}$ mol/cm³ for irradiated UFPNBR at the same gamma doses with UFPNR and UFPSBR. The molecular weight between crosslink of all rubbers was tended to decrease with increasing gamma irradiation dose. On the other hand, the crosslink density increased due to an increasing of crosslinked network. This phenomenon was a similar trend with latex form and can be observed in the irradiated polybutadiene rubber powder [10] and irradiated acrylonitrile-butadiene rubber [48].

5.2.4 Thermal Properties of UFPRs: Glass Transition Temperature and Thermal Stability

Glass transition temperature (T_g) was determined by a differential scanning calorimeter (DSC) as shown in Figure 5.19. The effect of gamma radiation at various doses on T_g of all UFPRs was evaluated. The T_g s of each un-irradiated UFPRs were -61.8, -25.5, and -24.7°C for UFPNR, UFPSBR and UFPNBR, respectively. The T_g values of irradiated UFPNR were found to be -61.6, -61.3, -61.8, -61.7 and -60.8°C while the T_g s of irradiated UFPSBR were measured to be -23.8, -23.4, -23.1, -22.5 and -21.6°C and the T_g s of irradiated UFPNBR were -23.3, -21.9, -21.8, -20.9 and -20.1°C at gamma irradiation doses at 50, 100, 150, 200 and 250 kGy, respectively. It could be observed that the T_g s of all UFPRs were increased with increasing the gamma radiation dose. Hence, considerable increase in T_g with the introduction of gamma crosslinking in the rubber can be observed. UFPSBR irradiated at 250 kGy, T_g shifts by more than +3.9°C compared to un-irradiated UFPSBR. The increase in T_g with the progressive increase in gamma

radiation dose (from 50 to 250 kGy) is attributed to the restriction imposed on the chain movement due to the crosslinking, as there are lesser number of free chains available at glassy to rubbery transition.

The thermal stability of UFPRs was measured by a thermogravimetric analyzer. The T_{d5} s of UFPNR were found to be 330, 333, 335, 337, 338 and 340°C for gamma irradiation doses at 0, 50, 100, 150, 200 and 250 kGy, respectively. At the same gamma doses, the values of T_{d5} of UFPSBR were 360, 368, 374, 376, 379 and 381°C whereas the T_{d5} values of UFPNBR were 377, 378, 379, 380, 382 and 383°C. It can be observed that thermal stability of all UFPRs increased with increasing of gamma irradiation dose due to the high three-dimensional network structure in irradiated UFPRs. Moreover, the enhancement of thermal stability of radiation cross-linked was due to the formation of C-C networks between the main chains that lead to high activation energy for degradation. This can be ascribed in terms of the nature of the networks; the C-C linkages formed during radiation vulcanization are less flexible and having high bond energy [49].

5.3 Characterization of Ultrafine Rubber Filled Polybenzoxazine Composites

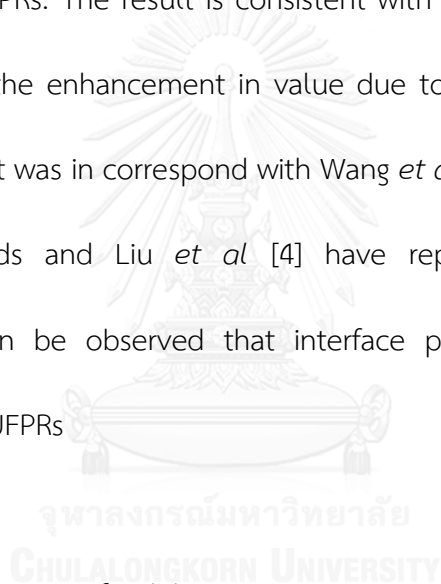
Ultrafine fully vulcanized powdered rubbers (UFPRs) has attracted much attention as a new type of toughening modifier that has many potential for polymers [16]. Polybenzoxazine is a new kind of phenolic resin that shows outstanding properties, i.e. high thermal stability, high glass transition temperature, low water

absorption, good adhesive properties, good mechanical strength and modulus [50]. However, polybenzoxazine network has low toughness and resistance of impact due to their highly crosslinked structure. This network structure leads to brittle behavior and causes the polymers to suffer from relatively poor resistance to crack initiation and growth. Therefore, a significant improvement in the toughness of polybenzoxazine by the addition of liquid rubbers has been previously reported [51]. Hence, we interested to study the effect of un-irradiated and irradiated UFPRs on thermal and mechanical properties including impact resistance of UFPRs filled polybenzoxazine (PBA-a/UFPRs).

5.3.1 Thermal Properties of Benzoxazine Resin (BA-a) Filled with Ultrafine Rubber

Glass transition temperature of PBA-a/UFPRs composites was also determined by a differential scanning calorimetry. The T_g value of the neat PBA-a was 163°C and PBA-a with an addition of un-irradiated UFPNR, UFPSBR and UFPNBR at 15 phr were measured to be 164, 165 and 165°C, respectively. In addition, an increase of gamma irradiation dose for vulcanized all types of UFPRs from 50 to 250 kGy affected to an improvement of the T_g s of the composites. At gamma doses of 50, 100, 150, 200 and 250 kGy, the T_g s for PBA-a/UFPNR composites were determined to be 165, 166, 167, 168 and 169°C, respectively. The T_g s of PBA-a/UFPSBR composites were 166, 167, 168, 169, and 170°C whereas the T_g s of PBA-a/UFPNBR composites were 167, 168, 169, 170 and 172°C with the same gamma doses. It was interesting to know that the rubber

particle can increase the heat resistance of PBA-a/UFPRs composites. The improvement of T_g of the polybenzoxazine with an addition of the UFPRs filler was attributed to a good dispersion of UFPRs in polybenzoxazine matrix thus higher temperature is required to provide the requisite thermal energy for the occurrence of a glass transition in the composites [52]. Furthermore, irradiated UFPRs can be improved the T_g value of composites because UFPRs had higher degree of crosslink than un-irradiated UFPRs. The result is consistent with crosslink density of irradiated UFPRs which shows the enhancement in value due to gamma radiation as seen in Figure 5.18. This result was in correspond with Wang *et al.* [52] that have studied NBR-UFPR/PVC compounds and Liu *et al* [4] have reported SBR-UFPR toughened polypropylene. It can be observed that interface played an important in heat resistance of plastic/UFPRs



5.3.2 Mechanical properties of Polybenzoxazine Composites Filled with Ultrafine Rubber

Mechanical properties of PBA-a/UFPRs composites including flexural strength and flexural modulus were investigated by a universal testing machine using three points bending mode. Figures 5.26 and 5.27 show the plots of flexural strength and flexural modulus of PBA-a/UFPRs composites as a function of gamma radiation doses. The value of flexural strength of the neat PBA-a was determined to be 134 MPa. The flexural strength of PBA-a filled with un-irradiated UFPNR, UFPSBR and UFPNBR were

measured to be 13.2, 25.6 and 37.9 MPa, respectively. A decreasing of the flexural strength of PBA-a/UFPRs composites was due to an addition of the softer rubber fraction in the greater flexural value of the polybenzoxazine. Moreover, the flexural strength values of PBA-a/UFPNR composites with various gamma doses of UFPNR were determined to be 14.8, 16.6, 29.9, 22.9 and 17.4 MPa, at 50, 100, 150, 200 and 250 kGy of gamma irradiation doses, respectively. The values of PBA-a/UFPSBR were determined to be 29.6, 48.1, 55.8, 43.7 and 35.0 MPa at gamma radiation dose of 50, 100, 150, 200 and 250 kGy, respectively. The flexural strength of PBA-a/UFPNBR composites was measured to be 37.9, 38.5, 63.9, 100.9, 68.5 and 53.4 MPa at gamma radiation dose of 50, 100, 150, 200 and 250 kGy, respectively. It was noticed that all of three PBA-a/UFPRs composite systems exhibited the maximum value of flexural strength at the dosage of gamma radiation of rubber at 150 kGy. At the radiation dose of all UFPRs over 150 kGy, the flexural strength decreased, which might be because the chain scission in rubber particle at high doses of gamma radiation was a dominant effect over crosslinking.

The flexural modulus of PBA-a/UFPRs composite was exhibited in Figure 5.27. In PBA-a/UFPNR PBA-a/UFPSBR and PBA-a/UFPNBR composites, the flexural modulus of these composites showed similar behavior with flexural strength that the value increased up to optimum dose of gamma irradiated rubber. For all UFPRs, the values were found to be increase with increasing the adsorbed dose up to 150 kGy. The flexural modulus of the neat polybenzoxazine was found to be 5.76 ± 0.40 GPa and

1.91±0.37, 3.38±0.15 and 3.22±0.20 GPa for PBA-a filled with un-irradiated UFPCR, PBA-a/UFPSBR and PBA-a/UFPNBR, respectively. This behavior could be related to the effect of viscous of rubber with much lower modulus than that of the PBA-a phase [53]. The flexural modulus of PBA-a/UFPCR composites were determined to be 2.36±0.29, 2.39±0.31, 2.49±0.20 2.68±0.30 and 2.39±0.35 GPa with UFPCR at gamma radiation dose of vulcanized NR latex of 50, 100, 150, 200 and 250 kGy, respectively. The flexural modulus of PBA-a/UFPSBR composites was found to be 4.07±0.26, 4.42±0.23, 4.59±0.47, 4.14±0.40 and 3.24±0.30 GPa with UFPSBR at gamma radiation dose of vulcanized SBR latex of 50, 100, 150, 200 and 250 kGy, respectively. For PBA-a/UFPNBR composites, the flexural modulus were evaluated to be 3.54±0.04, 3.93±0.04, 4.83±0.42, 4.36±0.17 and 4.23±0.22 GPa with UFPNBR at gamma radiation dose of vulcanized NBR latex of 50, 100, 150, 200 and 250 kGy, respectively. It can be observed that the flexural modulus of composites increased up to 150 kGy irradiated UFPCRs and then decreased. This result was possibly due to the fact that UFPCRs generates a predominant crosslinking at low irradiation dose. At the radiation dose over 150 kGy, the chain scission had greater effect than crosslinking; therefore, the flexural properties were decreased.

5.3.3 Impact strength of Polybenzoxazine Composites Filled with Ultrafine Rubber

Impact strength of PBA-a/UFPCRs composites was investigated by a pendulum impact tester in izod mode as shown in Figure 5.24. The impact strength value of the

neat PBA-a was 7.2 ± 0.21 kJ/m². Furthermore, the impact strength of PBA-a/UFPNR were 8.0 ± 0.26 , 8.4 ± 0.19 , 12.0 ± 0.32 , 8.3 ± 0.58 , 7.8 ± 0.24 and 7.4 ± 0.45 kJ/m² with UFPNR at gamma radiation dose of vulcanized NR latex of 50, 100, 150, 200 and 250 kGy, respectively. In PBA-a/UFPSBR system, the values were 8.1 ± 0.36 , 9.1 ± 0.29 , 12.5 ± 1.26 , 9.3 ± 0.21 , 8.2 ± 0.46 and 7.5 ± 0.35 kJ/m² with UFPSBR at gamma radiation dose of vulcanized SBR latex of 50, 100, 150, 200 and 250 kGy, respectively. Furthermore, the impact strength of PBA-a/UFPNBR composites were found to be 8.3 ± 0.29 , 9.8 ± 0.25 , 12.9 ± 0.89 , 15.0 ± 0.36 , 18.4 ± 0.59 and 13.4 ± 0.29 kJ/m² with UFPNBR at gamma radiation dose of vulcanized NBR latex of 50, 100, 150, 200 and 250 kGy, respectively. The results revealed that the impact strength of all PBA-a/UFPNRs composites higher than neat polybenzoxazine. According to the brittle characteristic of polybenzoxazine, an addition of soft segments of UFPRs in polybenzoxazine matrix can be increased the absorbed energy and decreased the cracking of the composites. This result was correlated with elastomeric nano-particles toughened epoxy [6, 54] that also shows an improvement of impact resistance. The other results of phenolic toughened by elastomeric [55] that impact strength of the composites were improved from 5.20 kJ/m² to 7.75 and 8.70 kJ/m² for toughened with NBR and carboxylic-NBR nanoparticles. The three types of rubbers showed the optimum gamma irradiation dose of rubber latex which resulted in the highest impact strength of the composites to be 100 kGy for UFPNR (12.0 kJ/m²) and UFPSBR (12.5 kJ/m²), and 200 kGy for UFPNBR (18.4 kJ/m²).

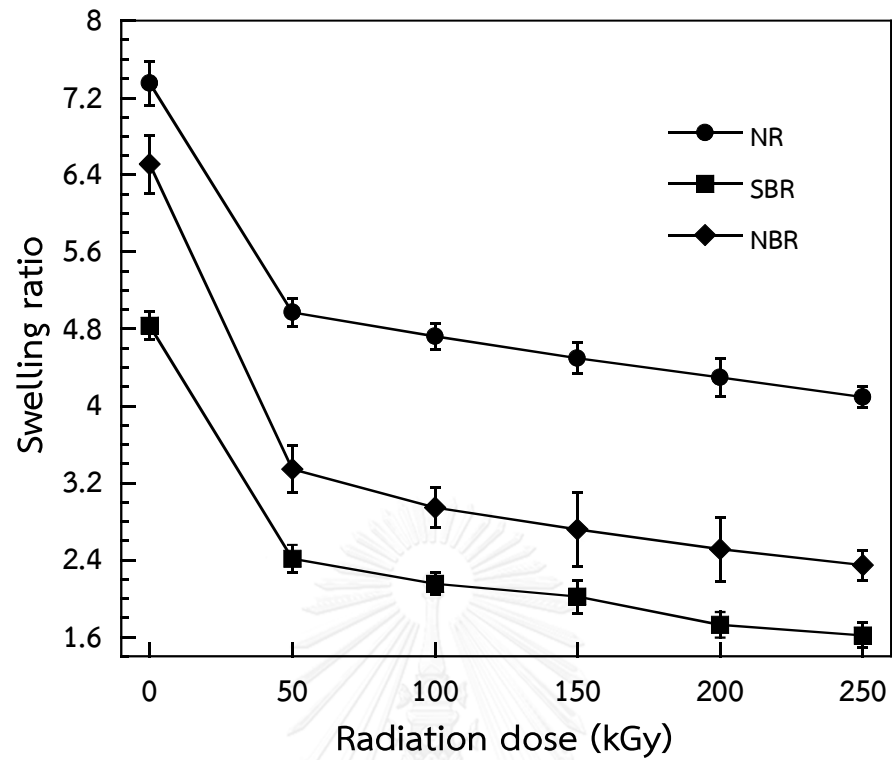


Figure 5.1 Swelling ratio of radiation irradiated rubber latex in toluene solvent at 0, 10, 30, 50, 100, 150, 200 and 250 kGy of gamma radiation doses: (●) rubber latex of NR, (■) rubber latex of SBR and (◆) rubber latex of NBR.

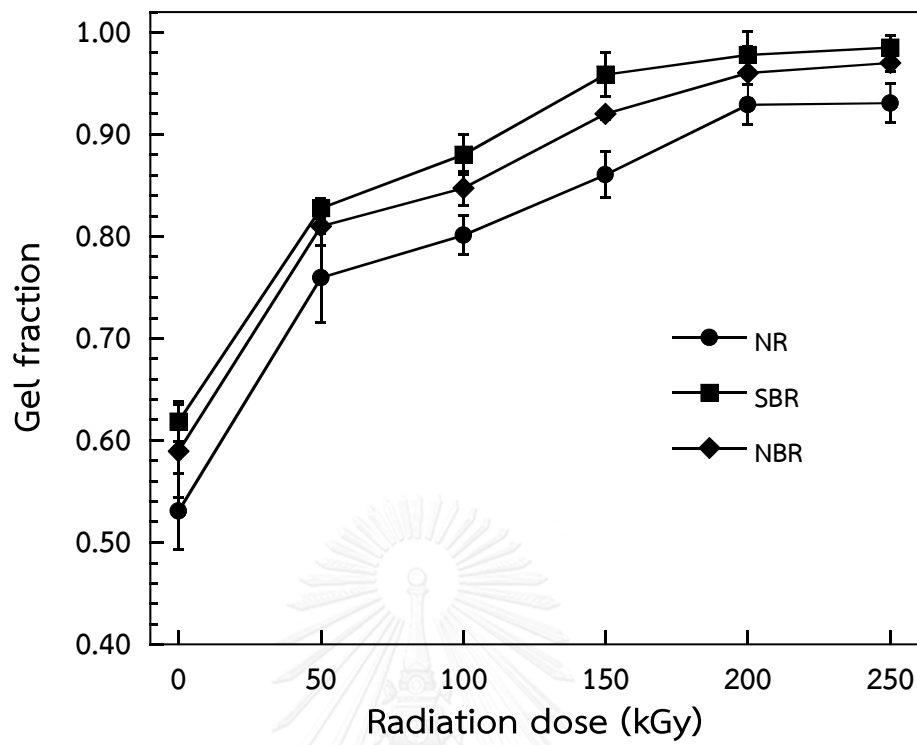


Figure 5.2 Gel fraction of rubber latex at 0, 10, 30, 50, 100, 150, 200 and 250 kGy of gamma radiation doses: (●) rubber latex of NR, (■) rubber latex of SBR and (◆) rubber latex of NBR.

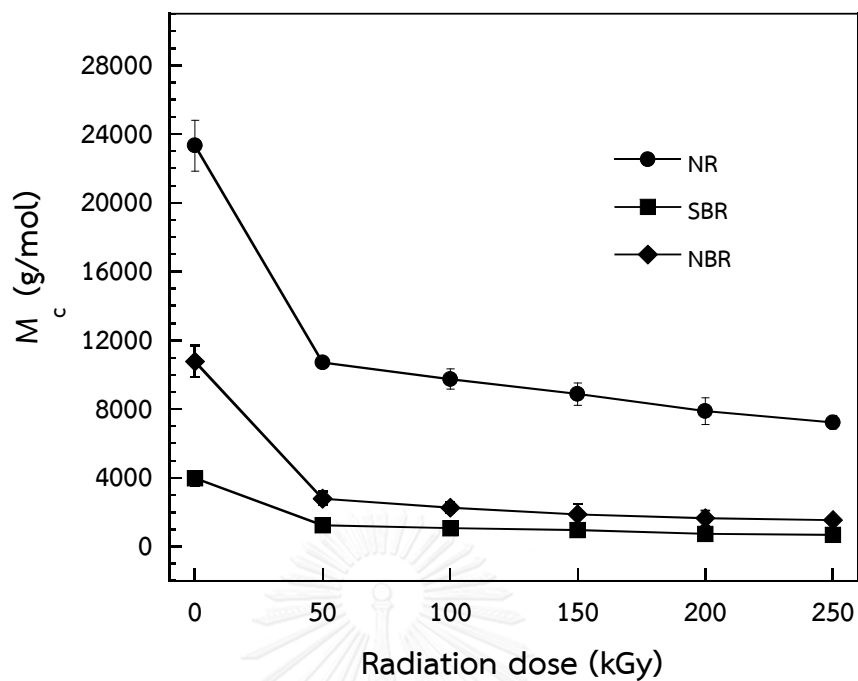


Figure 5.3 Molecular weight between crosslink of rubber latex that irradiated by radiation vulcanization in toluene solvent at 0, 10, 30, 50, 100, 150, 200 and 250 kGy of gamma radiation doses: (●) rubber latex of NR, (■) rubber latex of SBR and (◆) rubber latex of NBR.

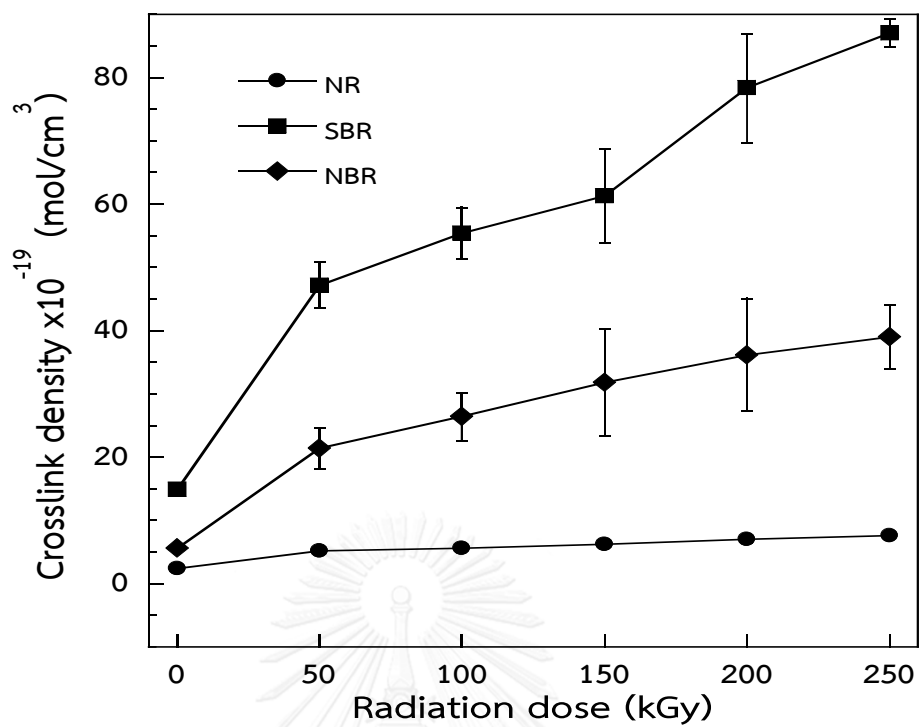


Figure 5.4 Crosslink density of un-irradiated and irradiated rubber latex in toluene solvent at 0, 50, 100, 150, 200 and 250 kGy of gamma radiation doses: (●) rubber latex of NR, (■) rubber latex of SBR and (◆) rubber latex of NBR.

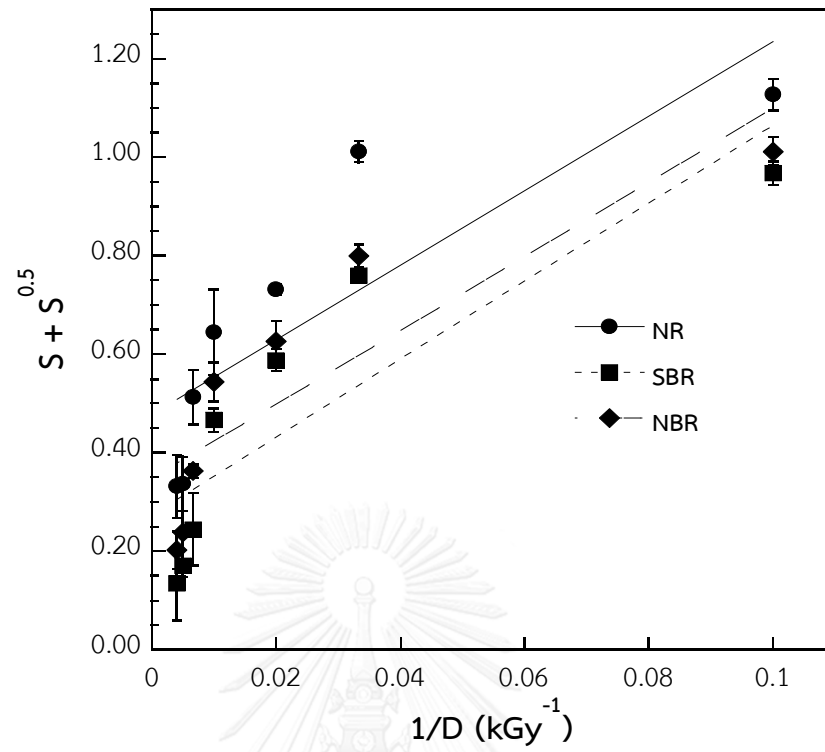


Figure 5.5 Sol-gel analysis of radiation crosslinking of rubber latices by Charlesby-Pinner equation (equation 5-1): (●) rubber latex of NR, (■) rubber latex of SBR and (◆) rubber latex of NBR.

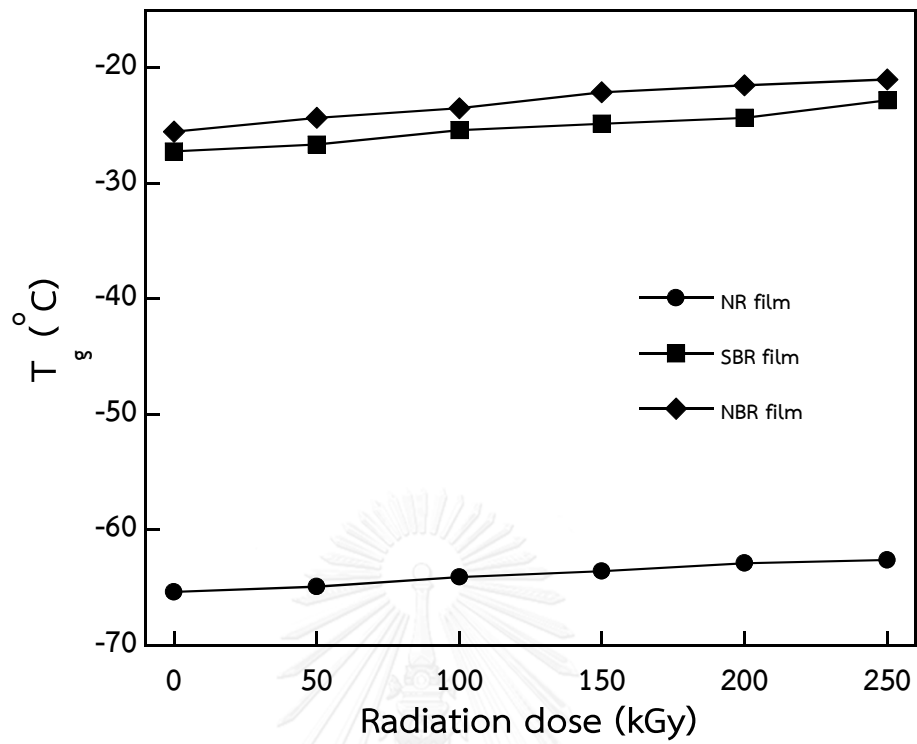


Figure 5.6 Glass transition temperature of rubber latex at 0, 50, 100, 150, 200 and 250 kGy of gamma radiation dose: (●) NR latex, (■) SBR latex and (◆) NBR latex.

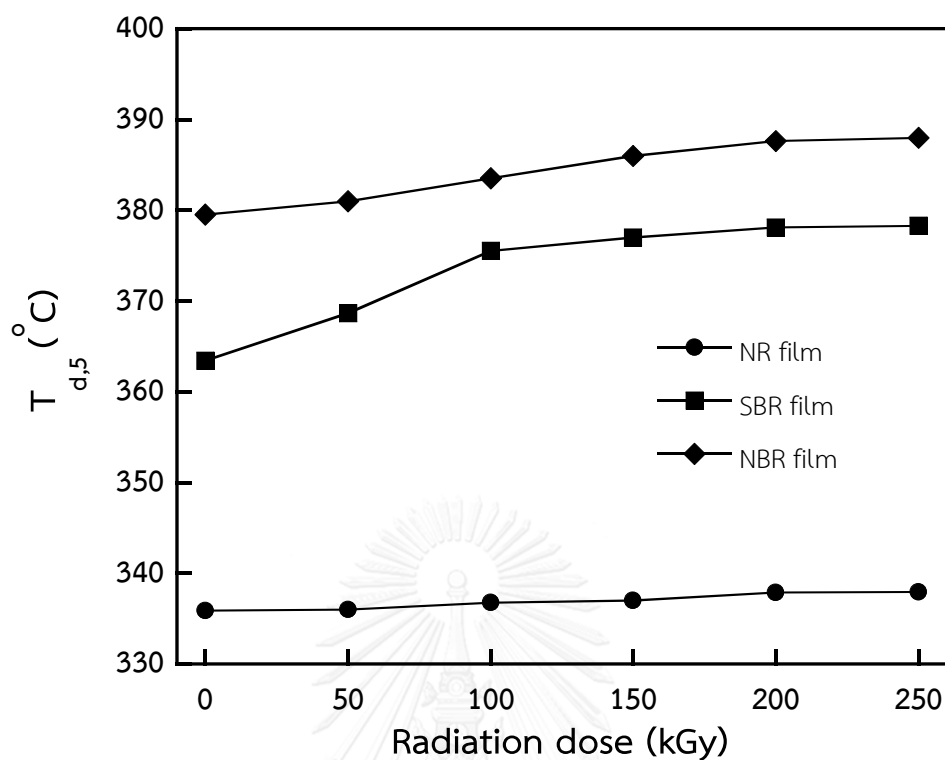


Figure 5.7 Degradation temperature at 5 percent weight loss of rubber latex at 0, 50, 100, 150, 200 and 250 kGy of gamma radiation doses: (●) NR latex, (■) SBR latex and (◆) NBR latex.

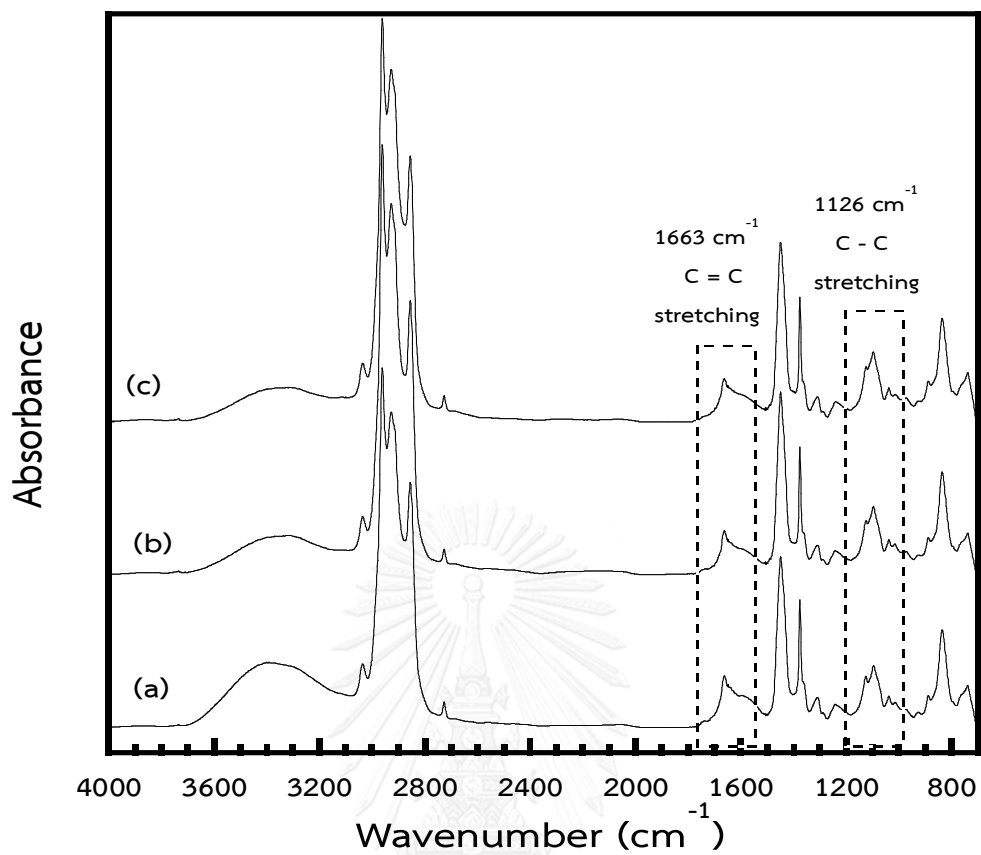


Figure 5.8 FT-IR spectra of (a) un-irradiated NR latex (b) 100 kGy, and (c) 200 kGy of gamma radiation irradiated NR latex.

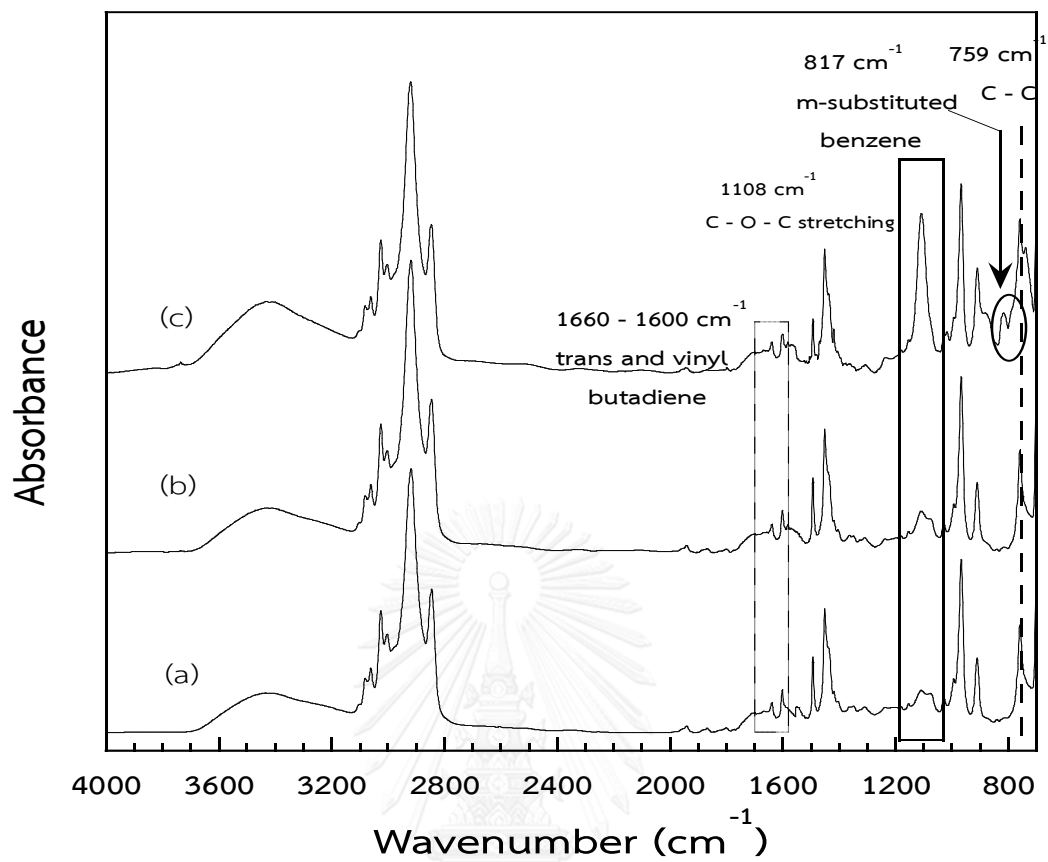


Figure 5.9 FT-IR spectra of (a) un-irradiated SBR latex and (b) 100 kGy, and (c) 200 kGy of gamma radiation irradiated SBR latex.

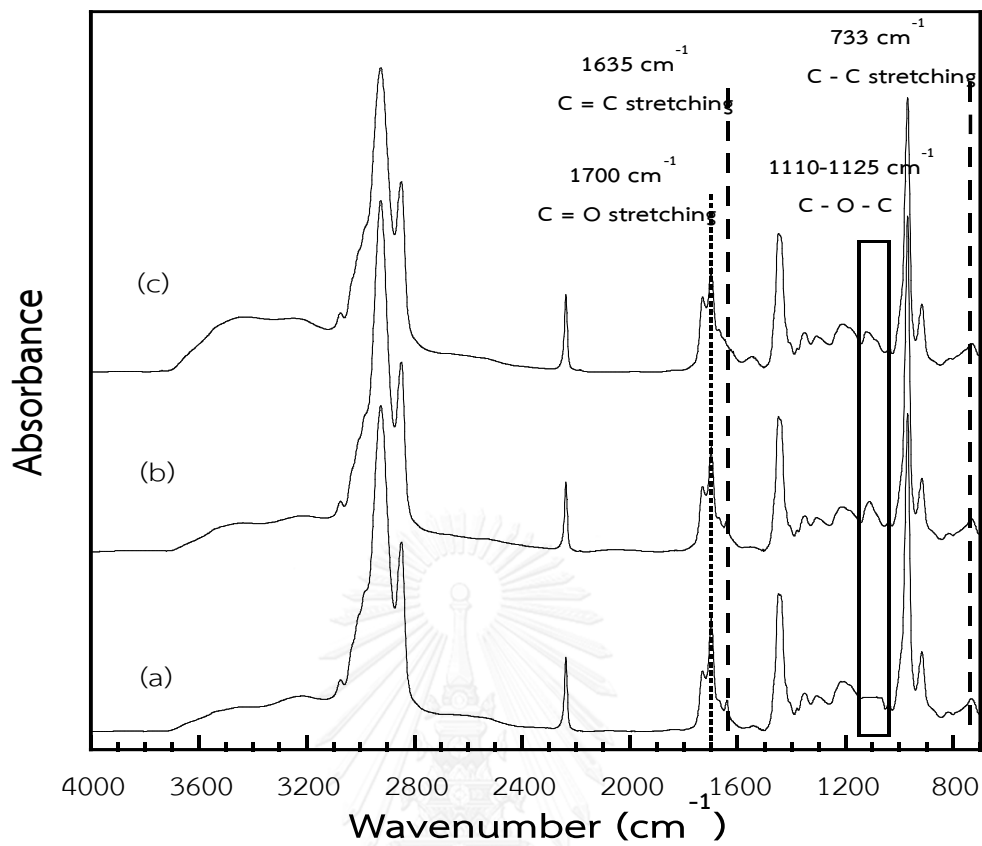


Figure 5.10 FT-IR spectra of (a) un-irradiated NBR latex and (b) 100 kGy, and (c) 200 kGy of gamma radiation irradiated NBR latex.

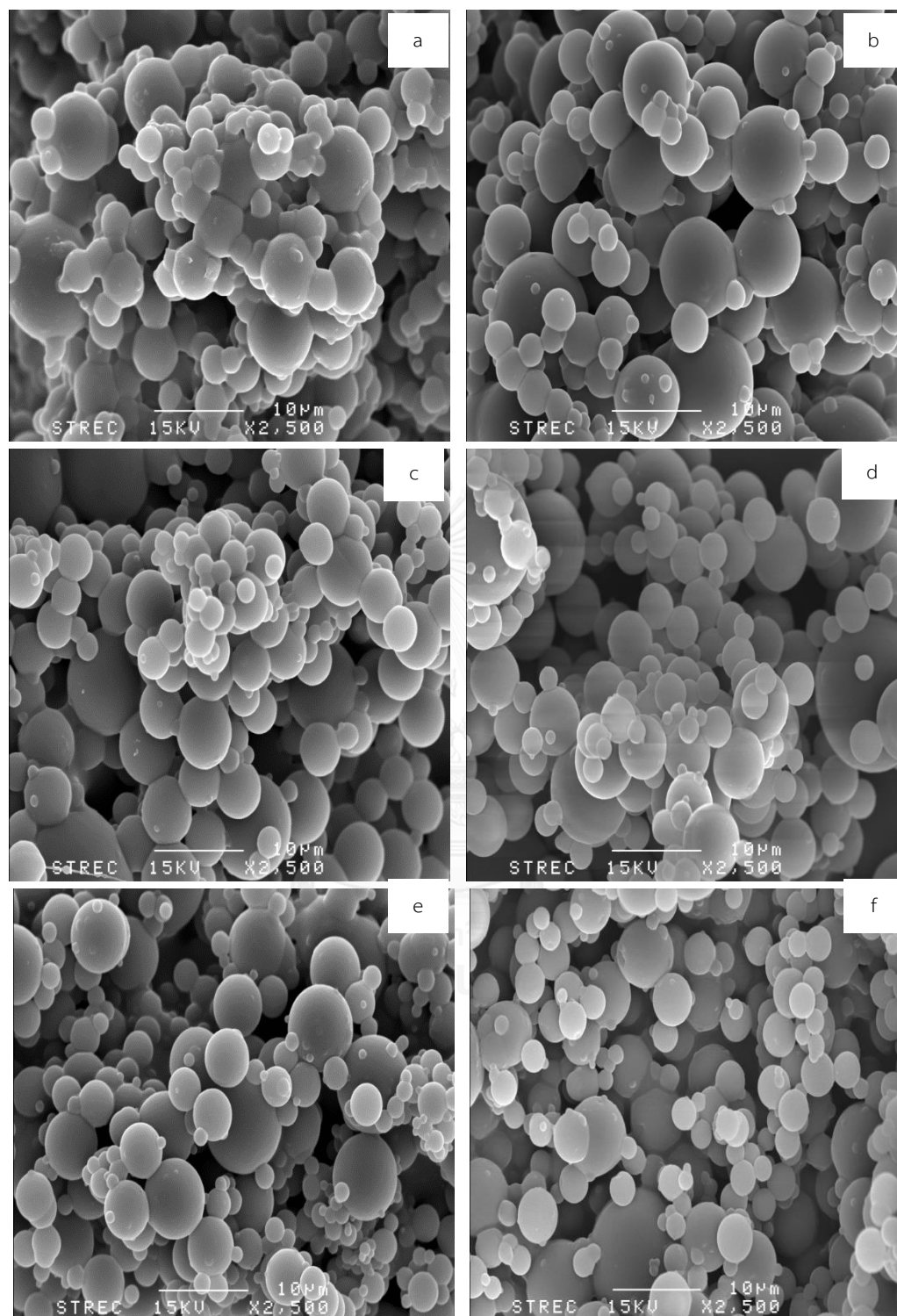


Figure 5.11 Morphology of ultrafine fully vulcanized powdered SBR for x2500 (a) 0 kGy, (b) 50 kGy, (c) 100 kGy, (d) 150 kGy, (e) 200 kGy and (f) 250 kGy.

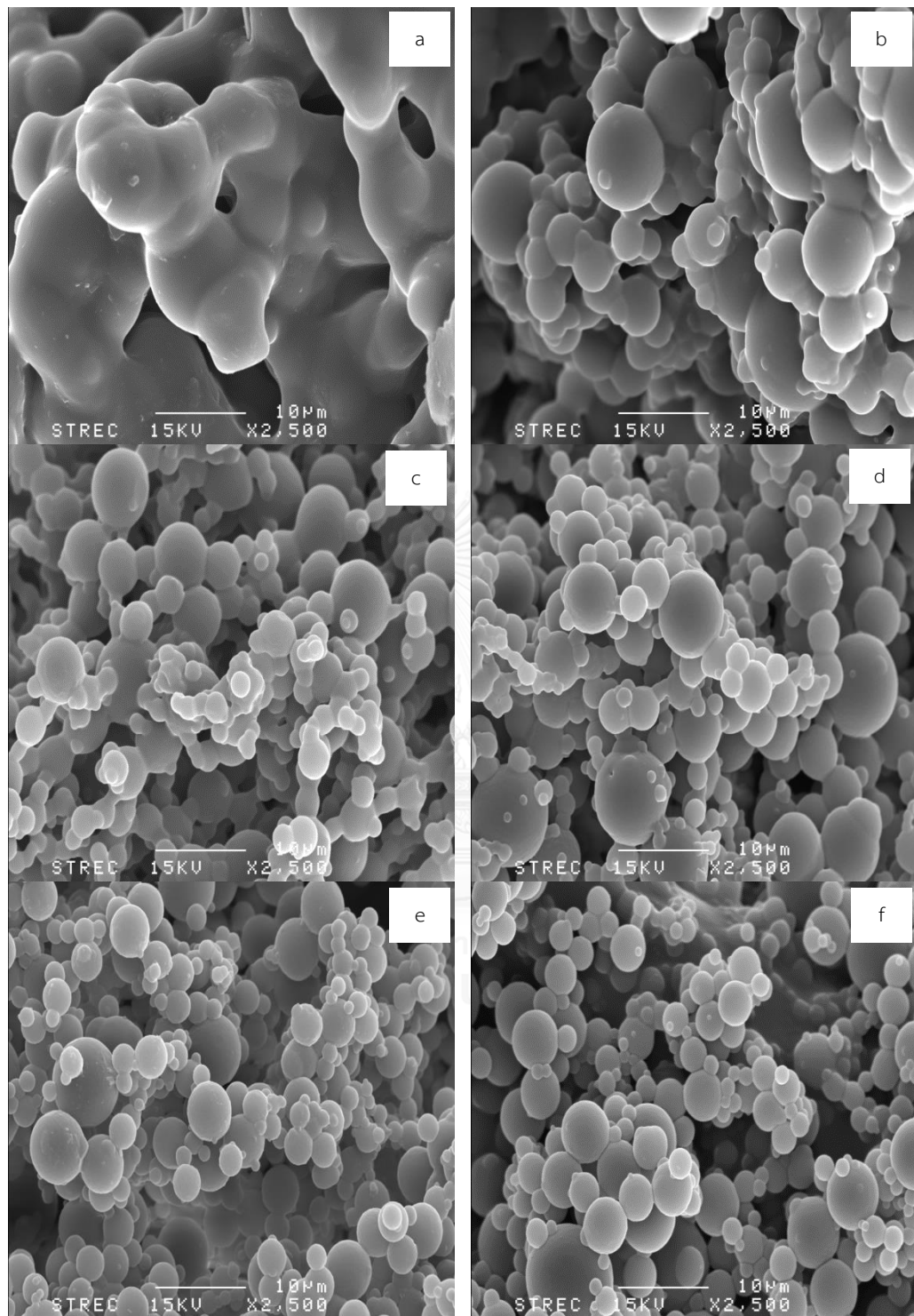


Figure 5.12 Morphology of ultrafine fully vulcanized powdered NBR for x2500 (a) 0 kGy, (b) 50 kGy, (c) 100 kGy, (d) 150 kGy, (e) 200 kGy and (f) 250 kGy.

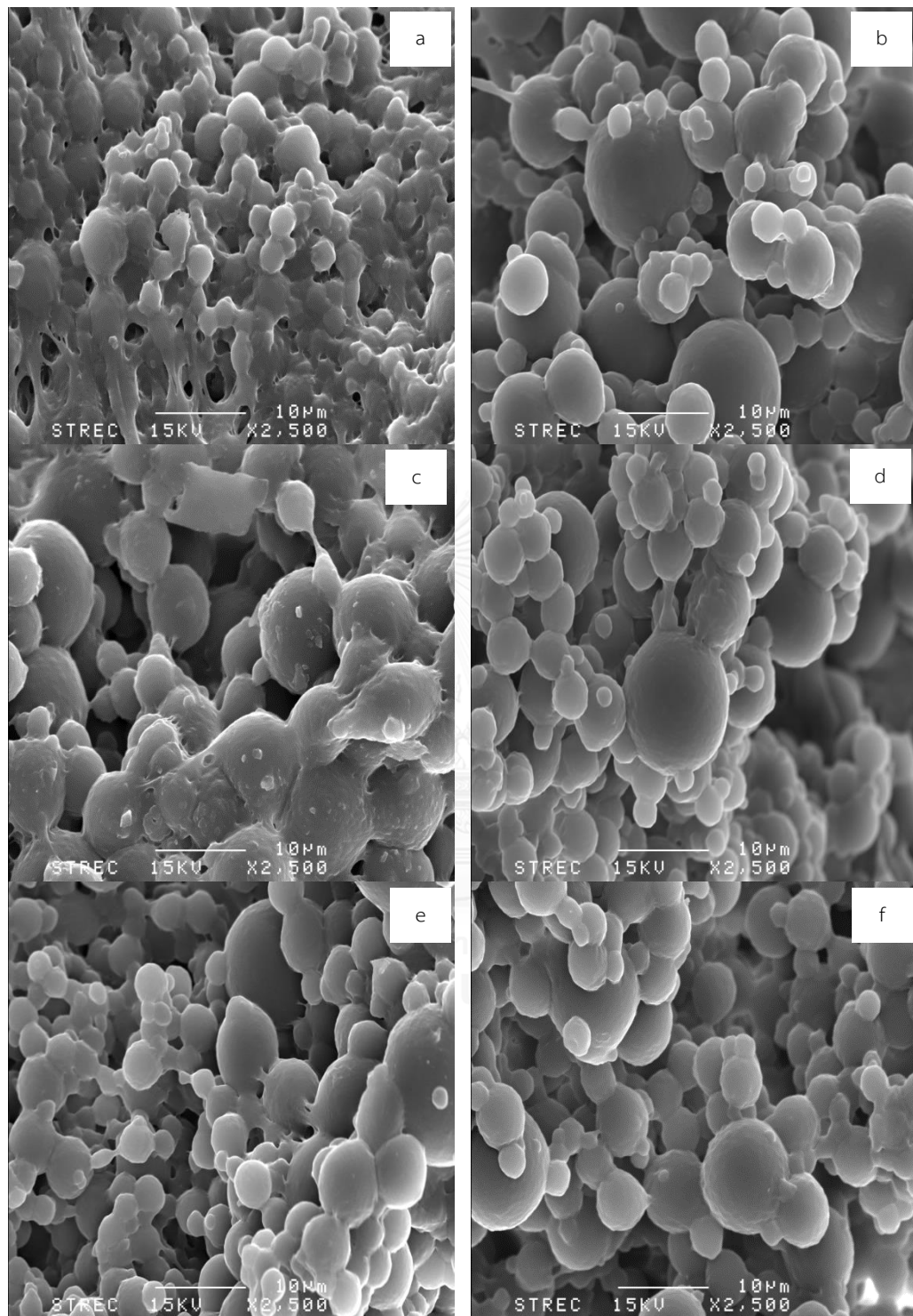


Figure 5.13 Morphology of ultrafine fully vulcanized powdered NBR for x2500 (a) 0 kGy, (b) 50 kGy, (c) 100 kGy, (d) 150 kGy, (e) 200 kGy and (f) 250 kGy.

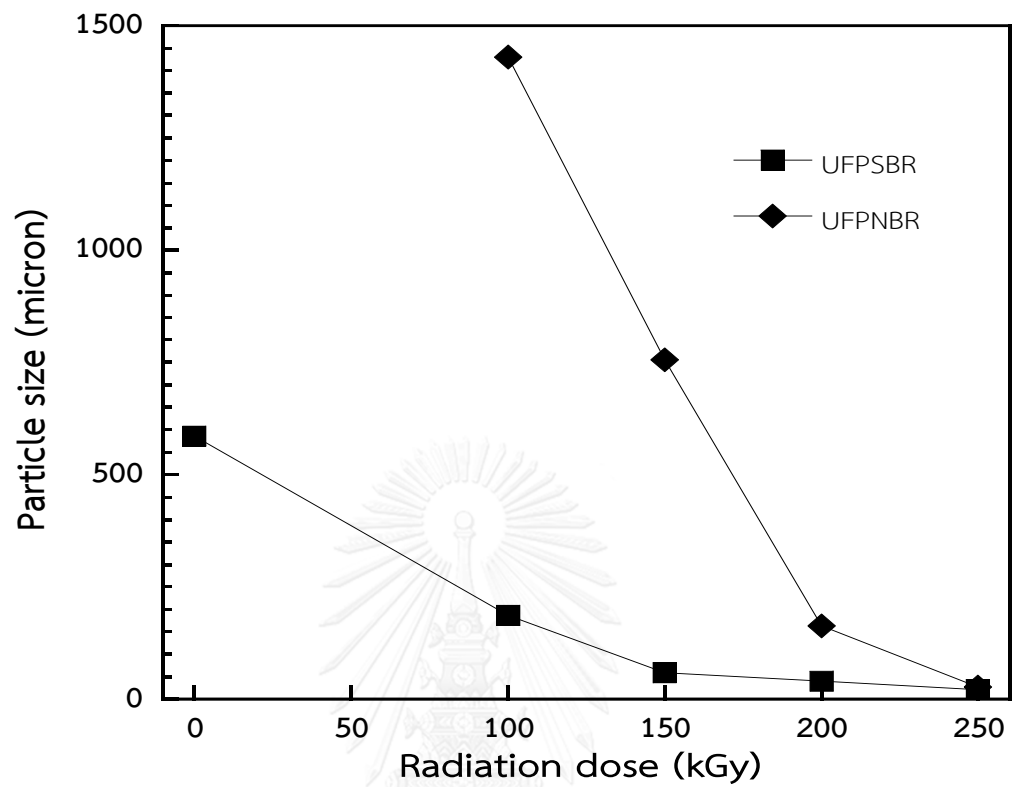


Figure 5.14 Average particle size of ultrafine SBR and NBR at various gamma radiation dose.

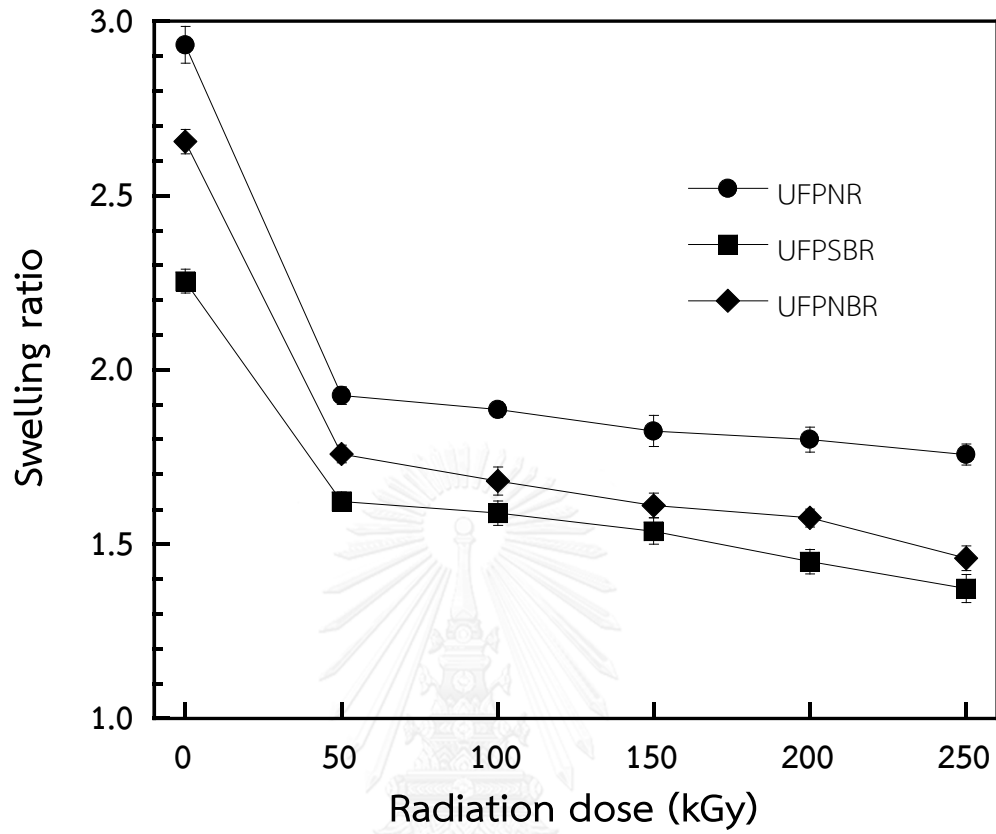


Figure 5.15 Swelling ratio of ultrafine rubber in toluene solvent at 0, 50, 100, 150, 200 and 250 kGy of gamma radiation doses: (●) ultrafine-NR (UFPNR), (■) ultrafine-SBR (UFPSBR) and (◆) ultrafine-NBR (UFPNBR)

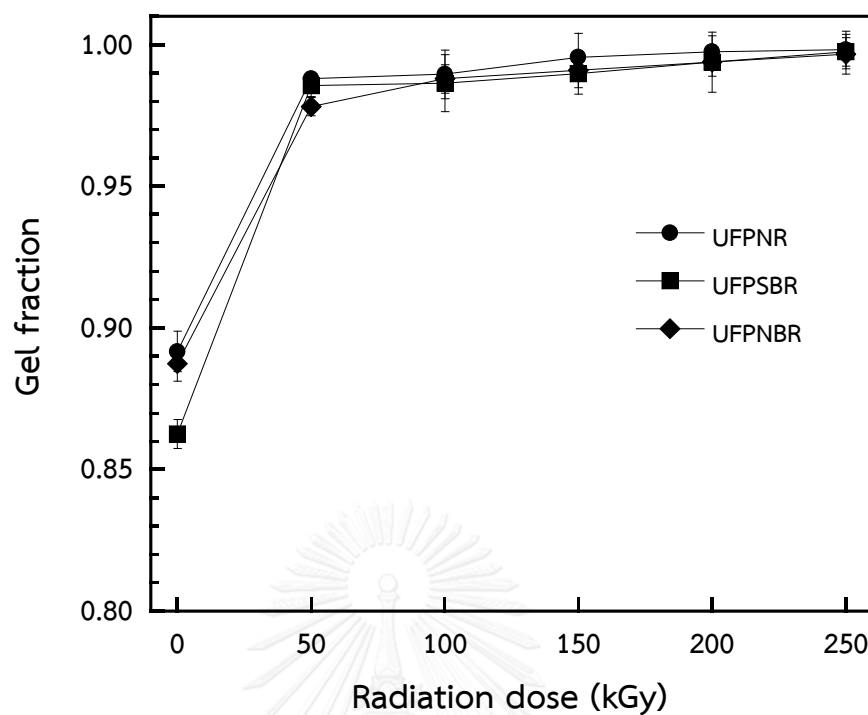


Figure 5.16 Gel fraction in toluene solvent of ultrafine rubber at 0, 50, 100, 150, 200 and 250 kGy of gamma radiation doses: (●) ultrafine-NR (UFNR), (■) ultrafine-SBR (UFPSBR) and (◆) ultrafine-NBR (UFNBR)

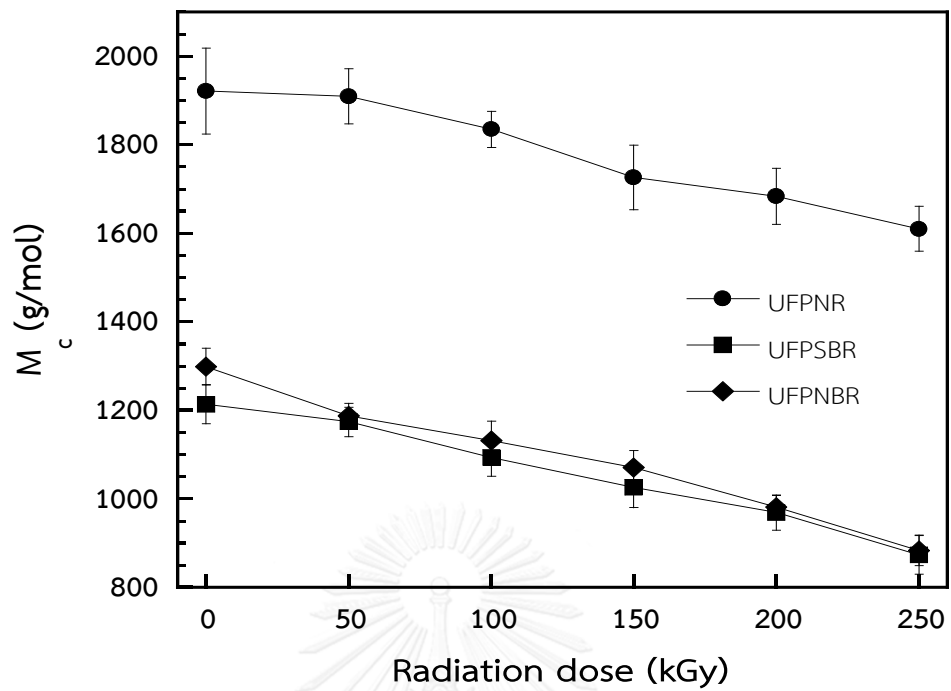


Figure 5.17 Molecular weight between crosslink of ultrafine fully vulcanized powdered rubber at different gamma radiation dose: (●) UFPNR, (■) UFPSBR and (◆) UFPNBR.

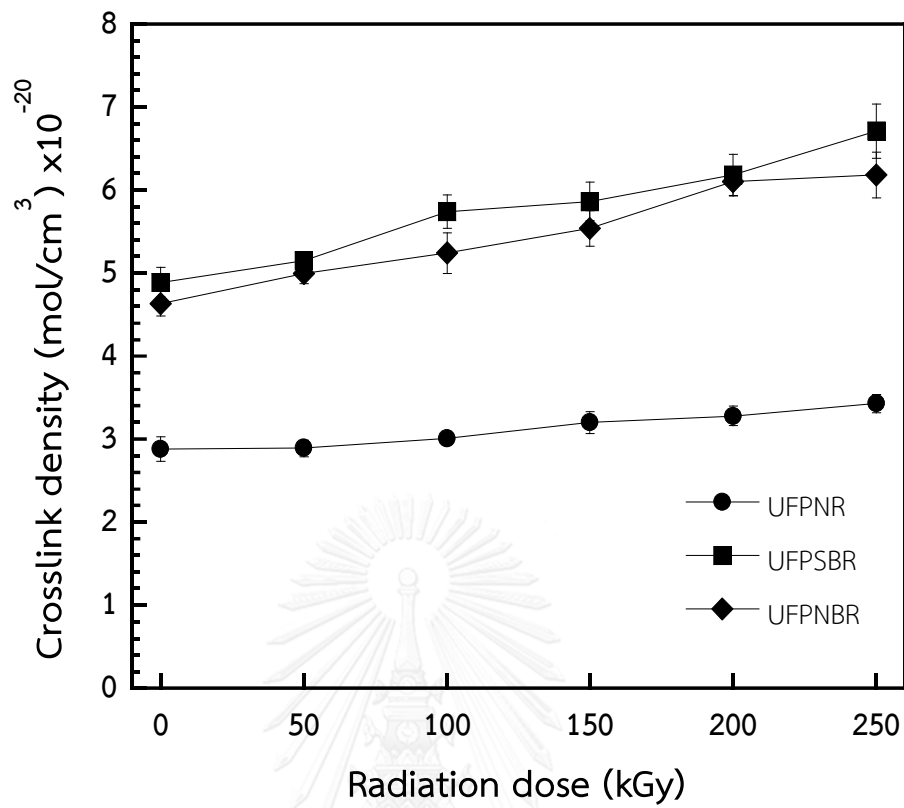


Figure 5.18 Crosslink density of ultrafine rubber at various gamma radiation doses after spray drying process: (●) ultrafine-NR (UFPNR), (■) ultrafine-SBR (UFPSBR) and (◆) ultrafine-NBR (UFPNBR).

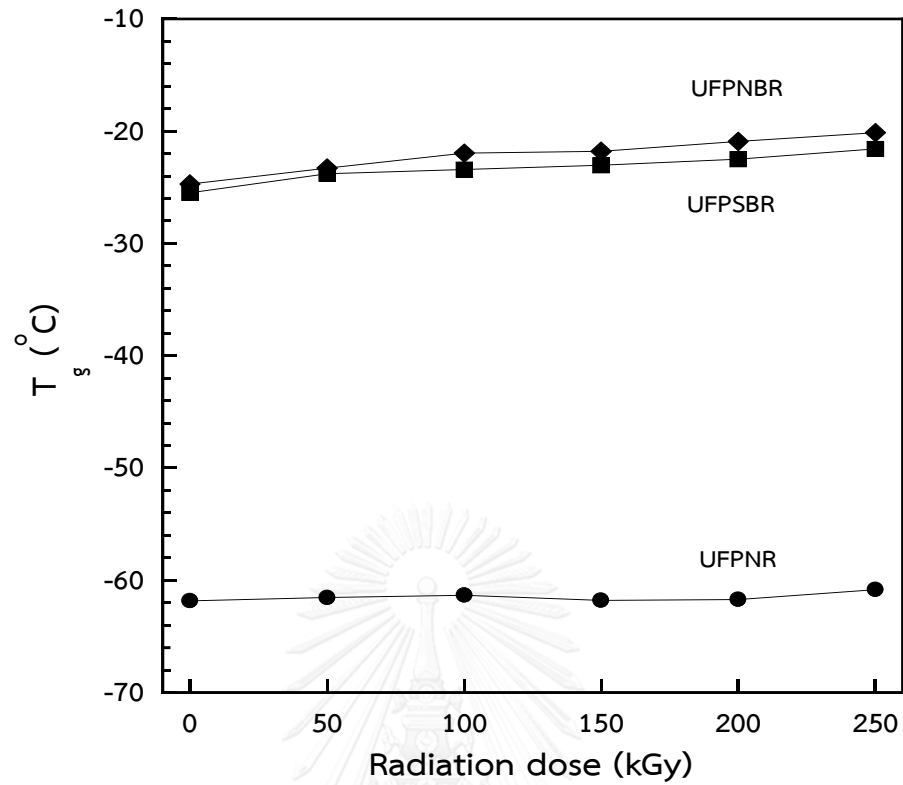


Figure 5.19 Glass transition temperature of UFPRs at different gamma irradiated dose: (●) ultrafine-NR (UFPNR), (■) ultrafine-SBR (UFPSBR) and (◆) ultrafine-NBR (UFPNBR).

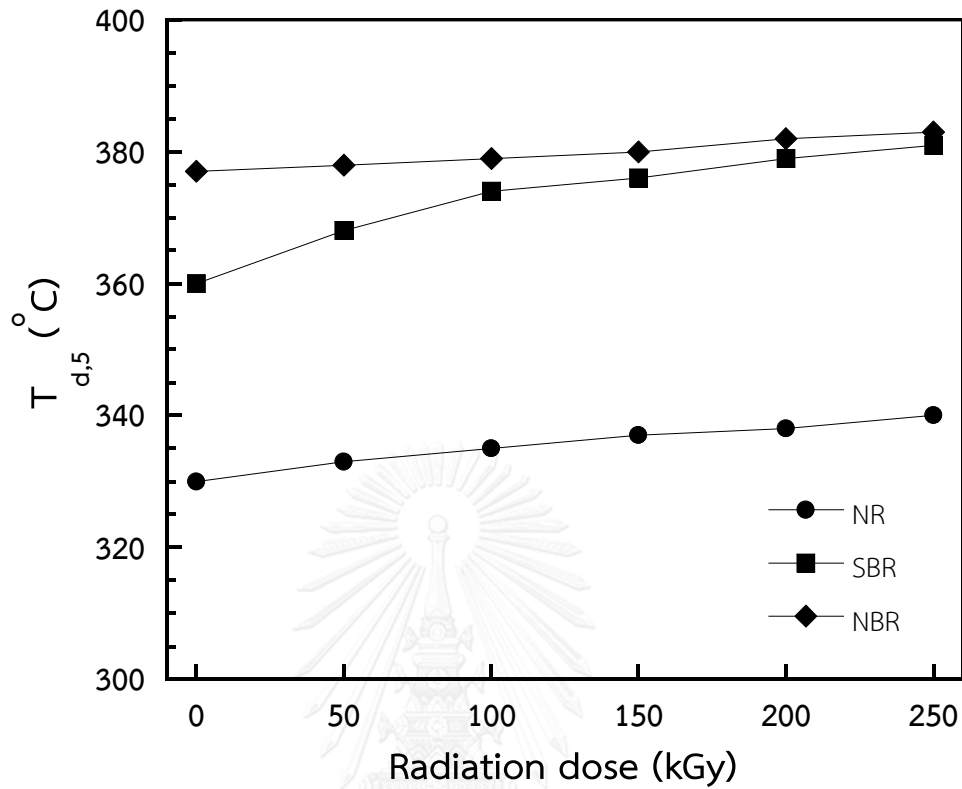


Figure 5.20 Degradation temperature at 5% weight loss of ultrafine rubber at 0, 50, 100, 150, 200 and 250 kGy of gamma rays: (●) ultrafine-NR (UFPNR), (■) ultrafine-SBR (UFPSBR) and (◆) ultrafine-NBR (UFPNBR)

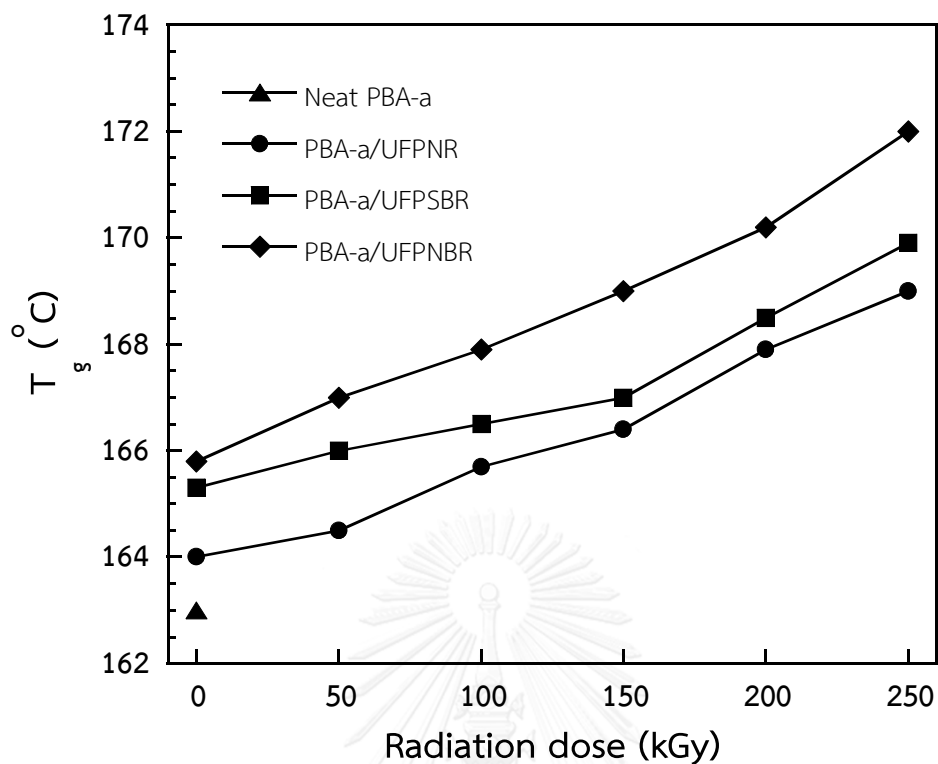


Figure 5.21 Glass transition temperature of polybenzoxazine composites at different doses of gamma rays: (▲) neat polybenzoxazine (PBA-a), (●) filled with ultrafine-NR (UFPNR), (■) filled with ultrafine-SBR (UFPSBR) and (◆) filled with ultrafine-NBR (UFPNBR).

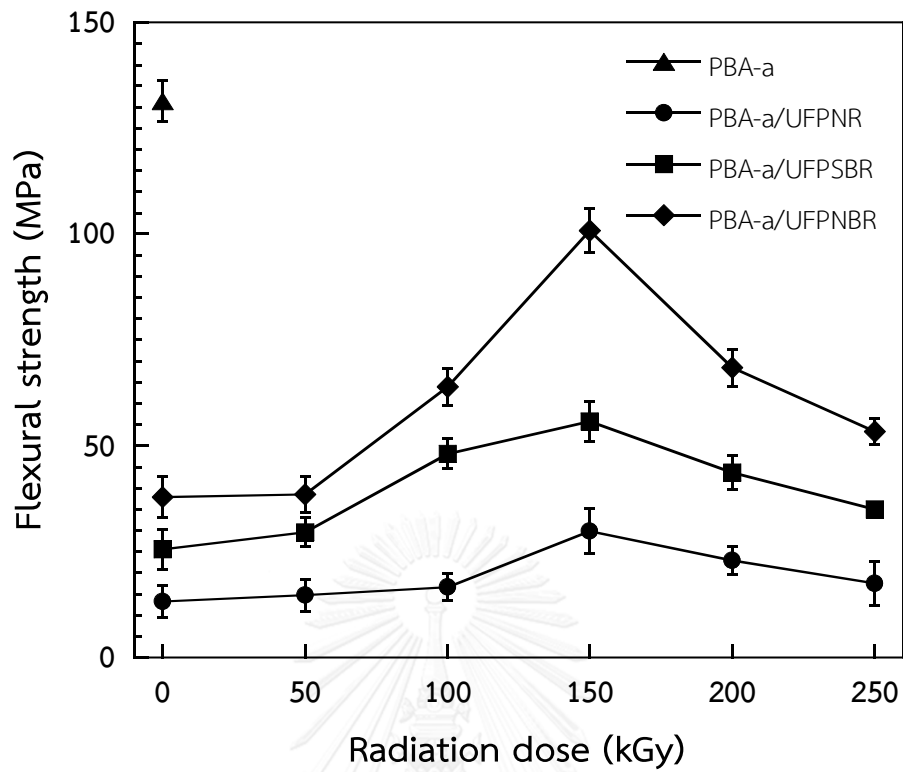


Figure 5.22 Flexural strength of (▲) neat polybenzoxazine and polybenzoxazine composites filled with (●) ultrafine-NR (UFPNR), (■) ultrafine-SBR (UFPSBR) and (◆) ultrafine-NBR (UFPNBR) at various gamma radiation doses.

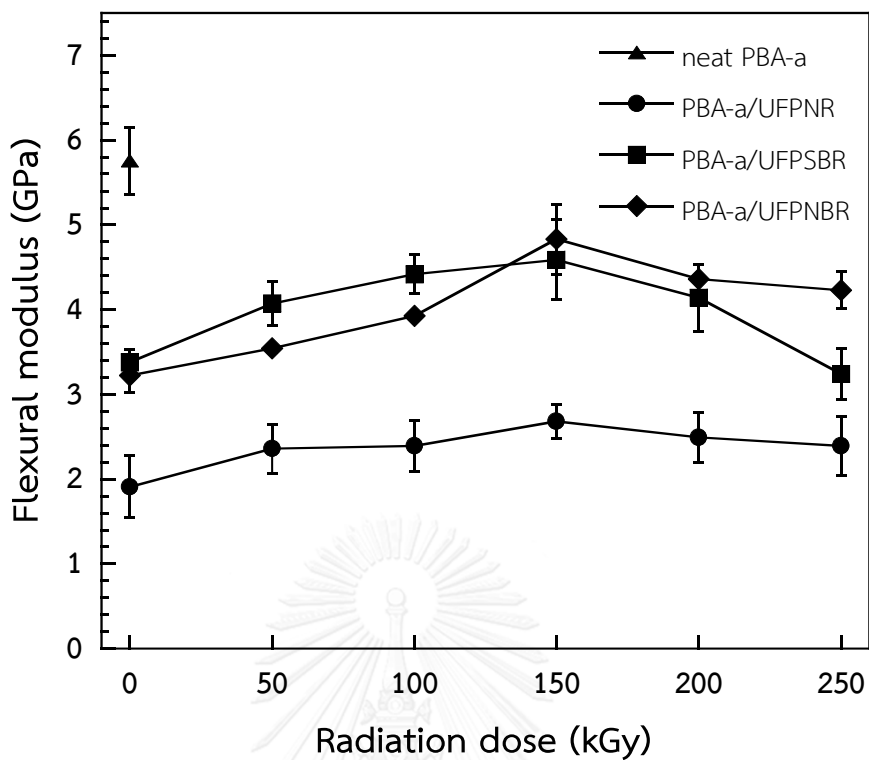


Figure 5.23 Flexural modulus of (▲) neat polybenzoxazine and polybenzoxazine filled with (●) UFPNR, (■) UFPSBR and (◆) UFPNBR at 0, 50, 100, 150, 200 and 250 kGy of gamma rays.

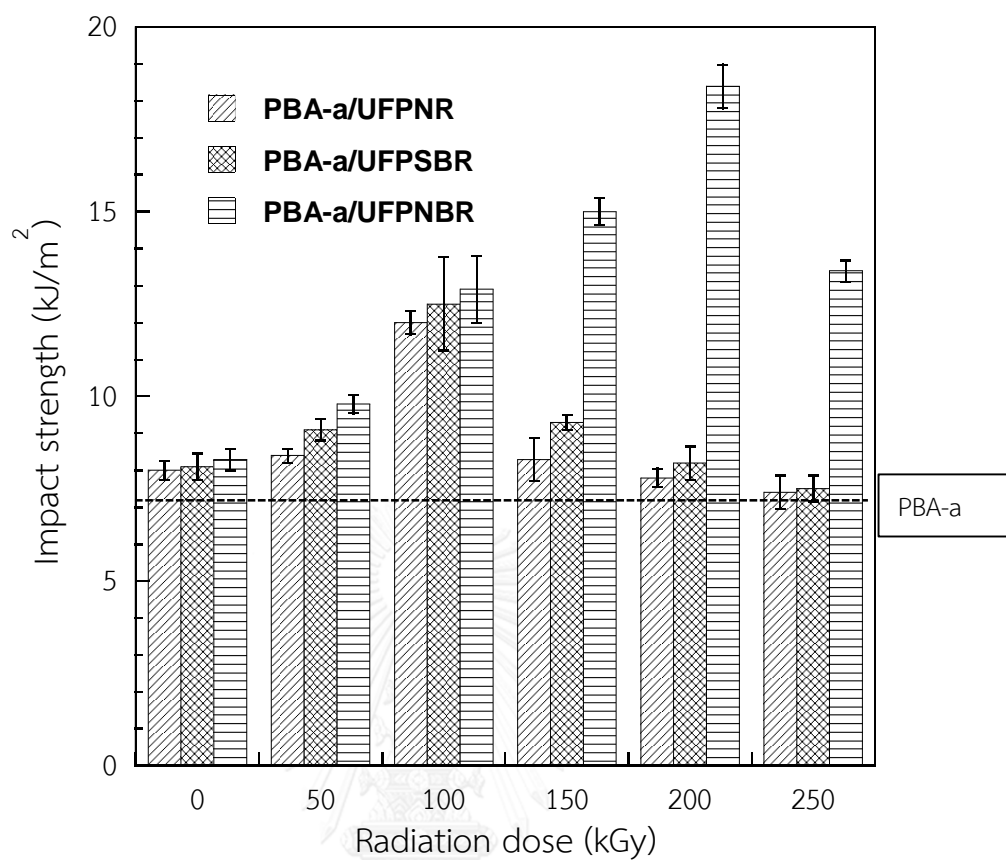


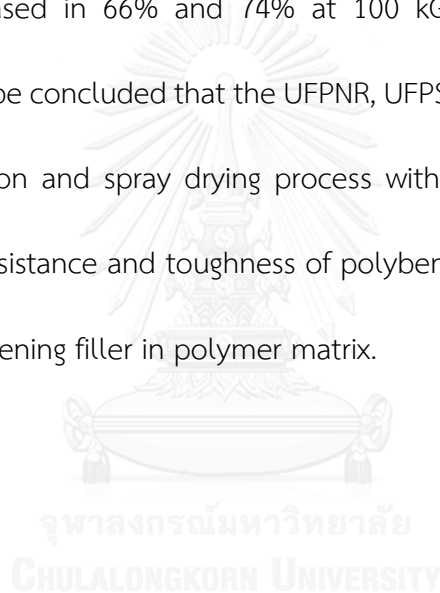
Figure 5.24 Impact strength of composites based on PBA-a at difference gamma dose irradiated UFPRs: (●) PBA-a/UFPNR, (■) PBA-a/UFPSBR and (◆) PBA-a/UFPNBR.

CHAPTER VI

CONCLUSIONS

Ultrafine fully vulcanized powdered rubber were successfully prepared by gamma radiation and spray drying process. An increase of gamma radiation dose of rubber latex led to an improvement on properties of rubber latices including swelling behaviors, gel fraction, crosslink density, glass transition temperature and thermal degradation temperature for all three types of rubber. On the other hand, swelling ratio and molecular weight between crosslink decreased. The gamma radiation on rubber latex affects to a decreasing of particle size of ultrafine rubber after spray drying process. Spherical shape with smooth surfaces UFPSBR and UFPNBR was observed at gamma irradiation dose of 250 kGy. The smallest particle size of UFPSBR was 21 μm at gamma radiation dose of rubber latex at 250 kGy. Moreover, swelling behaviors of UFPRs such as swelling ratio and crosslink density were also improved after spray drying process. With an addition of un-irradiated UFPRs into PBA-a, T_g of the composite increased compared with neat PBA-a composites. After irradiation of UFPRs, the T_g value of PBA-a/UFPRs composites increased at least 5°C for all three types of rubber. The flexural strength and flexural modulus of PBA-a/UFPR showed the optimum value at 150 kGy of gamma irradiation dose. The highest flexural strength of PBA-a filled with UFPNR, UFPSBR and UFPNBR were 29.9, 55.8 and 100.9 MPa, respectively. The optimum flexural modulus value of PBA-a/UFPNR, PBA-a/UFPSBR and PBA-a/UFPNBR was 2.68,

4.59 and 4.83 GPa, respectively. The impact strength of PBA-a filled with UFPRs was improved. Un-irradiated UFPRs revealed a slightly increased of impact strength from 7.2 kJ/m² of neat polybenzoxazine to 8.0, 8.1 and 8.3 kJ/m² of un-irradiated UFPNR, UFPSBR and UFPNBR filled in polybenzoxazine composites. The highest impact strength value of polybenzoxazine composites filled with UFPNBR increased in 155% at gamma irradiation dose of 200 kGy while the highest value of PBA-a/UFPNR and PBA-a/UFPSBR was increased in 66% and 74% at 100 kGy of gamma radiation dose. Consequently, it can be concluded that the UFPNR, UFPSBR and UFPNBR that obtained from gamma irradiation and spray drying process without vulcanizing agent can be improved the heat resistance and toughness of polybenzoxazine, in the other word it can be used as toughening filler in polymer matrix.



REFERENCES

- [1] Paiva, L.B.d., Oliveira, A.M.d., and Gavioli, R.R., Preparation and properties of rubber powder from modified-SBR latex by spray drying process. Powder Technology, 2014. 264: p. 507-513.
- [2] Li, D., Xia, H., Peng, J., Zhai, M., Wei, G., Li, J., and Qiao, J., Radiation preparation of nano-powdered styrene-butadiene rubber (SBR) and its toughening effect for polystyrene and high-impact polystyrene. Radiation Physics and Chemistry, 2007. 76(11–12): p. 1732-1735.
- [3] Zhang, M., Liu, Y., Zhang, X., Gao, J., Huang, F., Song, Z., Wei, G., and Qiao, J., The effect of elastomeric nano-particles on the mechanical properties and crystallization behavior of polypropylene. Polymer, 2002. 43(19): p. 5133-5138.
- [4] Liu, Y., Zhang, X., Gao, J., Huang, F., Tan, B., Wei, G., and Qiao, J., Toughening of polypropylene by combined rubber system of ultrafine full-vulcanized powdered rubber and SBS. Polymer, 2004. 45(1): p. 275-286.
- [5] Sae-Oui, P., Sirisinha, C., Sa-nguanthammarong, P., and Thaptong, P., Properties and recyclability of thermoplastic elastomer prepared from natural rubber powder (NRP) and high density polyethylene (HDPE). Polymer Testing, 2010. 29(3): p. 346-351.

- [6] Huang, F., Liu, Y., Zhang, X., Gao, J., Song, Z., Tang, B., Wei, G., and Qiao, J., Interface and properties of epoxy resin modified by elastomeric nano-particles. Science in China Series B: Chemistry, 2005. 48(2): p. 148-155.
- [7] Laura, D.M., Keskkula, H., Barlow, J.W., and Paul, D.R., Effect of rubber particle size and rubber type on the mechanical properties of glass fiber reinforced, rubber-toughened nylon 6. Polymer, 2003. 44(11): p. 3347-3361.
- [8] Peng, J., Zhang, X., Qiao, J., and Wei, G., Radiation preparation of ultrafine carboxylated styrene-butadiene rubber powders and application for nylon 6 as an impact modifier. Journal of Applied Polymer Science, 2002. 86(12): p. 3040-3046.
- [9] Liu, Y., Fan, Z., Ma, H., Tan, Y., and Qiao, J., Application of nano powdered rubber in friction materials. Wear, 2006. 261(2): p. 225-229.
- [10] Rezaei Abadchi, M. and Jalali-Arani, A., The use of gamma irradiation in preparation of polybutadiene rubber nanopowder; Its effect on particle size, morphology and crosslink structure of the powder. Nuclear Instruments and Methods in Physics Research Section B: Beam Interactions with Materials and Atoms, 2014. 320: p. 1-5.
- [11] Yoshida, K., Shimizu, K., and Hamada, M., *Method for producing silicone rubber powder*, 1988, Google Patents.
- [12] Harashima, A., Morita, Y., and Tachibana, R., *Silicone rubber powder and method for the preparation thereof*, 1998, Google Patents.

- [13] Qiao, J., Wei, G., Zhang, X., Zhang, S., Gao, J., Zhang, W., Liu, Y., Li, J., Zhang, F., and Zhai, R., *Fully vulcanized powdery rubber having a controllable particle size, preparation and use thereof*, 2002, Google Patents.
- [14] Spray Drying Systems, I. *WHY USE A SPRAY DRYER FOR YOUR DRYING APPLICATION?* 2014; Available from: <http://www.spraydrys.com/spray-dryers/spray-drying-advantages.htm>.
- [15] PALLMANN Industries, I. *Preparation of Rubber*. 2009; Available from: <http://www.pallmannindustries.com/rubber.htm>.
- [16] Zhao, Q., Ding, Y., Yang, B., Ning, N., and Fu, Q., Highly efficient toughening effect of ultrafine full-vulcanized powdered rubber on poly(lactic acid)(PLA). *Polymer Testing*, 2013. 32(2): p. 299-305.
- [17] Xiang, W., GuiCun, Q., XiaoHong, Z., JianMing, G., BingHai, L., ZhiHai, S., and JinLiang, Q., The abnormal behavior of polymers glass transition temperature increase and its mechanism. *Science China Chemistry*, 2012. 55(5): p. 713-717.
- [18] Tian, M., Tang, Y.-W., Lu, Y.-L., Qiao, J., Li, T., and Zhang, L.-Q., Novel Rubber Blends Made from Ultra-Fine Full-Vulcanized Powdered Rubber (UFPR). *Polymer Journal*, 2006. 38: p. 50-56.
- [19] Barlow, F.W., *Rubber Compounding: Principles, Materials, and Techniques, Second Edition*. 1993: Taylor & Francis.

- [20] Sumitomo Electric Industries, L. *Heat shrink tubing & Heat-resistant tubing/tapes*. 2015; Available from: <http://global-sei.com/products/industrial.html>.
- [21] M, A. *How To Make Rubber*. 2014; Available from: <http://scinote.tumblr.com/post/102908520388/how-to-make-rubber>.
- [22] *Spray Dryer ADL310*. 2012; Available from: <http://www.yamato-scientific.com/product/other/adl310.htm>.
- [23] Cleland, M.R., Parks, L.A., and Cheng, S., Applications for radiation processing of materials. *Nuclear Instruments and Methods in Physics Research Section B: Beam Interactions with Materials and Atoms*, 2003. 208: p. 66-73.
- [24] Parks, L.A. *Radiation Crosslinking of Polymers*. 2010; Available from: <http://www.sterigenics.com/crosslinking/crosslinking.htm>.
- [25] Li, X., Anton, N., Arpagaus, C., Belleteix, F., and Vandamme, T.F., Nanoparticles by spray drying using innovative new technology: The Büchi Nano Spray Dryer B-90. *Journal of Controlled Release*, 2010. 147(2): p. 304-310.
- [26] *Mini Spray Dryer B-290 : The world leading R&D solution for Spray Drying*. 2015 [cited 2015; Available from: <http://www.buchi.com/en/products/spray-drying-and-encapsulation/mini-spray-dryer-b-290>.
- [27] Mitra, S., Chattopadhyay, S., Sabharwal, S., and Bhowmick, A.K., Electron beam crosslinked gels—Preparation, characterization and their effect on the

mechanical, dynamic mechanical and rheological properties of rubbers.

Radiation Physics and Chemistry, 2010. 79(3): p. 289-296.

- [28] Ahmed, S., Basfar, A.A., and Abdel Aziz, M.M., Comparison of thermal stability of sulfur, peroxide and radiation cured NBR and SBR vulcanizates. Polymer Degradation and Stability, 2000. 67(2): p. 319-323.
- [29] Ishida, H., *Process for preparation of benzoxazine compounds in solventless systems*, 1996, Google Patents.
- [30] Flory, P.J. and Rehner, J., Statistical Mechanics of Cross-Linked Polymer Networks II. Swelling. The Journal of Chemical Physics, 1943. 11(11): p. 521-526.
- [31] Flory, P.J. and Rehner, J., Statistical Mechanics of Cross-Linked Polymer Networks I. Rubberlike Elasticity. The Journal of Chemical Physics, 1943. 11(11): p. 512-520.
- [32] Ltd, M.I. *Mastersizer 3000: Smarter particle sizing*. 2016; Available from: <http://www.malvern.com/en/products/product-range/mastersizer-range/mastersizer-3000/>.
- [33] Gordon, M.J., Industrial design of plastics products. 2003: Wiley-Interscience.
- [34] Charlesby, A. and Pinner, S.H., Analysis of the Solubility Behaviour of Irradiated Polyethylene and Other Polymers. Proceedings of the Royal Society of London. Series A. Mathematical and Physical Sciences, 1959. 249(1258): p. 367.

- [35] Chapiro, A., Radiation chemistry of polymeric systems. 1961: Interscience Publishers.
- [36] Giri, R., Naskar, K., and Nando, G.B., Effect of electron beam irradiation on dynamic mechanical, thermal and morphological properties of LLDPE and PDMS rubber blends. Radiation Physics and Chemistry, 2012. 81(12): p. 1930-1942.
- [37] Moustafa, A.B., Mounir, R., El Miligy, A.A., and Mohamed, M.A., Effect of gamma irradiation on the properties of natural rubber/styrene butadiene rubber blends. Arabian Journal of Chemistry, 2011.
- [38] Rolere, S., Liengprayoon, S., Vaysse, L., Sainte-Beuve, J., and Bonfils, F., Investigating natural rubber composition with Fourier Transform Infrared (FT-IR) spectroscopy: A rapid and non-destructive method to determine both protein and lipid contents simultaneously. Polymer Testing, 2015. 43: p. 83-93.
- [39] Dinsmore, H.L. and Smith, D.C., Analysis of Natural and Synthetic Rubber by Infrared Spectroscopy. Analytical Chemistry, 1948. 20(1): p. 11-24.
- [40] Kishore, K. and Pandey, H.K., Spectral studies on plant rubbers. Progress in Polymer Science, 1986. 12(1): p. 155-178.
- [41] Nallasamy, P. and Mohan, S., Vibrational spectra of cis-1,4-polyisoprene. Arabian Journal for Science and Engineering, 2004. 28(1 A): p. 17-26.
- [42] Baeta, D.A., Zattera, J.A., Oliveira, M.G., and Oliveira, P.J., The use of styrene-butadiene rubber waste as a potential filler in nitrile rubber: order of addition

- and size of waste particles. Brazilian Journal of Chemical Engineering, 2009. 26: p. 23-31.
- [43] Liu, W.-W., Ma, J.-J., Zhan, M.-S., and Wang, K., The toughening effect and mechanism of styrene-butadiene rubber nanoparticles for novolac resin. Journal of Applied Polymer Science, 2015. 132(9): p. n/a-n/a.
- [44] Martínez-Barrera, G., López, H., Castaño, V.M., and Rodríguez, R., Studies on the rubber phase stability in gamma irradiated polystyrene-SBR blends by using FT-IR and Raman spectroscopy. Radiation Physics and Chemistry, 2004. 69(2): p. 155-162.
- [45] Crompton, T.R., 1.20 Nitrile-Butadiene, in Thermal Methods of Polymer Analysis. 2013, Smithers Rapra Technology.
- [46] N., K.P. Study on the use of Nanokaolin, MWCNT and graphene in NBR and SBR. Ph.D, Department of polymer science and rubber technology, Cochin university of scienc and technology, 2013.
- [47] Laskowska, A., Zaborski, M., Boiteux, G., Gain, O., Marzec, A., and Maniukiewicz, W., Ionic Elastomers Based on Carboxylated Nitrile Rubber (XNBR) and Magnesium Aluminum Layered Double Hydroxide. eXPRESS Polymer Letters, 2014. 8(6): p. 374-386.
- [48] El-Nemr, K.F., Effect of different curing systems on the mechanical and physico-chemical properties of acrylonitrile butadiene rubber vulcanizates. Materials & Design, 2011. 32(6): p. 3361-3369.

- [49] Stephen, R., Jose, S., Joseph, K., Thomas, S., and Oommen, Z., Thermal stability and ageing properties of sulphur and gamma radiation vulcanized natural rubber (NR) and carboxylated styrene butadiene rubber (XSBR) latices and their blends. Polymer Degradation and Stability, 2006. 91(8): p. 1717-1725.
- [50] Ishida, H. and Allen, D.J., Physical and mechanical characterization of near-zero shrinkage polybenzoxazines. Journal of Polymer Science Part B: Polymer Physics, 1996. 34(6): p. 1019-1030.
- [51] Jang, J. and Seo, D., Performance improvement of rubber-modified polybenzoxazine. Journal of Applied Polymer Science, 1998. 67(1): p. 1-10.
- [52] Wang, Q., Zhang, X., Liu, S., Gui, H., Lai, J., Liu, Y., Gao, J., Huang, F., Song, Z., Tan, B., and Qiao, J., Ultrafine full-vulcanized powdered rubbers/PVC compounds with higher toughness and higher heat resistance. Polymer, 2005. 46(24): p. 10614-10617.
- [53] Jubsilp, C., Taewattana, R., Takeichi, T., and Rimdusit, S., Investigation on Rubber-Modified Polybenzoxazine Composites for Lubricating Material Applications. Journal of Materials Engineering and Performance, 2015. 24(10): p. 3958-3968.
- [54] Liu, Y.-q., Zhang, X.-h., Wei, G.-s., Gao, J.-m., Huang, F., Zhang, M.-l., Guo, M.-f., and Qiao, J.-l., SPECIAL EFFECT OF ULTRA-FINE RUBBER PARTICLES ON PLASTIC TOUGHENING. Chinese Journal of Polymer Science, 2002. 20: p. 93-98.

- [55] Ma, H., Wei, G., Liu, Y., Zhang, X., Gao, J., Huang, F., Tan, B., Song, Z., and Qiao, J., Effect of elastomeric nanoparticles on properties of phenolic resin. Polymer, 2005. 46(23): p. 10568-10573.
- [56] Drobny, J.G., Modification of Polymers by Ionizing Radiation: A Review, in ANTEC 2006 Plastics: Annual Technical Conference Proceedings. Society of Plastics Engineers.





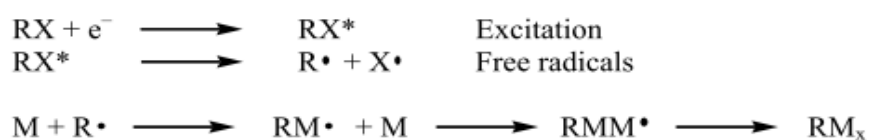
APPENDIX

จุฬาลงกรณ์มหาวิทยาลัย
CHULALONGKORN UNIVERSITY

APPENDIX A

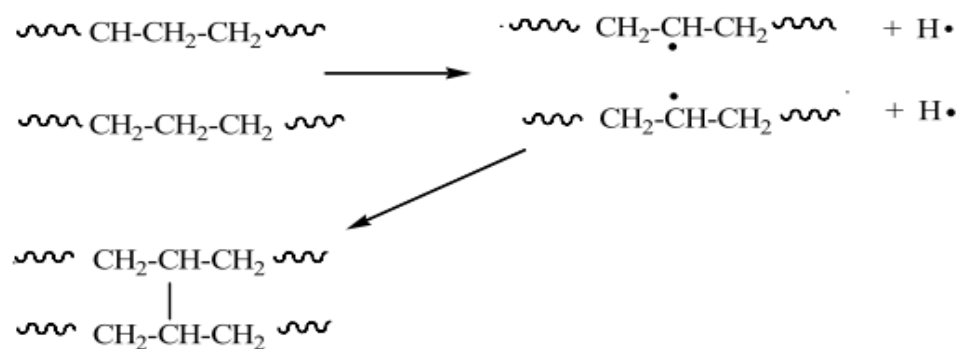
Appendix A1 Reactions induced by ionizing irradiation [56]

1. Free Radical Polymerization

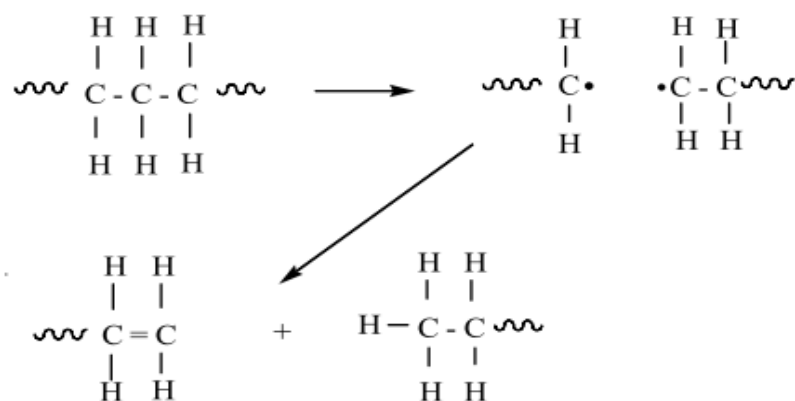


M – Monomer
 R• – Free radical

2. Cross-linking



3. Main Chain Scission - Polymer Degradation



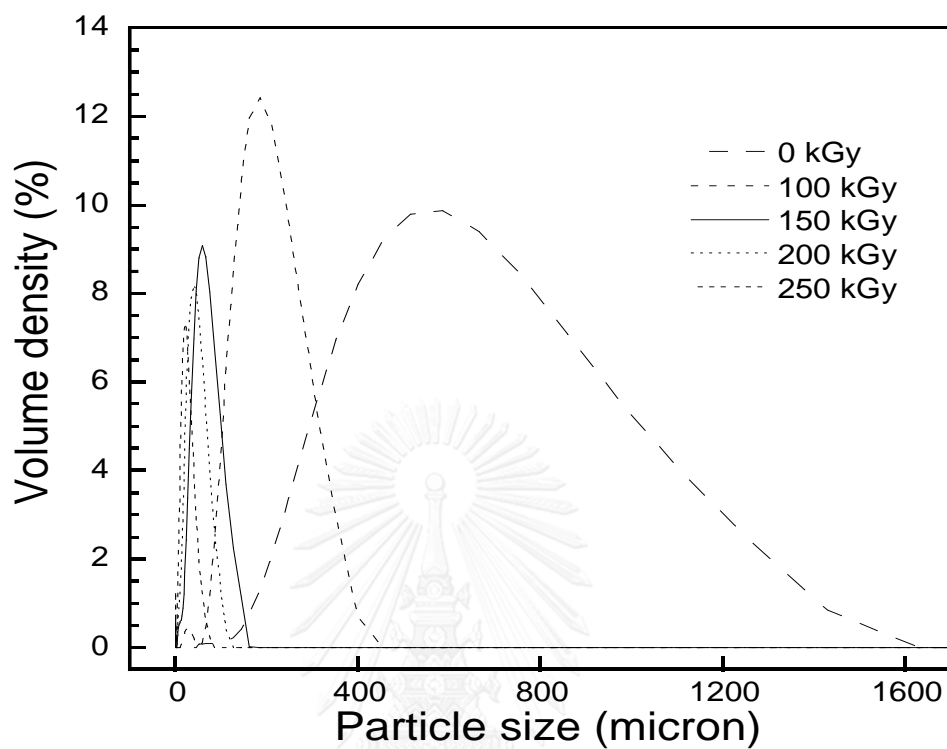
Disproportionation

Appendix A2: Particle size of UFPSBR and UFPNBR

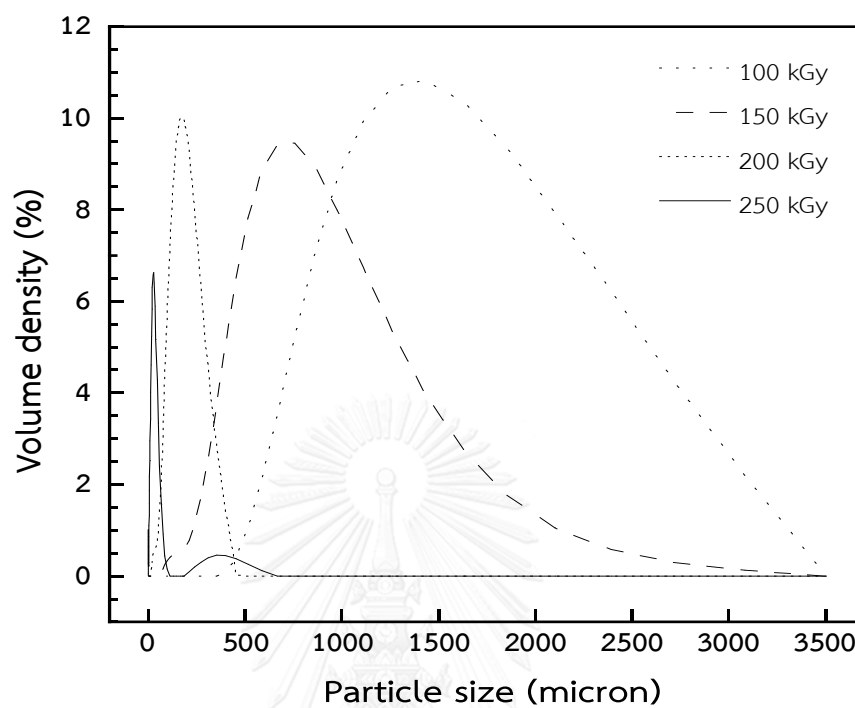
Radiation dose (kGy)	UFPSBR (micron)			UFPNBR (micron)		
	smallest	average	largest	smallest	average	largest
0	51.8	586	1430	-		
	58.9	586	1430			
	58.9	586	1430			
100	12.7	186	400	400	1430	-
	12.7	186	400	144	1430	-
	12.7	186	400	127	1430	-
150	0.188	58.9	163	66.9	756	3080
	0.188	58.9	144	66.9	756	3080
	0.188	58.9	163	66.9	756	2710
200	0.314	40.1	111	12.7	163	454
	0.314	40.1	111	12.7	163	454
	0.314	40.1	111	12.7	163	454
250	0.276	21.2	76	0.357	27.4	586
	0.276	21.2	86.4	0.357	27.4	756
	0.276	21.2	76	0.405	27.4	586

Note: - proposed to the sample cannot characterized by this machine

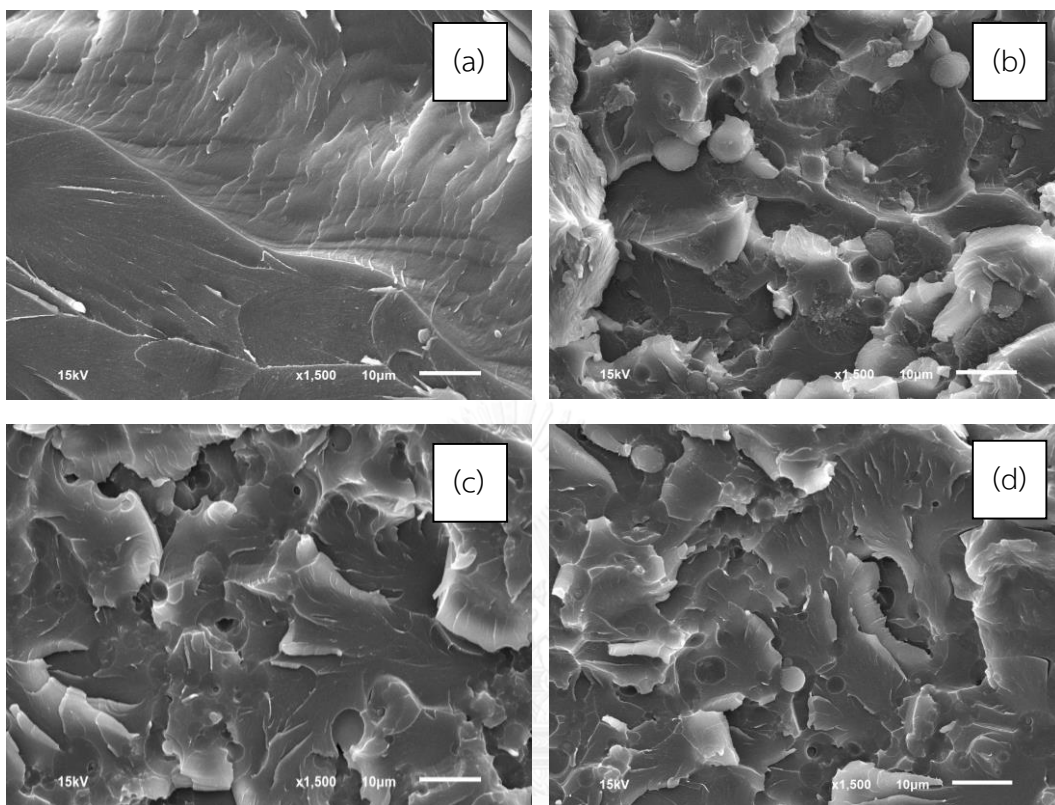
Appendix A3: Particle size distribution of UFPSBR at different radiation doses of gamma rays.



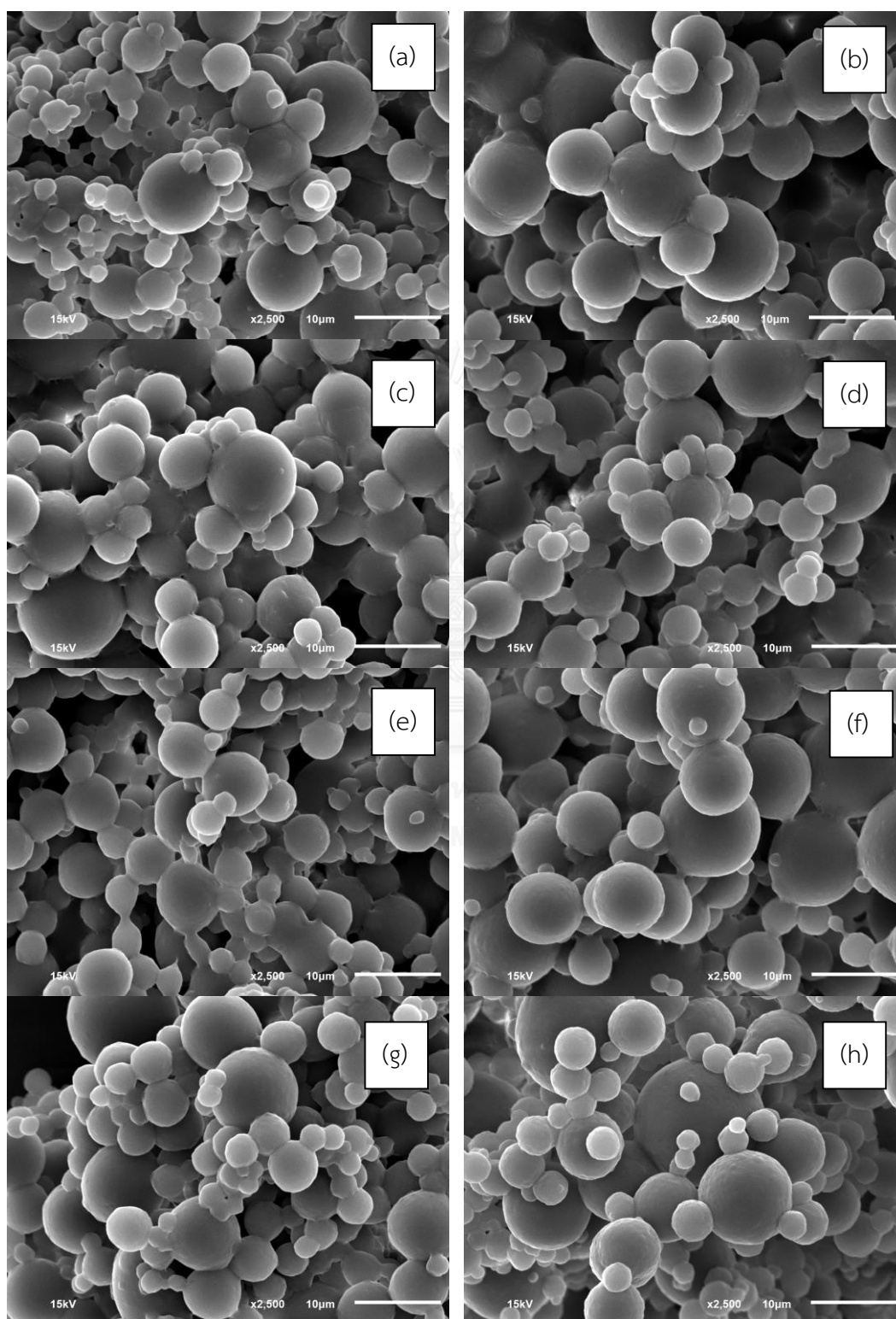
Appendix A4: Particle size distribution of UFPNBR prepared at different radiation doses.



Appendix A5: SEM Micrographs of PBA-a/UFPR Composites; (a) PBA-a, (b) PBA-a/UFPNBR-200kGy, (c) PBA-a/UFPNR-200kGy and (d) PBA-a/UFPSBR-200kGy.



Appendix A6: SEM Micrographs of UFPNR with TMPTMA 3 (left) and 5 phr (right); (a-b) 100 kGy, (c-d) 150 kGy, (e-f) 200 kGy and (g-h) 250 kGy.



VITA

Ms. Rapiphan Taewattana was born in Bangkok, Thailand. She graduated at high school level in 2010 from Sainampeung School under the Patronage of HRH Princess Petcharat Rajsuda Sirisopaphannawadee. She received the Bachelor's Degree of Engineer with major in Chemical Engineering from the Faculty of Engineer, Srinakharinwirot University, Thailand in 2014. After graduation, she entered study for a Master's Degree of Chemical Engineering at the Department of Engineering, Faculty of Engineering, Chulalongkorn University. Some part of this work were selected for oral presentation in The Pure and Applied Chemistry International Conference 2016 or PACCON2016 which was held during February 9-11, 2016 at Bangkok International Trade & Exhibition Centre (BITEC), Bangkok, Thailand and The International Polymer Conference of Thailand or PCT-6 which was held during June 30 - July 1, 2016 at Pathumwan Princess Hotel, Bangkok, Thailand.